DOCTOR OF PHILOSOPHY

Preparation and characterization of electrografted polymer films for surface functionalization

Easter, Penelope Anne

Award date:
2008

Awarding institution:
Bangor University

Preparation and characterization of electrografted polymer films for surface functionalization.

By Penelope Anne Easter

PhD thesis, University of Wales, Bangor. 2008.

Summary

Electrografting is an attractive technique with the potential for controlling the electrochemical conditions required for producing functionalized polymeric macrostructures of a predictable, well-defined composition and thickness. The aim of this study was to investigate the electrografting process for the prototype electron deficient vinylic monomer, acrylonitrile, with the purpose of extending the technique to other more functional monomers. The experimental preparation and set-up used here has evolved via a series of improvements to a technique used previously in these laboratories in line with those adopted by the laboratories at CEA, Saclay for the electrografting of PAN (polyacrylonitrile). Although the requirement for stringent conditions is similar, the simplicity of the current set-up contrasts markedly with previous workers. Various experimental parameters such as the composition of the electrolyte, electrode preparation, environment conditions and potentiostat control were explored to establish the optimum growing conditions.

The effects of changing these parameters were monitored electrochemically using cyclic voltammetry and also by evaluating the morphology and chemical structure of electrografted films using a combination of AFM, ellipsometry, FTIR, Raman and UV-VIS spectroscopies. In establishing the fundamental features of the electrografting technique, the study has highlighted the limitations of cyclic voltammetry as the sole technique for controlling the electrografting process.

Based on the AFM and FTIR data, the PAN films produced in this study were comparable in quality to those reported by CEA, Saclay, and the University of Liege groups. Their electrografted nature was confirmed by their ability to withstand a peel test and their insolubility in DMF (*N, N*-dimethylformamide). The FTIR spectra provide convincing evidence that the previous assignment of the 1670 cm^{-1} band to PAN structural transformations is incorrect and actually arises from DMF incorporated into the PAN films.

This study was the first to use Raman spectroscopy to investigate the electrografting of PAN films and revealed new, previously unreported Raman peaks at 1096, 1520 and 1580 cm^{-1}, which are attributed to the formation of a ladder type network of vertically stacked polymer chains connected by azine bridges.

Promising results from the experimental trials using a series of vinyl monomer derivatives have revealed the potential of the nitrile moiety as a useful electrografting engine to introduce more reactive functional moieties (protected by THP) into the polymeric macrostructure. However, further work is necessary to fully characterise the electropolymer and to investigate the in-plane and out-of-plane attachment after deprotection.

Acknowledgements

I would like to thank Professor Martin Taylor, my supervisor for his constant support, suggestions and unwavering belief in my capability during this research work.

During the time spent in the department I have had the pleasure of meeting and working with a number inspirational people, I thank them for their generosity: Catalina, Ignacio, David, Hmoud, Brynmor, to name a few. I would also like to say a special thank you to Janet who has been such a good friend and colleague during the completion of this study, sharing many an entertaining moment. I apologise for anyone I have left off the list. It has been quite a journey.

I would sincerely like to thank the following for their support; John Cambridge for his technical knowledge and expertise during the Raman /AFM work, Iwan Jones for the Teflon fittings cell design, Gwyn Williams for technical expertise, Wendy Halstead for admin, John Charles Chemistry for glass blowing and electrode work David Lacey and Kirsty Rump for the supply of the monomers (including measuring water content) and ellipsometry measurements and I would also like to pay heartfelt respects to the late John Tame for all his support.

And lastly and most importantly to my family and friends, my father who insisted I finish with a twinkle in his eye I thank him for all his love, my children Sion and Gavin who have been a constant source of support and encouragement throughout, my good friend Fiona, my mother and sister for their nurturing words of wisdom and my brothers Geoff, Nigel and Andy for their teasing and of course my sheepdogs for their healthy outdoor distraction.

Contents:

Chapter 1: Introduction

1.1 Introduction to Electrografting

A traditional industrial engineer will take a slab of metal and machine away vast quantities of metal 'swarf' in a top down process to create the intricate parts of a machine. Nanotechnology on the other hand offers the modern engineer a bottom up process whereby simple devices can be assembled at a molecular level. Electrografting is just such one of these techniques. The interested entrepreneur can, given the right conditions initiate a chemical bond at a metal/molecule interface and then carefully grow a functional surface molecule by molecule. If this is to be a viable technique for industry the ability to control this molecule assembly line is essential if well-defined functional surfaces are to be achieved.

Surface functionalization of polymer films prepared on a variety of substrates has potential applications in a wide range of demanding fields: electronics, catalysis, biotechnology, space etc. The modification of metallic surfaces using a polymer coating to confer certain properties e.g. optical, adhesive, electrical, friction etc. has attracted much interest. Electropolymerization is an attractive technique offering potential control of the electrochemical conditions with the prospect of producing polymer films of a predictable, well-defined composition and thickness. Early developments and successes in this technique were mainly due to the adoption of the anodic process for film deposition by Tourillon et al (Deniau 1992a). The restrictive conditions demanded by the cathodic process have been a serious hindrance to its development as an established technique for surface preparation. Various combinations of monomers, solvents and supporting salts were investigated. Aqueous media were considered with the purpose of minimizing cost and impact on the environment. However, organic solvents became the preferred choice with the advantage of suitable working potential windows, ability to dissolve most salts and swell the polymer. Protection of metals against corrosion was one of the main applications driving the research. The main problems encountered were poor coverage, adhesion and chemical stability of the polymer films until the appropriate electrochemical conditions were identified.

In 1975 Dubois et al (Deniau 1992a) using more stringent conditions cathodically electropolymerized a well-defined polyacrylonitrile film on an iron substrate. Initially the polymer deposition was seen as an unwanted side reaction. Then in 1979 Mengoli et al reviewed the electropolymerization as a potential technique for coating metals. The coating could efficiently protect oxidisable metals from corrosion. But the lifetime and adhesion of such coatings was disappointing. The breakthrough came in 1982 when Lecayon et al successfully electrografted a polymer film onto a nickel electrode. The polyacrylonitrile (PAN) film remained attached to the metal even in a good solvent of the polymer. The process involved the electroreduction of the acrylonitrile (AN) in dry acetonitrile (ACN), a solvent of the monomer. Voltammetric scans showed two reduction steps (Figure 1.1). Viel (1990)[1] in his Ph.D. thesis described the first peak (I) at the less cathodic potential as 'a passivation peak' and the second larger peak (II) at the more negative potentials as 'a diffusion peak'. The electrografting reaction appeared to occur between the two peaks. Lecayon proposed an anionic mechanism for the reduction of acrylonitrile independent of the cathodic potential and suggested the grafting process involved the exchange of one electron. The stability of the polymer-metal interface has been attributed to the formation of covalent chemical bonds as confirmed by Deniau et al (1992b) using XPS and UPS studies.

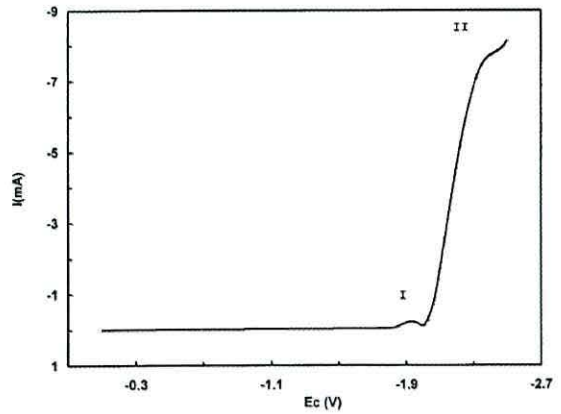

Figure 1.1 *Cathodic response of a 0.1M AN solution in Acetonitrile; TEAP = 0.05M, $v = 20mVs^{-1}$, Baute et al (1998).*

[1] in Mertens et al (1996).

Since the 1980's there has been an increasing interest in the field with the emergence of two separate groups; the laboratories at Centre D'Etudes de Saclay, France and the University of Liege, Belgium, leading the work on the electrografting technique with the aim of producing high quality stable polymer films with a functional purpose for industrial applications.

1.2 Illusive peculiarities

The history of the interpretation of the mechanisms involved in the electrografting of vinyl monomers is riddled with conflicting proposals. So far the experimental observations of the process have escaped a completely satisfactory interpretation. There remain a number of illusive peculiarities. The shape of voltammograms is very sensitive to the initial monomer concentration. The occurrence of a double peak for particular concentration ranges of AN in anhydrous ACN when the system involves only one charge transfer step in the electro reduction of AN is yet to be fully understood. The reason for the comparatively higher concentrations of methacrylonitrile (MAN) in anhydrous ACN required for the occurrence of a similar double peak is not clear either. Bureau et al (1999) compared the voltammograms from the electropolymerization of pure MAN and 0.05M AN/ACN and found smaller current intensities for MAN which is surprising considering the difference in concentrations and given that the surface area of the electrode and the scan rate is the same. Mertens et al (1996) proposed the electrografting of PAN occurs at Peak I as a result of a radical process; the only definite evidence being the existence of a grafted PAN layer at the end of the experiment. Bureau et al (1997) reviewed this proposal and showed that the initiation of PAN in connection with the occurrence of Peak I can only be ionic. Tanguy et al (1996) in an in-situ electrochemical quartz crystal microbalance (EQCM) study observed a significant change in frequency and suggested that the asymmetry of Peak I was due to the sudden blocking of the electrode. Viel et al (1999) showed that under the drastic stirring conditions of a rotating disc electrode (RDE), that the grafted polymer is initiated from the surface and not precipitated from solution. Charlier et al (1999) in the in-situ study of N-vinyl-2-pyrrolidone (NVP) and MAN using complementary frequency and resistance measurements from an EQCM showed much of the frequency changes observed during

electropolymerization were due to viscosity effects arising from polymerization occurring in solution. The delays observed by Tanguy et al (1996) between the voltammetric and EQCM responses were seen as artificial and induced by the zooming of the scale. The detection of a grafted PMAN well before Peak I shows that the peak is not due to passivation. However the subsequent strong variations in equivalent resistance masked any further evidence of the grafting mechanism.

The interpretations of the grafting reaction tend to focus on the double peak regime of the voltammograms since it appears as the most obvious deviation from the standard behaviour and as the monomer is the only electro-reactive species present. The only evidence for Peak I being the 'signature' of the electrografting reaction is the detection of the products of the reaction i.e. the grafted polymer.

Bureau et al (1999) has been able to show by numerical simulations of voltammograms that the peculiar double peak can occur as the result of a homogeneous polymerization in solution coupled to a charge transfer. If the model is correct in its simulation of all the experimental observations it leaves us with a predicament. Most of what appears visible in a voltammogram is accounted for by polymerization occurring in solution. The voltammetric current is a measure of the reaction rate of a charge transfer reaction. If the grafting reaction is comparatively fast compared to the other reaction steps it will not be rate determining. Voltammetry can only detect rate determining steps. The 'experimental footprint' of the grafting reaction will therefore remain illusive. However the coincidence of Peak I and the grafting reaction has proved to be a productive indicator.

Despite the arguments for and against the visibility of the electrografting signature in voltammograms, cyclic voltammetry has provided a method of initiating and monitoring the growth of films. Not knowing the exact potential at which the electrografting occurs has not deterred the production of good quality films. However the electrografting of PAN films has been shown to be sensitive to high negative potentials. Mertens et al (1996) observed the straining and subsequent debonding of electrografted PAN films at high potentials.

The electrografting technique is a specialized form of electropolymerization. The technique imparts a strong chemical bond between the metal and monomer during the

initiation of the electropolymerization. Different forms of polymer (acrylonitrile) /metal interaction can be achieved using electrografting. As mentioned earlier Lecayon et al (1982) have shown that when the electrode acts as a cathode it behaves as a basic initiator for anionic polymerization through a 1,4 Michael type addition from the metal surface to the vinylic carbons of the acrylonitrile molecule to form a polymeric structure. Whereas Bureau et al (1996) have shown that when the metal surface is used as an anode, it acts as a Lewis acid towards a methacrylonitrile (MAN) molecule resulting in a 1-2 nucleophilic addition on the nitrile group forming a conjugated polymeric structure. Therefore by changing the nature of the electropolymerization then, potentially at least, different macroscopic structures can be chemically bonded to a metal surface.

Mills et al (2000) using a simple three electrode setup and a two-step technique (adapted by Taylor et al, 1991 for the electropolymerization of poly-3-methylthiophene) successfully managed to electropolymerize a range of monomers; acrylonitrile, acrylic acid and 2-cyanoprop-1-en-ol using both polarities. This work formed the basis of the present study; an investigation into the design and construction of functionalized macrostructures using electrografting.

1.3 Aim of the study

The aim of the work was to develop the electrografting technique to produce functionalized polymeric macrostructures or command surfaces, for a range of potential applications. Command surfaces containing functional groups at the surface could provide grafting sites for active moieties such as sensor units, NLO chromophores etc. The selective grafting nature of different metals could offer control over structures for device configurations for novel arrays. The debonding process also has potential to produce well defined free-standing films of a desired tactic nature.

This study set out to explore what type of monomer undergoes electrografting, how the structure is built from the surface, what factors affect the growth of the structure from the metal surface and which metals initiate electrografting. Using a standard 3-electrode cell connected to a potentiostat the optimum growth conditions for cathodic/ anodic electrografting were investigated. The effect of changing growth conditions was monitored by investigating the resulting film morphology and chemical structure.

The above aim was achieved by focusing on the following objectives:

- establish the fundamental features and limitations of the electrografting technique
- electropolymerize in a systematic way a range of monomers under cathodic/anodic conditions on a number of different metal substrates
- investigate the resulting polymer structures and relate it to the growth conditions
- investigate the 'debonding' process
- develop the technique for the preparation of quality well defined macrostructures for academic / industrial use.

1.4 References

Bureau, C., Deniau, G., Valin, F., Buittet, M. J., Lécayon, G., Delhalle, J., *Surf. Sci.,* **355,** (1996), 4910.

Bureau, C., Deniau, G., Viel, P. and Lécayon, G., *Macromolecules,* **30**, (1997), 333.

Bureau, C., *J. Electroanal. Chem.,* **479**, (1999), 43.

Charlier, J., Bureau, C. and Lécayon, G., *J. Electroanal. Chem.,* **465**, (1999), 200.

Deniau, G., Lécayon, G. and Viel, P. *Langmuir*, **8**, (1992a), 267.

Deniau, G., Viel, P. and Lécayon, G. *Surf.Interface Anal.*, **18**, (1992b), 443.

Lécayon, G., Bouziem, Y., Le Gressus, C., Reynaud, C., Boiziau, C. and Juret, C., *Chem. Phys. Lett.*, **91** (1982), 506.

Lécayon, G., Viel, P., Le Gressus, C. and Boiziau, C., *Scanning Electron Microscopy*, **1**, (1987), 85.

Mengoli, G., *Adv. Polym. Sci.,* **33**, (1979),2

Mertens, M., Calberg, C., Martinot, L. and Jérôme, R., *Macromolecules,* **29**, (1996), 4910.

Mills, C.A., Lacey, D., Stevenson, G. and Taylor, D.M., *J. Mater. Chem.,* **10**, (2000), 1551.

Tanguy, J., Deniau, G., Zalczer, G. and Lécayon, G., *J. Electroanal. Chem.,* **417**, (1996), 175.

Viel, P., Bureau, C., Deniau, G., Zalczer, G. and Lécayon, G., *J. Electroanal. Chem.,* **470**, (1999), 14.

Chapter 2: Literature Review

2.1 Introduction

This review traces the development of the electrografting technique from its discovery in 1982 to the present day in an attempt to extract the intimate mechanisms from a lengthy debate lasting over 20 years. To date only a handful of organic species have been successfully grown. For progress in this field to continue the investigation must be broadened to encompass more functional monomers. Alternative supporting environments must be explored in order to establish optimum propagation for the selected species and its proposed application. All of the work included in the review has used the same experimental set-up. Adhering to strict guidelines regarding purity and dryness of experimental conditions has been shown by successive methods to be essential for the effective grafting of a polymer. The review explores the main factors controlling the kinetics of the electrografting process. Voltammetric techniques were employed to study the electron transfer kinetics during electrografting so, before taking the reader on an historical review of the technique, a brief introduction on cyclic voltammetry is appropriate.

Cyclic voltammetry is a standard electroanalytical technique generally used by electrochemists to acquire both qualitative and quantitative information about electrochemical reactions; electrode mechanisms and their kinetic parameters. It is an active method whereby the experimenter drives the electrochemical reaction by incorporating the chemistry into a circuit and then controlling the reaction by circuit parameters such as the voltage. It is often the preferred electroanalytical method for providing a fast and convenient evaluation of any changes to the chemistry. It is assumed the reader has a basic understanding of electrochemistry; electrolysis, electron transfer, mass transfer etc. and are referred to *Instrumental Methods in Electrochemistry* produced by the *Southhampton Electrochemistry Group (2001)* for background text.

2.2 Cyclic voltammetry

Cyclic voltammetry involves cycling the potential of a stationary electrode immersed in a quiescent solution containing a redox couple and measuring the resulting current (see Figure 2.1). The potential scan normally follows a triangular waveform in which the scan rates can range from a few millivolts per second to hundreds of volts per second. During a cycle the potential of the working electrode is swept back and forth between two switching potentials. This has the advantage that the product of the electron transfer reaction that occurred in the forward scan can be probed again in the reverse scan. Thus, a negative potential scan is chosen for the first half cycle during which a cathodic current is observed. Because the solution is quiescent, the product generated during the forward scan is available at the surface of the electrode for the reverse scan resulting in an anodic current. One complete cycle produces a complete voltammogram with cathodic (reduction) and anodic (oxidation) asymmetrical waveforms as shown in Figure 2.2. The current at the stationary working electrode is measured under diffusion-controlled, mass-transfer conditions. The potential scan is usually terminated after one cycle but certain applications can require repeated cycles. The scan rates and switching potentials can easily be varied.

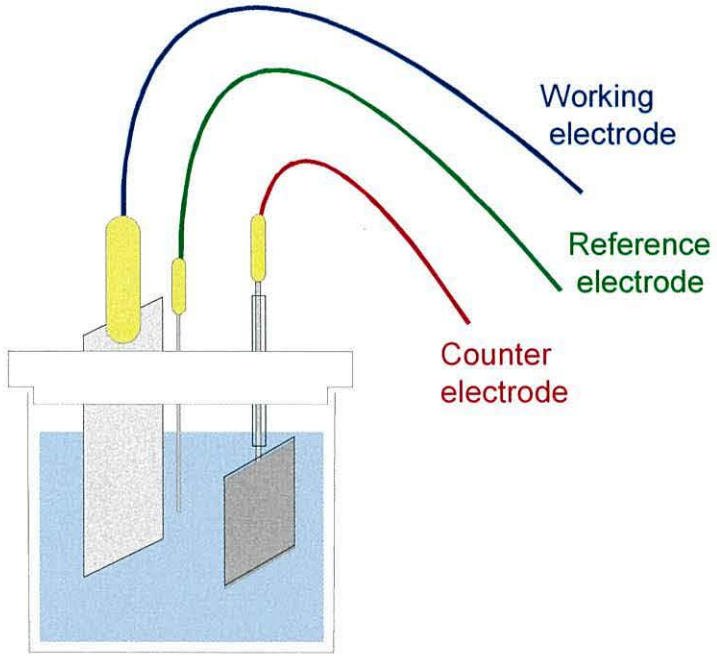

Figure 2.1 *A diagram of a simple electrochemical cell*

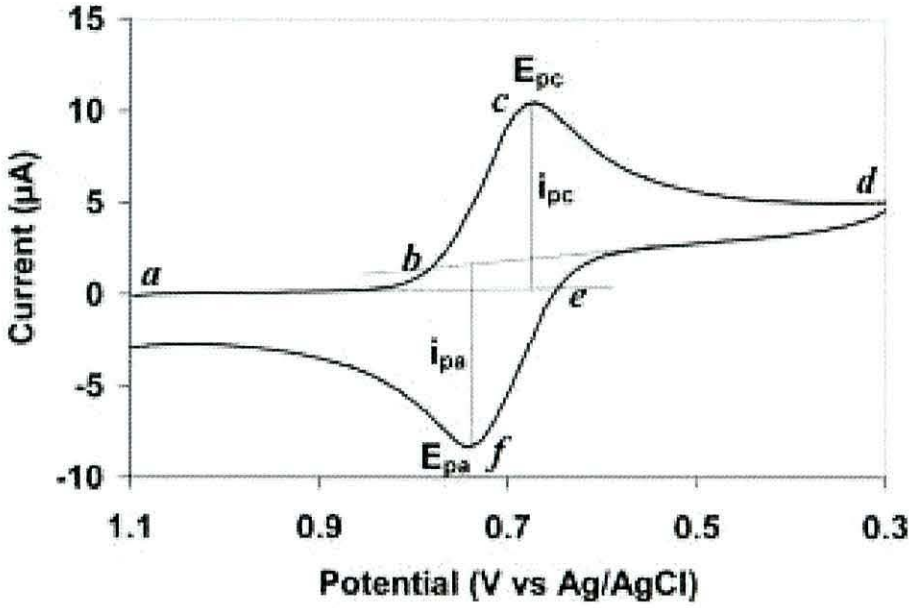

Figure 2.2 *Cyclic voltammogram for a reversible process.*

The cyclic process illustrated in Figure 2.2. is explained as follows. At the start of the experiment, the bulk solution contains only the oxidised form of the redox couple (O) so that at potentials lower than the redox potential, i.e. the initial potential, there is no net conversion of O into R, the reduced form (point *a*). The potential is then scanned in a negative direction. As the redox potential is approached there is a net cathodic current (point *b*) which increases exponentially with potential. As O is converted into R, concentration gradients are set up for both O and R, and diffusion occurs down these concentration gradients. At the cathodic peak (point *c*), the redox potential is sufficiently negative that any O that reaches the electrode surface is instantaneously reduced to R. Therefore, the current now depends upon the rate of mass transfer to the electrode surface and decays as $(\text{time})^{-1/2}$ according to the Cottrell equation (Willard et al, 1988), resulting in an asymmetric peak shape. The final rise at *d* is caused by the discharge of the supporting electrolyte. Upon reversal of the scan (point *d*), the current continues to decay with a $(\text{time})^{-1/2}$ until the potential nears the redox potential. At this point, a net oxidation of R to O occurs which causes an anodic current which eventually produces a peak shaped response (point *f*). The anodic current then decays as the concentration of R formed from the forward scan is depleted.

The important parameters in a cyclic voltammogram are the magnitudes of the anodic peak current $(i_p)_a$, the cathodic peak current $(i_p)_c$, the anodic peak potential $(E_p)_a$, the cathodic peak potential $(E_p)_c$ and the half peak potential $(E_{p/2})_c$. The separation between the peak potentials $((E_p)_a - (E_p)_c)$ provides information on the reversibility of the reaction.

2.2.1 Reversible and irreversible reactions

The form of the cyclic voltammogram can be determined mathematically by solving Fick's second law of diffusion with the appropriate initial and boundary conditions. Fick's second law predicts the rate of diffusion in a solution of constant viscosity

$$\frac{\partial[c]}{\partial t} = D\left(\frac{\partial^2[c]}{\partial x^2}\right) \tag{2.1}$$

where D is the proportionality constant known as the diffusion coefficient, $[c]$ the analyte concentration, x the direction normal to the electrode and t time.

In the absence of an applied voltage and indeed under a constant voltage, equation (2.1) is readily solved. However application of a time dependent potential increases the complexity of the solution. Nevertheless, for planar diffusion it can be shown that the peak current density i_p, is directly proportional to the analyte concentration, c, as described by the Randles-Sevcik equation:

$$i_p = -0.4463nFAc\left(nFvD/RT\right)^{1/2}. \tag{2.2}$$

In this equation, n is the number of electrons appearing in a half-reaction of the redox couple, v is the rate at which the potential is swept (V/s), F is Faraday's constant (96485 C/mol), A is the electrode area (cm^2), R is the universal gas constant (8.314 J / mol K), T is the absolute temperature (K), and D is the diffusion coefficient (cm^2/s). Note that if the temperature is assumed to be 25°C (298.15 K), the Randles-Sevcik equation can be re-written in a more concise form namely

$$i_p = -(2.687x10^5)n^{3/2}v^{1/2}D^{1/2}Ac \qquad (2.3)$$

where the numerical constant is understood to have units of C mol^{-1} $V^{-1/2}$. For a reversible wave, the peak potential (E_p) is independent of the scan rate, and i_p as well as any other point on the wave is proportional the square root of the scan rate. A convenient normalized current function is $i_p/v^{1/2}C$, which depends on $n^{3/2}$ and $D^{1/2}$. For a simple diffusion controlled reaction, this current function is a constant independent of the scan rate. This constant can be used to estimate n for an electrode reaction if a value of D can be estimated. The number of electrons transferred in the electrode reaction can be determined from the separation between the peak potentials i.e.

$$(E_p)_a - (E_p)_c = 0.057/n \,. \qquad (2.4)$$

This is valid when the switching potential is at least 100/n mV past the cathodic peak potential. The formal potential for a reversible couple is centred between the peak potentials. Electrochemical quasi-reversibility is characterized by a separation of peak potentials greater than the value indicated by the above equation and irreversibility by the disappearance of the reverse peak. On the reverse scan the position of the peak depends on the switching potentials. In the case of a reversible system the electron transfer rates at all potentials are significantly greater than the rate of mass transport, so Nernstian equilibrium is always maintained at the electrode surface. If the electron transfer rate is insufficient to maintain this equilibrium, then the shape of the cyclic voltammogram changes. At low potential sweep rates the rate of electron transfer is greater than that of mass transfer, and a reversible cyclic voltammogram is recorded. As the sweep rate is increased, the mass transport increases and becomes comparable to the rate of the electron transfer. This has the effect of increasing the peak separation and reducing the peak height. In the limit for a totally irreversible process, the shape of the cyclic voltammogram is given by a different solution to Fick's second law of diffusion i.e.

$$i_p = -(2.99x10^5)n(\alpha_c n_\alpha)^{1/2}v^{1/2}D^{1/2}Ac \qquad (2.5)$$

where n_α is the number of electrons transferred up to and including the rate determining step. The half peak width (E_p- $E_{p/2}$) for an irreversible case is given by:

$$\left(E_p - E_{p/2}\right) = 47.7/(\alpha_c n_\alpha) \qquad \text{mV at } 25^\circ\text{C} \qquad (2.6)$$

2.3 The two peak regime

Lecayon et al (1982) were the first to report the two peak regime (Figure 1.1) and the electrografting of PAN films on nickel electrodes using cathodic polymerization. The success was attributed to the use of an aprotic organic medium, relatively high monomer concentrations and a metal electrode whose surface oxide was removed electrochemically. The purpose behind such conditions was to produce pure homogeneous films of a predictable chemical composition and molecular structure. The majority of workers in this field used the standard three electrode cell set-up composed of a working, reference and counter electrode. The choice of reference was limited due to the necessity for stringent conditions.

2.3.1 A model growing mechanism

Lecayon et al (1982) recognized that the adsorption of a layer of monomer molecules is the first step in the electrografting of a homogeneous film. A model growing mechanism was proposed for film formation (see Figure 2.3). The AN molecule has a large dipole moment, 3.9 D from the nitrile group, and this coupled with a vinyl bond gives it a conjugated structure (delocalized π electrons). The molecule will orientate easily in an electric field aligning the dipole moment perpendicular to the electrode. The double layer at the electrode has an electric field strength of the order of 10^7 V/cm due to the build up of charge of the opposite sign. It was proposed that this field strength was strong enough to influence the electronic configuration of the molecule, transferring the π electrons towards the nitrile group and resulting in the opening of the vinyl bond. If the energy levels are favourable the ionic-type molecule will then participate in an electron transfer to form a metal / AN bond. One electron too many on the CHCN group will then allow the electronic doublet to interact with an available polarized monomer in a Michael

type addition – polymerization. Energy levels must be compatible for the metal/ AN bond to occur. The electric field will broaden and lower the ionization energies of the metal substrate. Lecayon et al (1987) compared different metal electrodes and attributed the success of electrografting on nickel and not on aluminium to the difference in the energy levels of their oxidized states.

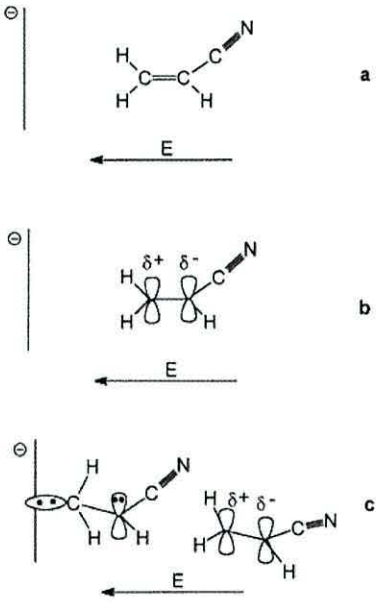

Figure 2.3 *Molecular model for the acrylonitrile/metal interaction in the cathode double layer according to Lecayon et al (1987): a) orientation of monomer, b) monomer is polarized and c) formation of chemisorbed radical anion which can initiate the propagation of an anionic polymerization.*

Lecayon et al (1987) proposed the occurrence of two phenomena a) a reduction process and the formation of a radical anion as a result of a direct electron transfer from the cathode to monomer to account for the electrolytic current and b) a secondary reaction in which the simultaneous grafting of a polymer film onto the metal occurs. The electrode potential was adjusted to initiate the polymerization reaction.

Cyclic voltammograms of solutions containing 0.5M AN in ACN and 0.05M tetraethyl ammonium perchlorate (TEAP) showed two reduction peaks. At the lower negative potential an 'inhibition' peak so called by Lecayon et al due to its shape and low current intensity consistent with an irreversible change on the electrode, and at a higher negative potential a diffusion controlled peak, the current intensity of which is much

higher and increases with an increase in monomer concentration. It is at the first peak that the electrografting of well-adhered films is thought to occur. In contrast, thicker yellow films formed at the second peak could easily be removed by a known solvent for the polymer. Lecayon proposed a unique mechanism independent of the cathodic potential. The mechanism is described in Section 2.3.2.

2.3.2 Alternative conduction pathways - hopping

High current densities were measured during the electrografting process. The formation of a metal/AN bond followed by the triggering of one polymer chain only involves one electron and the calculations of the limited number of possible sites could not account for these values alone. Also considering that the development of a dense polymer layer may prevent further access to the electrode surface Lecayon et al (1987) speculated on alternative conduction pathways. As the polymer backbone was saturated and structural transformations usually seen after extensive heat treatment were not possible considering the conditions, the involvement of nitrile groups was suggested to explain the electrical conduction. In the model, electrons were assumed to hop from site to site facilitated by the orientation of the dipoles in the electric field. The decrease in current observed after the curve maximum followed by a sharp rise was thought to correspond to the change from Faradaic to the suggested hopping behaviour. The mathematical model devised by Bureau et al (1999) however shows that the voltammograms are as a result of a Radical-to-Radical Coupling initiated polymerization linked to an irreversible charge transfer from the electrode. Whether a polymer grows from the surface or in solution both processes are electroinitiated at the surface. So the charge injected into the solution is unlikely to give the yield for the grafting process.

2.4 Radical mechanism?

Jérôme et al (1995) repeated the work of Lecayon et al, in particular work investigating the effect that replacing the supporting solvent had on the electrografting reaction. PAN is insoluble in ACN yet soluble in *N, N*-dimethylformamide (DMF). Homogeneous well defined PAN films electrografted in DMF at peak I was seen as good evidence of electrografting. No film was observed at peak II in DMF. The films formed

at peak II in ACN were rapidly dissolved in DMF. The current density dependency on the scan rate was investigated and it was concluded that Peak I did not fit a classical electrochemical model, either Faradaic or capacitive. In contrast, Peak II followed a Faradaic diffusion process involving a one electron transfer. Jérôme et al (1995) proposed that AN polymerization occurred at the two different potentials by two distinct mechanisms and that the electrografting mechanism occurred at Peak I.

2.4.1 Radical probe

In an attempt to validate this proposal tests were carried out to identify the active species involved in Peak I and Peak II. The radical probe molecule, 2,2-di-(4-t-octylphenyl)-1-picrylhydrazyl (DPPH) was added to the electrolyte. The immediate disappearance of DPPH's violet colour near the electrode during a scan of Peak I was seen as evidence of grafted AN radical species which propagates the proposed radical polymerization. In contrast a scan of Peak II shows no immediate colour change in the vicinity of the electrode which supports the formation of radical anions. No grafting occurs and the radical anion dimerizes in solution to form a dianionic species which reacts with further AN molecules propagating the anionic polymerization.

Mertens et al (1996) studied the electroreduction of AN and supported the proposal that electrografting of PAN occurs at Peak I as a result of a radical process. Experiments involving voltammetry, chronoamperometry, chronopotentiometry and various spectroscopic methods; secondary ion mass spectroscopy (SIMS), x-ray photoelectron spectroscopy (XPS), Fourier transform infrared (FTIR) spectroscopy, scanning electron microscopy (SEM) and atomic force microscopy (AFM) were all used to gain insight into the electrografting mechanism. In particular the investigation was directed at identifying the potential at which the electrografting occurred and whether a radical or anionic mechanism was involved. The study confirmed the essential requirements of astringent conditions and the electrochemical reduction of the metal oxide. PAN films formed at Peak I were confirmed using FTIR (see Figure 2.4).

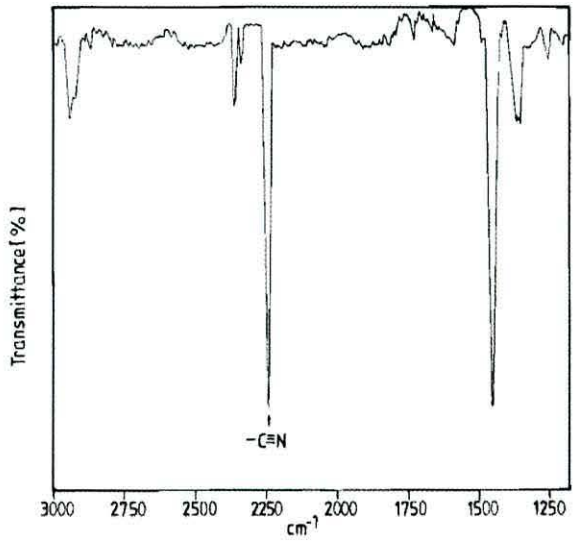

Figure 2.4 *IR spectrum of a PAN film grafted onto nickel, in a TEAP (0.05M) solution in ACN, [AN] = 1M, (Mertens et al, 1996).*

Voltammograms of the electroreduction of AN in ACN / TEAP (0.05M) showed the two peak regimes to be dependent on the monomer concentration in quite separate ways. For Peak I the current intensity decreases and shifts to more positive potentials as the monomer increases (see Figure 2.5) in contrast to Peak II intensity which increases and shifts to more negative potentials.

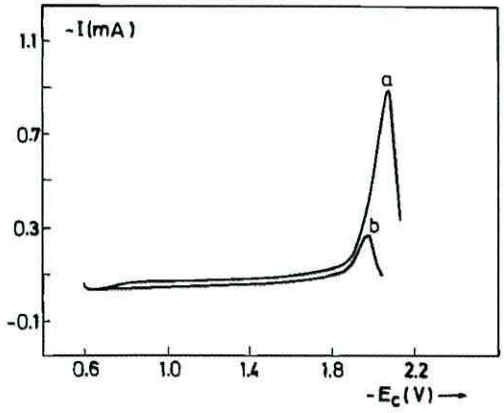

Figure 2.5 *Voltammograms showing Peak I dependency on monomer concentration for TEAP (0.05M) solution in ACN on nickel; (a) [AN] =0.1M, (b) [AN] =0.5M, (Mertens et al, 1996).*

The two peaks are only evident for monomer concentrations between 10^{-2} M and 2M. Viel (1990)[1] in his Ph.D thesis interpreted the peak disappearance at lower monomer concentrations to be an overlap of the two peaks. Mertens et al concluded that the kinetics

[1] in Mertens et al (1996)

of the polymerization of AN was controlled by the monomer concentration. They explained that higher concentrations increased the availability of the monomer at the surface thereby reducing the time to form an insulating PAN layer and consequently reducing the intensity of Peak I.

To calculate the density D, of grafted chains, Mertens et al (1996) used the equation for a Faradaic reaction i.e.

$$D = \frac{IN}{FSn} \tag{2.7}$$

where I is the current associated with the reduction peak, F is the Faraday constant, N is Advogadro's number, S is the actual surface area and n is the number of electrons involved.

For Peak I, D was estimated to be ~ 0.2 chain/Å^2 assuming a purely Faradaic reaction and that more than one electron was involved in the reduction of each AN monomer. Mertens et al found this value to be 4 times larger than a value obtained by Favis et al (1983) for the stacking of stearic acid perpendicular to an air water interface and rationalized if more than one electron is involved in the electrografting process a more reasonable value would be obtained. Early work by Langmuir et al (1917) on monolayer films of fatty acids with different chain lengths, oriented with the polar functional group immersed in the water and the long non-polar acyl chain directed nearly vertically up from the interface were shown to occupy molecular areas of ~ 20 Å^2, giving a value of 0.05 chain/Å^2. Much higher values of D were estimated from Peak II suggesting that grafting was unlikely to be occurring at the higher potential.

Chronoamperometry and chronopotentiometry experiments were carried out to try and identify the potential at which the electrografting occurred. Chronoamperometry results showed that for a potential beyond Peak I the curve shows two effects. After the initial transient a decrease in current occurred followed by an increase in current showing a linear dependence on the square root of the pulse duration. The former was interpreted to be an auto-inhibition phenomenon and the latter a nucleation reaction with a constant number of active sites. Chronopotentiometry results revealed a 'superpolarisation'

characteristic which was compared to the behaviour seen in the nucleation of metal deposition. The film formed at Peak I was thin and colourless but changed to a thicker yellow deposit when the potential was increased. SEM images of a film formed at Peak II showed 'cauliflower aspects' to the structure (see Figure 2.6).

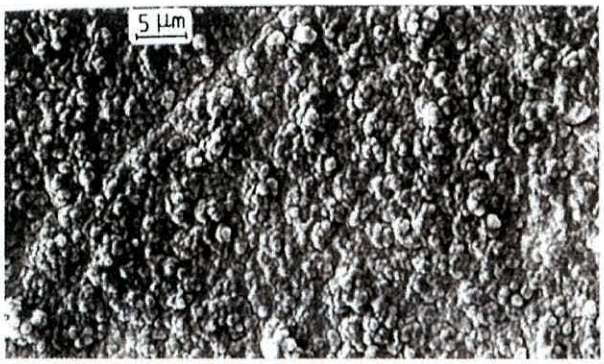

Figure 2.6 *Scanning electron micrograph of PAN film deposited on Nickel in a 0.05M TEAP solution in ACN at potentials between Peaks I and II, (Mertens et al, 1996).*

Mertens et al suggested that the film formed at peak I is strained at higher potentials developing defects in the film which allows the reaction associated with Peak II to occur. They proposed that the films produced at the different potentials/peaks were due to different mechanisms and their findings supported this conclusion. The thicker yellow films formed at Peak II were found to be soluble in dry DMF. Based on the work of Funt et al (1964) on the electropolymerization of PAN by an anionic mechanism (Figure 2.7), Mertens et al speculated that the yellow colouration was the result of nitrile attack, as films electropolymerized at -30°C showed no such colour.

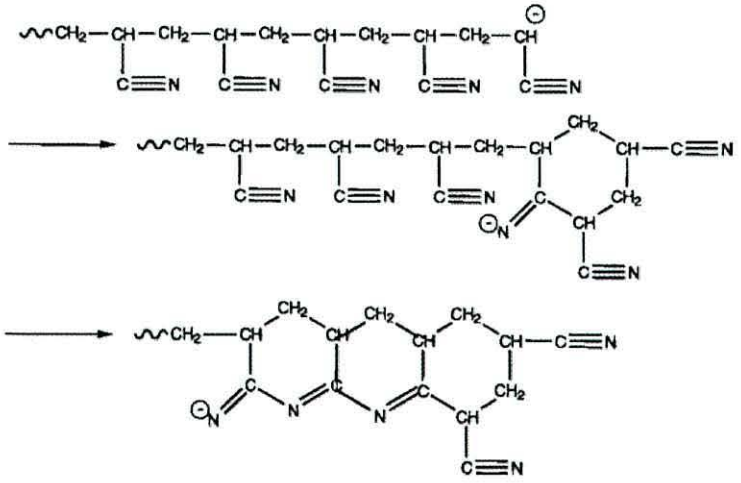

Figure 2.7 *Anionic mechanism as reported by Funt et al (1964).*

Mertens et al (1996) concluded that the electrografting reaction was irreversible since no peak was observed on the reverse scan. The peak current did not scale with the square root of the scanning rate, suggesting that the process was not Faradaic in nature. However in differential pulse polarographic measurements, the peak height was proportional to pulse height suggesting it was Faradaic.

Equation (2.6) for the irreversible reaction of an insoluble product (Bard and Faulkner, 1980) was used to estimate the number of electrons involved. On the premise that one electron gave a reasonable answer, Mertens et al (1996) proposed the formation of radicals at the cathode. However, the supporting requirement that the 'oxidation at the anode does not create or consume any charged species' does not make any electrochemical sense.

2.4.2 Radical & anionic probes

Further to the work carried out by Jérôme et al (1995) using the radical probe DPPH to identify the active species involved in the electrografting process, Mertens et al (1996) continued the investigation into the chemical influence on Peak I, now considered the signature of the electrografting reaction. An increase in the concentration of DPPH resulted in both a decrease in the intensity of Peak I and the thickness of the resulting PAN films. Addition of DPPH was also observed to increase the passivation efficiency, which was measured by comparing the first and second scans. SIMS signals confirming the presence of DPPH was taken as evidence for the presence of radicals, the premature terminating of the polymerization by DPPH accounting for the decreases in efficiency and film thickness. The loss of violet colour near the electrode confirmed the involvement of DPPH. To complete the argument, the anionic probe ε-caprolactone (ε-Cl) known for its selective ionic ring opening reaction was used to rule out the involvement of anions in the process. Addition of ε-Cl to the electrolyte had no effect on the intensity of Peak I or on the resulting SIMS and FTIR data.

For comparison Mertens et al (1996) studied the reduction of AN on zinc. Only one peak was observed in the voltammogram irrespective of the monomer concentration see Figure 2.8.

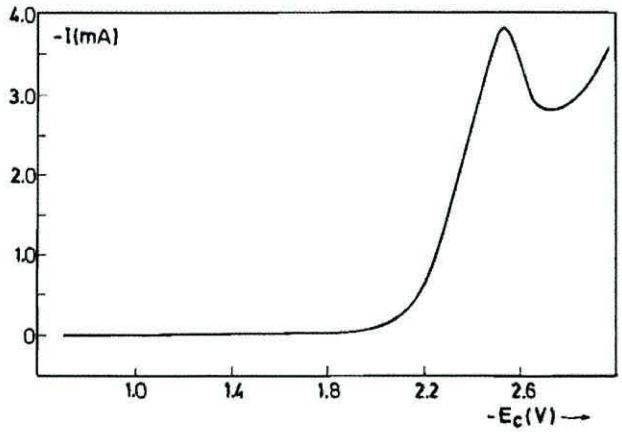

Figure 2.8 *Voltammetry of AN on zinc in a 0.05M TEAP solution in ACN. AN = 0.5M, v = 20mVs^{-1} (Mertens et al,1996).*

The behaviour of the peak intensity is comparable to that of Peak II i.e. peak intensity proportional to both the square root of the scan rate and monomer concentration. Differential pulse polarographic measurements confirmed the reaction to be Faradaic. Similar voltammograms were recorded irrespective of whether ACN or DMF was used. ε-Cl was added to the electrolyte to probe the nature of the active species involved. FTIR and proton nuclear magnetic resonance (^{1}H NMR) spectra confirmed the presence of ε-Cl in the yellowish PAN precipitate extracted from the electrolyte. The electropolymerized PAN had been repeatedly precipitated before analysis in toluene, a solvent for ε-Cl,but a non-solvent for PAN. The IR spectra of the precipitate were compared to the spectrum of a mixture of preformed PAN and poly(ε-Cl). The existence of an IR absorption at 1725cm^{-1} found only in the spectrum of the precipitate confirmed the copolymerization of ε-Cl and PAN.

As a result of their experimental findings Mertens et al revised the reaction scheme (Figure 2.3) of Lecayon et al. They proposed that Peak I was the result of a one electron partial reduction of AN to form a radical species grafted on to the electrode (Figure 2.9).

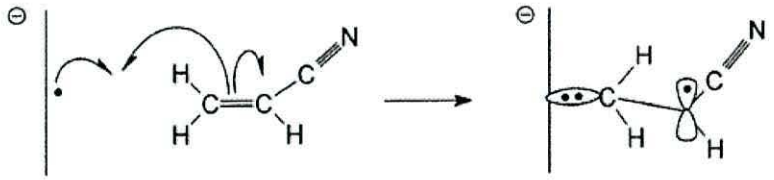

Figure 2.9 *Mechanism proposed by Mertens et al (1996) for the electrografting reaction of AN at Peak I.*

The unusual electrochemical signature, the lack of film colour typical of free radical polymerized PAN and the limited thickness of the electrografted films as a result of rapid termination of the growing radicals gave validity to the proposal. On the other hand, Peak II results from the reduction of AN according to a Faradaic process involving one electron to form a radical anion which quickly forms a dimer by radical coupling (Figure 2.10). This dianionic species then propagates the polymerization of PAN in solution. Bhadani et al (1992) had previously proposed such a scheme for the cathodic electropolymerization of PAN.

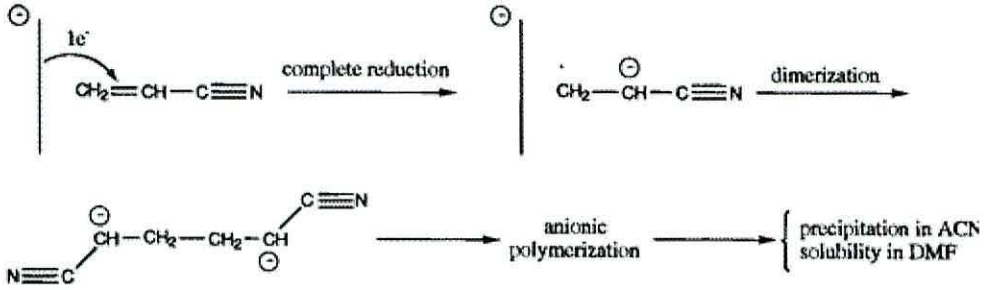

Figure 2.10 *Anionic polymerization of PAN in solution, (Bhadani et al, 1992).*

Mertens et al also proposed that the yellow colour of the precipitate PAN films deposited on electrodes at higher potentials was due to the interaction of the nitrile groups (Figure 2.7) as seen in anionic polymerization where secondary nucleophilic attack of the nitrile group occurs (Funt et al, 1964).

2.5 Anionic mechanism

Bureau et al (1997) reviewed the findings of Mertens et al (1996), challenging the assumptions and the evidence for the radical mechanism. The use of equation (2.6) for an irreversible electrochemical reaction was questioned. While agreeing that the electron transfer and subsequent polymerization was irreversible Bureau et al challenged the

assumed irreversible nature of the electron transfer step evident in the voltammogram. Lewis structures were used to identify charge transfers and to demonstrate that the electronic configurations for the formation of a surface radical were not feasible.

The results and conclusions relevant to Peak I may be summarized as follows. Lecayon et al proposed a unique mechanism for the reduction of AN even though two distinct peaks are observed. Bureau et al (1997) explained that the multiple peak response seen in voltammograms can be the result of a single organic molecule involved in adsorption phenomena. The authors referred to Wopschall and Shain (1967) to explain the shift in Peak I to a lower potential. Bureau et al speculated that the existence of pre and post peaks maybe due to the dynamic interplay between the kinetics of adsorption and diffusion. Voltammograms give information on the rate limiting step only. Mertens et al (1996) studied the effect DPPH and ε-Cl had on Peak I. Bureau et al questioned the deduction that the effect of DPPH on the peak intensity was evidence of a radical reaction, as the results only give information on whether the chemical is involved in the rate determining step. The thoroughness of the investigation was also queried, as the DPPH is known to readily poison surfaces and suggested thorough rinsing and surface analysis. With respect to ε-Cl, no change in Peak I response does not necessarily eliminate ε-Cl involvement only that it is not involved in the rate determining step. The Peak I response may be due to a number of reasons; the blocking of the electrode as a result of the surface being covered by electro-inactive molecules, the exhaustive reduction of available electro-active species or a change in relevant competition between the kinetic steps. Bureau et al demonstrated using Lewis structures that an anionic mechanism is the only feasible mechanism capable of accounting for all the results. The adsorbed electroactive molecule is reduced by the transfer of one electron to form an anionic species. Bureau et al (1998) explained the monomer always has to chemisorb onto the surface to accept an electron. There is only one type of charge transfer between the surface and that the monomer. It is only the relaxation process of the reduced monomer after the transfer of charge that can vary.

2.6 Adsorption

Peak I is not necessarily the result of surface passivation as assumed by Mertens et al. According to Wopshall and Shain a reduction current can start at a more positive potential because the adsorption of a molecule can lower the activation energy for the transfer of electrons. If the negative potential is then increased the number of molecules reduced will be driven to increase as will the reduction current. This current will then continue to increase as long as the reduced molecules can desorb in time to allow for further molecules to be reduced. The current will reach a maximum where desorption cannot keep up and it will then start to decrease. Whether the lifetime of the adsorbed species is infinite leading to passivation, or non-infinite with the current being controlled by the adsorption/desorption process, both processes can give rise to a current pre-peak. Peak I was also observed to change with increasing scan rate. This can be explained by considering the competition between adsorption and electron transfer which may vary with the scan rate. Bureau et al refers to the Semi-integral Voltammetry results (Bernard et al, 1997) which reveal absorption phenomena even for low monomer concentrations.

Tanguy et al (1994) also compared Peak I to an absorption peak and referred to the work by Wopschall and Shain's on modelling the effect that adsorption has on the cyclic voltammetric peak for a reversible electrochemical reaction. However the model does not account for the irreversibility of the monomer reduction.

2.7 Electrografting or crosslinking?

Forming a polymer film on an electrode from a solution containing a solvent for the polymer is seen as definitive evidence of electrografting. However a polymer will precipitate onto an electrode if it becomes insoluble as a result of cross-linking. A number of studies have investigated this possibility.

Jérôme et al (1995) compared the reduction of AN to the oxidation of N-vinylpyrrolidone (NVP) on a platinum anode. In the electropolymerization of NVP only one peak is observed in the voltammogram and polarographic measurements indicate a one electron transfer which Jérôme et al proposed to be the formation of a radical cation. For monomer concentrations < 0.5M no polymerization was evident and the peak intensity increased with monomer concentration. However above 0.5M a polymer film of

poly-n-vinylpyrrolidone (PNVP) film formed at the electrode and the peak intensity was independent of monomer concentration. The formation of PNVP, on the electrode in ACN, a solvent for the polymer, would indicate grafting unless cross-linking could account for the insolubility. The authors considered the possibility of the ionization of the pyrrolidone group triggering the PNVP insolubility through inter and intramolecular interactions. However TOF-SIMS experiments performed on similar films (Doneux, 1998) show that the grafted polymer was not cross-linked. PNVP is a so-called bench mark polymer since it only grafts.

In situ EQCM study of MAN and NVP (Charlier et al, 1999) showed from calculated mass changes on the quartz crystal electrode that the PNVP grows progressively from the surface in a brush type conformation.

A Rotating Disc Electrode spinning at a high rate was used by Viel et al (1999) to test for precipitate formation of poly-methyl-methacrylate (PMAN) during the electrografting process. Homogeneous PMAN films of a reasonable thickness (~20nm) were electrografted despite the extremely effective stirring conditions. This is clear evidence that electrografting started from a strong surface bond.

Palacin et al (2004) draws attention to NEXAFS measurements carried out by Tourillon et al (1990) on very thin electrografted PAN films which show that polymer chains orientate perpendicular to the metal surface with the nitrile groups sticking out parallel to the surface. This provides further evidence for the electrografting process being initiated from the electrode under the influence of an electric field.

Electrografted films firmly adhere to the metal substrate resisting peeling tests and even sonication in a known solvent for the polymer. Chemical bonds between the carbon atoms of an electrografted PMAN and the nickel atoms of the metal electrode were confirmed using XPS and UPS studies by Deniau et al (1992b) (see Figure 2.11).

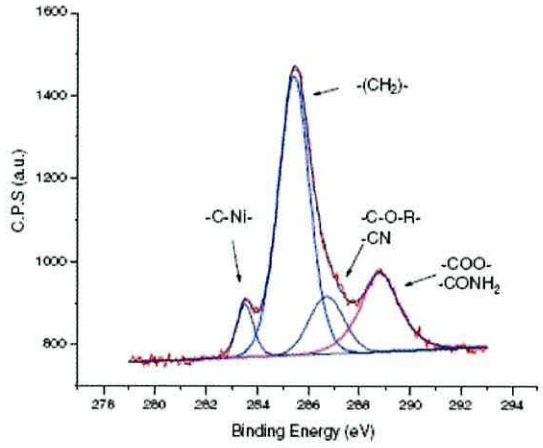

Figure 2.11 *XPS spectra showing the carbon to metal bond for a PMAN film electrografted onto nickel (Deniau et al, 1992b).*

The durability of a grafted polymer coating on a metal was tested by Deniau et al (1997). They coated a steel electrode with an electrografted PAN film (40μm) and subjected it to aerated sea water for 1 month. The results showed a remarkable resistance comparable to coatings of varnish several times thicker (300 μm).

Cross-linking (Figure 2.7) was proposed to account for the insolubility of electropolymerized PAN films prepared by Funt et al (1964). The propagation mechanism was interpreted to be anionic in nature and polarographic measurements were indicative of a direct electron transfer to the vinyl double bond. Current efficiencies of 300% (3 polymer units per electron) were calculated and chain transfer was suggested to account for this. The insoluble PAN precipitate formed on the electrode was noted to be a darker yellow than the soluble polymer. The colour change with insolubility was investigated by electrolyzing a white sample of soluble PAN in DMF saturated with sodium nitrate. The solution turned red and an insoluble polymer formed at the electrode.

Grassie et al (1962) proposed that the PAN's insolubility in DMF was due to cross-linking from the successive combination of the nitrile groups. A sharp absorption peak at 1670 cm^{-1} and a broad weak band centred about 1575 cm^{-1} in the infrared spectra of the insoluble PAN films were assigned to the presence of –C=N- and –(C=N)- chains respectively. Funt et al (1964) proposed that the change in the colour of PAN was catalyzed by an electron and that the insolubility was as a result of intermolecular cyclizations. However DMF is known to have a sharp infrared absorption peak at 1670

cm^{-1}. The thermal analysis of PAN fibres polymerized in DMF reported by Sánchez-Soto et al (2001) show that amide molecules are difficult to eliminate completely, even after prolonged heating at temperatures of 110 °C. Formation of a possible PAN/DMF complex by dipolar bonding was postulated.

2.8 Investigating the influence of molecular structural differences

Deniau et al (1992a) investigated the influence that molecular structural differences have on the electrografting process. The study compared four isomeric derivatives of AN, namely 2-methyl-2-propenenitrile, trans-2-butenenitrile, cis-2-butenenitrile and 3-butenenitrile. The first three are methyl derivatives of AN with the nitrile group directly attached to the vinylic group, while the fourth was included to assess the influence of distancing the nitrile group from the vinyl group. The structural and electronic properties of the isolated monomers were calculated at the *ab initio* level to assist in the interpretation of the results. Molecular orbital calculations, geometrical data, electron density maps, polarizability, the propensity to accept and donate electrons, energies of highest occupied molecular orbitals (HOMO) and lowest unoccupied molecular orbitals (LUMO) were all investigated to assess the ability of the different monomers to react with the cathode and form a stable anion capable of polymerizing with further monomers.

Voltammograms show all four monomers to be electroactive. Peak I was evident for all four monomers, yet only AN and 2-methyl-2-propenenitrile successfully formed electrografted homogeneous films ranging in thickness from 50 nm – 100 nm. Infrared reflection absorption spectroscopy (IRRAS), UPS and XPS spectra confirmed the existence of chemically pure polymer films. The theoretical investigation confirmed the propensity of AN to electrograft yet did not predict the success of 2-methyl-2-propenenitrile, which is also known to be soluble in the supporting solvent ACN, thus providing further evidence of electrografting. The authors recognized the inadequacy of the LUMO model which did not include the subsequent relaxations after electron transfer. Such additional calculations would assess the ability of monomer to accommodate an electron and stabilize. Steric hindrance of the methyl groups in the 2-butenenitriles was proposed to account for the failure of these monomers to polymerize

and there are no reports of the anionic or radical polymerization of these monomers in the literature.

2.9 Quantum chemical calculations

Boiziau et al (1992) compared experimental results with quantum chemistry calculations to assess the likelihood of a monomer electrografting and polymerizing. The experimental work also compared the four isomeric derivatives of AN isomers to assess the dependence of the electrografting process on steric characteristics. The theoretical study then compared the two monomers which were selected for the largest difference in the ability to electrograft. AN producing well defined films was compared to the inactive 3-butenenitrile. The work focused on the role played by the frontier orbital in the grafting and the subsequent polymerization reaction. Electronic isodensity curves of the HOMO and LUMO of the monomers subjected to an electric field were modelled to predict the probability of a reaction between an occupied base orbital of the metal and an empty acid orbital of the monomer to form a covalent bond. The AN showed a high overlapping probability of its LUMO with the valence orbital of the metal compared to the 3-butene nitrile. The probability of polymerization was then assessed by the overlap of the HOMO of the chemisorbed anion and the LUMO of a monomer activated by an electric field. Predictably AN showed a high probability compared to an impossible overlap from the 3-butenenitrile thus reflecting the experimental outcome.

2.10 Thickness of films

Calberg et al (1997) characterised electrografted PAN films using ellipsometry, AFM and X-ray reflectivity. The aim of the work was to explore the factors affecting the thickness and roughness of the films with the purpose of controlling film quality for particular applications. Peak I was again taken as the signature of the electrografting reaction and films were grown at the corresponding potentials. The thickness of PAN films was found to be independent of the technique used be it chronoamperometry, chronocoulometry or voltammetry. Voltammetry was the preferred technique with a repeat scan assessing the inhibition of the electrode. The authors anticipated and confirmed the film thickness dependency on the monomer concentration from the Peak I

response. They proposed that this dependency was evidence of the radical nature of the species grafted to the electrode as the propagation of radical poly-addition is known to be dependent on the monomer concentration. The quality and thickness of the PAN was also found to be strongly dependent on the nature of the solvent i.e. whether it was a good solvent for PAN (DMF) or not (ACN).

ACN produced thinner films than DMF. In ACN the film thickness is dependent on the loss of solubility of the growing chains. At a critical length the chain precipitates onto the electrode hindering further propagation irrespective of available monomer. This does not occur in DMF as chains remain solvated and propagation continues following diffusion controlled dynamics.

AFM results by Baute et al (2001) support this explanation. Films grown in ACN were found to be heterogeneous in contrast to the more uniform and regular PAN films from DMF. AFM images show that PAN films grafted from high AN concentrations in DMF were thick enough to mask substrate defects. Films grown from low concentrations show small grain-like formation of the order of 40 nm-60 nm irrespective of the solvent used. In contrast higher concentrations produced films with quite different morphologies depending on the solvent used. DMF- grown films were thicker with larger more nodular structures (100-150 nm) compared to the ACN films which had a similar grain size to the film from more dilute concentrations and were only slightly thicker. Calberg et al (1997) recorded optimum thicknesses typically > 2000 Å (DMF) and >250 Å (ACN) which conflicted with those reported by Leroy et al (1985) who reported thicknesses of thousands of Å for PAN films grown in ACN. Calberg et al suggested the films to be a mixture of grafted and precipitated ungrafted PAN.

2.11 Solvent influence

Mertens et al (1996) studied the reduction of AN in DMF confirming the findings of Jerome et al (1995). Voltammograms showed the characteristic two peak regime. The success of the PAN film formation at Peak I in DMF was seen as definitive evidence of electrografting. However the possibility of cross-linking accounting for the PAN film's insolubility could not be ruled out. A change in polymer solubility may well be misinterpreted as successful electrografting. Drawing on the work of Deniau et al (1990)

on the electrografting of poly-p-chlorostyrene in ACN, Baute et al (1998) suggested that the insolubility of the polymer was better described by Levisailles et al (1973) i.e. the parasitic loss of chlorine triggering cross-linking.

The films adhered strongly to the metal substrate even resisting peeling tests and ultrasonic radiation. For comparison a spun-coated PAN film was found to rapidly dissolve in DMF. AFM images of PAN films electrografted in different solvents show significant differences. PAN films grown in ACN are quite rough in comparison to the smoother PAN films formed in DMF. Interestingly PAN films grown in DMF showed an increase in the polarization resistance, possibly due to the solvation properties of DMF allowing for further chain growth. DMF was selected as the preferred solvent to ensure effective electrografting. The precipitation of PAN due to its insolubility in ACN would interfere with the propagation process when the chains reach a certain length. The work also showed that the polymer film formed at Peak I and 'debonded' as the potential was increased. Voltammograms and SIMS measurements of the electrode confirmed that 'debonding' had occurred.

Mertens et al (1998) continued this investigation into the effect of the solvent on the electrografting of AN on nickel. The work explored the influence of four different solvents ACN, DMF, and for the first time pyridine (PY) and propylene carbonate (PC). The solvents were selected to compare the results of a solvent and a non solvent of similar polarity to the results from three non-solvents of different polarity. The study confirmed that the resolution between the Peak I 'inhibition peak' and the Peak II 'diffusion peak' was concentration dependent, the two peaks overlapping for low concentrations and Peak I disappearing above AN concentrations of 5M which the authors suggested was as the result of quasi-instantaneous passivation.

Interestingly, DMF was found to improve peak resolution when compared to ACN, with current intensities correspondingly smaller than those for ACN. The authors proposed that this was the result of a more efficient inhibition of the electrode as a result of much faster growth of the solvated polymer chains. Similarly smaller current intensities for DMF than ACN were recorded in chronoamperometric experiments, with comparably shorter observation times for DMF supporting the proposal of faster formation of an insulating PAN film in DMF.

Mertens at al (1998) explored these differences using a QCM. A comparison of the voltammograms and the corresponding frequency changes showed noticeable differences between ACN and DMF. In particular when scanning to high negative potentials the resonant frequency was recovered for DMF indicating debonding while in ACN a larger decrease in frequency occurred showing further precipitation. When comparing the voltammogram results of all four solvents, the current intensity of Peak I was found to increase as the dipole moment of the solvent increased (with the AN concentration constant) and decrease as the monomer concentration was increased. Films were successfully electrografted in all four solvents. Mertens et al assumed throughout this work that Peak I was an indicator for electrografting and interpreted the changes in the peak current intensity in association with the film quality as a measure of the effectiveness of the process. The solvent influence on Peak I was interpreted as evidence of the competition between solvent and monomer for localization in the double layer.

Baute et al (1999) using an EQCM coupled with cyclic voltammetry also compared the electroreduction of AN in different solvents; ACN and DMF. Similar frequency changes were observed coinciding with Peak I showing the formation of an electrografted PAN film. This concurrence of the frequency changes with Peak I was seen as strong evidence for the electrografting signature. However the different electrolytes showed contrasting responses at Peak II. A larger frequency response was noted for ACN suggesting further precipitation whereas the resonant frequency was recovered showing 'debonding' of the film in DMF. Resonant frequency changes can be converted to mass changes if the ideal behaviour of a rigid layer is assumed (Sauerbrey, 1964). The work showed that the frequency changes associated with Peak I varied linearly with the thicknesses measured ex-situ by ellipsometry. Assuming ideal behaviour holds, the masses of the electrografted PAN films were estimated using the Sauerbrey equation and compared to masses calculated using an alternative method from thickness and commercial PAN density values. The results were comparable, particularly for films grafted in DMF.

2.11.1 Anhydrous conditions

The influence of the conducting salt and solvent dryness on Peak I was also investigated by Mertens et al (1998). Increasing the concentration of the salt or increasing

the size and hydrophobicity of the tetra-alkyl-ammonium supporting salt increased the current intensity of Peak I and reduced the film thickness. The reduction in film thickness was visibly different; films grown in tetra-butyl ammonium perchlorate (TBAP) were barely detectable in contrast to the thicker more visible films in TEAP. These results were seen as further evidence of competition for the electrode surface, the conditions for AN being more favourable when the concentration and size of the cation are smaller.

The intensity of Peak I was also noted to increase when the water content of the supporting electrolyte was increased but only up to a critical level dependent on the solvent used. Above 400 ppm in ACN or 1000 ppm in DMF the reduction of water dominates and no film growth occurs.

Baute et al (2001) reviews the following studies on the effects of contamination. Mertens (1995) shows the effect that increasing impurities such as water and oxygen have on Peak I. An increase in water content was observed to increase the peak current intensity and shift it to lower potentials. Viel (1990)[1] proposed that Peak I was dependent on the polymerization kinetics, the inhibition time of the electrode being controlled by the rate of formation of an insulating film. An increase in Peak I intensity can then be seen as a slower inhibition of the electrode. Ellipsometry measurements carried out by Calberg et al (1997) show thinner films for increased water contamination suggesting earlier termination of grafted chains. The electrografting of AN can also be influenced by any oxygen dissolved in the electrolyte. The reduction potential of oxygen is lower than AN. By-products formed as a result of oxygen reduction can initiate the polymerization and interfere with the grafting process as shown by Mertens (1995).

These studies show that the quality of the resultant PAN film is dependent on the competition between the monomer, solvent, salt and contamination for the electrode surface and that any condition affecting the local concentration of AN in the double-layer will affect the electrografting process.

2.12 Substrates

Chemisorption of AN onto the metal electrode is recognised as the first step in the electrografting process. Parent et al (1995) in a study of the adsorption of AN on Pt (111)

[1] in Baute et al (2001)

and Au (111) using NEXAFS and UPS showed that AN physisorbed on Au and chemisorbed on Pt via nitrogen lone pair orbitals. Pt and Au were selected for the differences in their surface density of states - different filling of the Pt 5d [9] and Au 5d [10] orbitals. NEXAFS probe unfilled states. UPS gives information on the chemical activity of the nitrogen lone pair and π orbitals. The physisorption of AN on Au was confirmed by UPS by the preservation of the valence bands on adsorption. In contrast the NEXAFS results showed a strong interaction between nitrogen and Pt adsorption sites.

Fredriksson et al (1996) carried out a combined theoretical and experimental study of the electrochemical induced chemisorption of AN on nickel, copper and zinc. The aim of the work was to gain an insight into the chemisorption mechanism, so as to extend the range of polymer materials. Quantum chemical calculations performed using density functional theory within the local spin density (LSD) approximation, showed AN molecules are likely to form stable π – d bonds with Ni and Cu atoms but not with the Zn. Ni and Cu both have partially filled 3d levels compared to Zn 3d and 4s orbitals which are completely filled. The computational results showed that the electron affinity of an AN molecule is greatly increased on adsorption with the likely formation of a radical anion rather than an anion as the initiator for polymerization. The work studied the influence a strong electric field had on the AN molecule and agreed with Lecayon et al (1982) that the field was strong enough to increase the polarization of the nitrile group assisting the orientation but not strong enough to open the C=C bond. It was recommended that the chemisorption model needed further work.

The experimental work demonstrated the selective role of the electrode material. The voltammograms showed two responses. The distinct shape of peak I was observed for Ni and Cu and grafting occurred but for Zn no such peak or film were observed. However when the cathodic potential was increased all three electrodes showed a peak II response and the resulting polymer was soluble in DMF.

Rault-Berthelot et al (1995) carried out a study of the cathodic polymerization of AN on a polyfluorene-modified electrode. They proposed that the electrodes had a catalytic effect on the anionic polymerization/ electrografting of AN because insoluble PAN films formed at more positive potentials (potential shift up to 400 mV) compared to nickel or platinum. An FTIR spectral analysis of the insoluble PAN film detached from

the electrode and a sample of PAN extracted from the electrode apparently showed no difference. However the FTIR spectrum shown was of a mixture of PAN products extracted from different electrodes and electrolytes and showed structural alterations. Bands associated with vinylic terminal bonds and conjugated imino groups suggested cyclization while amine bonds and iminonitrile groups suggested degradation of the nitrile group. Reduction of the AN was recognised by a yellow colouration at the electrode.

It is questionable from the results presented that electrografted films were obtained. The ability to detach films from electrodes for analysis is not consistent with electrografting. Spectra of the attached films were not presented for individual assessment and, contrary to the conclusion of the authors, the spectra that were presented do not compare well to spectra of electrografted PAN films.

2.13 Grafting ratio

Tanguy et al (1993) combined electrochemical impedance spectroscopy, chronoamperometry and linear sweep voltammetry to study the electrografting of AN and MAN. The aim of the work was to monitor the relative changes in the double-layer capacitance to investigate the growth of the polymer. Impedance measurements are possible due to the swelling properties of ACN, the supporting solvent. The polymer is transparent to the electrolyte and changes in the double layer can be measured through the polymer. Capacitance measurements taken before and after the polymer deposition were used to estimate the surface coverage and hence the grafting ratio. The dependence of grafting ratio on surface preparation, monomer concentration and cathodic potential was investigated. Impedance measurements showed that the grafting ratio could be increased significantly by applying a pre-electrolysis step i.e. the reduction of the nickel oxide, thereby increasing the number of active sites available for polymerization.

In situ ellipsometric measurements carried out by Bouizem et al (1984) showed that the grafting reaction is likely to be initiated from sites released from the oxide. Successive cycles to improve the grafting ratio for low monomer concentrations justified the need for high monomer concentrations to improve the efficiency of surface

passivation. The formation of a dense polymer layer blocked the electrode from further monomer reduction.

Significant differences were observed in the grafting ratios for PAN and PMAN, the latter requiring high monomer concentrations (80 vol.%) and successive cycling in order to achieve a comparable grafting ratio. The steric hindrance of the methyl group was proposed to account for the difference. The study demonstrated that the quality of the films i.e. thickness and morphology depended on the grafting ratio.

2.13.1 Grafted and ungrafted polymer chains

Tanguy et al (1994) continued the study of the electrografting of MAN to establish the best conditions for optimum quality films, which were found to be highly dependent on the monomer concentration and applied potential. For a monomer concentration of 30 vol.%, no Peak I was observed in the voltammogram and no film formed on the electrode. The peak current density varied approximately linearly as the square of the scanning rate suggesting a diffusion controlled process. Above 30 vol.% an increase in monomer concentration decreased Peak I and shifted it to more positive potentials. Tanguy et al argued that the current density required to form a layer of reduced monomers on the electrode is normally independent of the monomer concentration, assuming the radical anion is stabilised by polymerization pushing the negative charge away from the electrode. If, however, the anion is not stabilized by the polymerization process it will desorb freeing the active site. The probability of polymerization increases with increasing monomer concentration. So for low monomer concentrations higher currents are required to compensate for the desorbed anions which have not been stabilized. However at higher monomer concentrations the probability of grafting is higher. But the process is complicated by polymerization occurring in solution in the vicinity of the electrode. For 100 vol.% monomer concentrations, electrografting was seriously hindered by the rapid polymerization leading to insoluble polymer occurring in solution so that films deposited on the electrode were composed of a mixture of grafted and ungrafted polymer chains.

No reverse scans are reported for the electroreduction of AN. The presence of the methyl group in MAN affects its reactivity. Reverse scans show current density peaks

appearing on successive cycles for monomer concentrations above 50 vol.% suggesting desorption and further reduction. Tanguy et al studied the desorption adsorption processes by measuring the changes in the double layer capacitance during the polymerization process. The results supported the formation of two types of polymer: a) grafted polymer strongly bound to the electrode which cannot desorb during a reverse scan and b) ungrafted polymer which only remains attached to the electrode under the influence of an electric field. The ratio of grafted to ungrafted chains was observed to be highly dependent on the monomer concentration and the number of successive voltage pulses/cycles.

Infrared spectra confirmed the quality of PMAN when compared to a commercial sample. Insolubility of the polymer film firmly attached to electrode was attributed to grafting since the spectra showed no structural changes associated with interchain reticulation. The length of the grafted chain depended on the monomer concentration and solvent used. Optimum grafting occurred for a monomer concentration of 80 vol.%.

In their review Palacin et al (2004) referred to a study by Viel et al (1996) which showed that by selectively poisoning the electrode, thus partially inhibiting the surface, the grafting ratio was reduced and the relative ratio of ungrafted chains to grafted chains was increased. This demonstrated the competitiveness of the polymer initiation mechanism.

2.13.2 Comparing the electrochemical behaviour of acrylic and methacrylic monomers.

An investigation into the electropolymerization of AN, ethyl-acrylate (EA) , MAN and methyl-methacrylate (MMA) using a EQCM coupled with cyclic voltammetry was also carried out by Baute et al (1999) with the purpose of comparing the electrochemical behaviour of acrylic and methacrylic monomers. By simultaneously recording the current/voltages of the electrochemical reaction and respective changes in resonant frequency of the QCM, changes at the electrode and the progress of the reactions were compared. A number of differences were noted when comparing the methacrylics; the formation of ungrafted chains at Peak I, the interplay of adsorption/desorption allowing for further grafting evident by frequency changes and reverse scan peaks and the necessity for high monomer concentrations. Methacrylics form both bonded and non-bonded chains simultaneously at Peak I, whereas acrylic

polymers tend to only graft suggesting that they would be more suitable for the efficient coating and long term protection of metals.

2.14 Precipitation of special soluble polymers with reactive heads

Tanguy et al (1996) using EQCM, cyclic voltammetry and electrochemical impedance spectroscopy carried out an in-situ study of the electropolymerization of MAN to investigate the progressive changes to the polymer layer at the electrode. Following Viel (1990)[1], chronoamperometric methods were utilized for determining optimum growing conditions. Current and quartz crystal frequencies were recorded simultaneously. A delay was observed between the beginning of the current curve and a significant change in frequency. The authors interpreted the delay as the time required for the polymer to reach a critical length before precipitating on the electrode and blocking further reduction. Cyclic voltammograms also showed a similar delay which was found to be dependent on the scan rate and the monomer concentration. Tanguy et al proposed elaborate changes in the polymer conformation to explain irregularities seen in the experimental QCM and CV responses. The interplay of adsorption and desorption, allowing further reduction to occur, was observed during repeated scans and was thought to be due to the progressive organisation of polymer chains on the electrode. As the density of polymers growing from the electrode increased the chains became stiffer and aligned perpendicular to the surface to form a thicker denser brush-type structure.

The evolution of polymer growth during successive scans was also followed by ellipsometry measurements of polymer thickness and compared with the corresponding frequency changes of the QCM. Changes in capacitance were observed due to the loss of the double-layer as polymer covered an increasing fraction of the electrode area. Tanguy et al (1996) referred to work by Fleers et al (1993) on polymers at interfaces and discussed the possibility of adsorbing special soluble polymers with reactive end groups which have the capability of forming a bond with the metal electrode. An alternative mechanism for the grafting process was proposed to explain the successive frequency changes and the asymmetry of Peak I. Tanguy et al described the formation of a local critical concentration of polymer chains bearing radical active ends which on precipitation and if in direct contact of the electrode, will react with the metal to form a

[1] in Tanguy et al (1996)

strong bond. It is clear from the above that further work using a rotating disc electrode would test this proposal.

2.15 Structure of the polymers formed before and after Peak I

In a study by Deniau et al (2001) samples of polymer recovered before and after Peak I were compared. Steric exclusion chromatography, infrared spectroscopy and C^{13} NMR spectroscopy revealed no significant difference between the solution and grafted polymer samples. This suggests that both polymers are formed from the same charge transfer mechanism (Figure 2.12). However a slight difference of the 1710 cm^{-1} infra red absorption band not characteristic of PMAN is seen in the grafted polymer and is compatible with the presence of a carbonyl group. Nitrile groups can be turned into carbonyl groups as a result of nucleophilic attack by O^{2-} anions which are formed during the electrochemical cleaning of the metal. This shows that the grafted polymer is unlikely to be a precipitate of a polymer formed in solution.

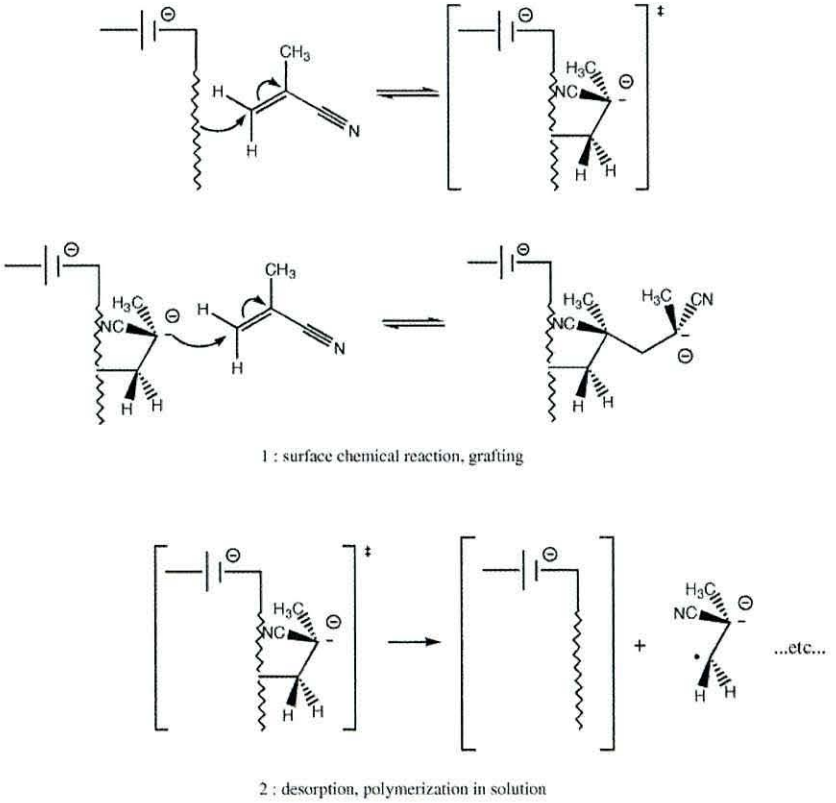

Figure 2.12 *Proposed mechanism showing that both grafted and solution polymer are formed from the same charge transfer mechanism (Deniau et al, 2001).*

2.16 Rotating disc electrode – test for precipitation

Viel et al (1999) studied the electropolymerization of MAN 80%vol/ACN on a RDE at a high spinning rate. The characteristic shape of Peak I was observed and XPS and ellipsometry measurements confirmed the existence of a PMAN film after the experiment even in ACN which is a solvent of the polymer. Convection rate estimated from the spinning rates using the Navier Stokes equation show a considerable stirring effect very close (~ 1 nm) to the surface. This was seen as firm evidence for the electrografting of the polymer being initiated from the surface and not as previously suggested by precipitation from solution. RDE's can produce extremely effective stirring conditions displacing the solution element near the surface several centimeters during the experiment. Several parameters were investigated to explore the influence of the RDE's highly efficient stirring conditions. The slight changes to Peak I with increased spinning rate, coupled with a consistent map of the film thickness from centre to edge of the RDE (Figure 2.13) would suggest that drastic stirring conditions have little or no effect on the rate limiting mechanism responsible for Peak I nor indeed on the grafting process.

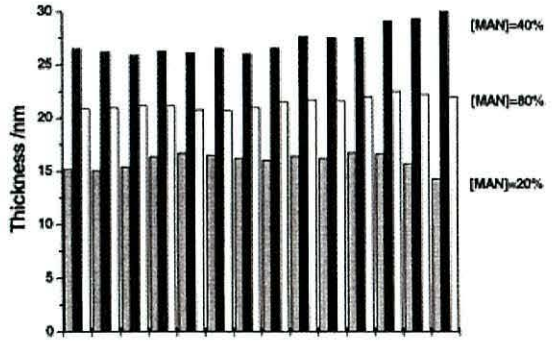

Figure 2.13 *Profiles of thicknesses along a diameter of the RDE polarized in a solution containing 20, 40, and 80% of MAN, (Viel et al, 1999)*

2.17 Mass changes versus viscosity changes – Is the grafting signature invisible?

Charlier et al (1999) monitored the electropolymerization of MAN and NVP in situ using EQCM. The work questioned the ideal assumption that the frequency of the quartz electrode is attributed solely to mass changes arising from the electro-polymerization of MAN at the electrode. Other effects could give rise to changes in the resonant frequency e.g. solution properties such as viscosity and density, and film properties such as roughness and homogeneity. The aim of the work was to differentiate

between the grafting and viscosity changes in solution as a result of polymer formation to gain further insight into the electrografting mechanism.

In the experiments both the resonant frequency and equivalent resistance of the quartz crystal were measured during electropolymerization. The resonant frequency of the EQCM is affected by both mass and viscosity and the resistance is mainly affected by viscosity. If there were no changes due to viscosity i.e. no change in the equivalent resistance of the quartz crystal the authors assumed that the electrografted polymer film demonstrated ideal rigid behaviour following the Sauerbrey equation. NVP and MAN are two monomers with contrasting electrografting behaviour; NVP only forms a grafted polymer whereas MAN forms both the grafted and solution-type polymer. Donneux (1998) showed using TOF-SIMS measurements that PNVP obtained via electropolymerization is not cross-linked. EQCM measurements made during the electropolymerization of NVP by Charlier et al (1999) show mainly frequency changes which were attributed to mass changes since the equivalent resistance was essentially constant, see Figure 2.14.

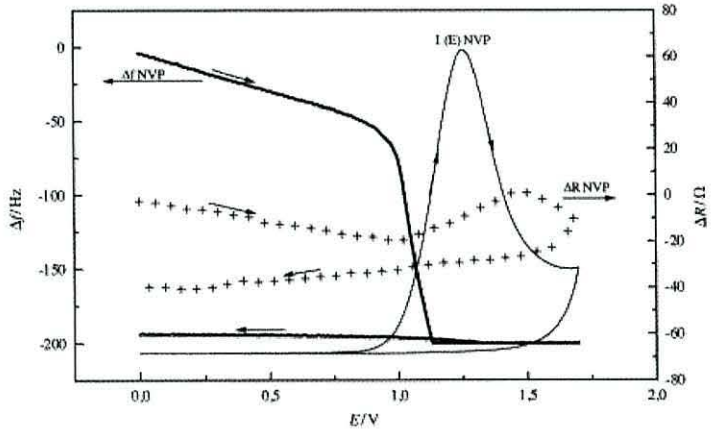

Figure 2.14 *Simultaneous plot of the oxidation current (solid line), the quartz frequency variation (bold line) and the resonant resistance intensity variation (+ + +) vs. potential (Ag/Ag+) during the first cyclic voltammetric experiment in a solution 5M NVP in ACN, v = 5mVs^{-1}, (Charlier et al, 1999)*

Based on these findings the mass of PNVP was calculated using the Sauerbrey equation and by considering the area of the electrode and polymer density, the conformation of the film was evaluated to be dense and brush-like. This suggests PNVP grows progressively from the surface. In contrast, the EQCM measurements made during

the electropolymerization of MAN show some interesting yet inconclusive results. The formation of a rigid coating is first detected at 700 mV before the onset of Peak I. At 200 mV before the onset of Peak I, a large change in resistance indicates the significant polymer production in solution which completely masks any clues to the grafting process occurring at Peak I.

2.18 Competition between the solvent and monomer.

2.18.1 The Gutmann approach.

The concept of competition between monomer and solvent was further investigated by Baute et al (1998) with the aim of extending the range of monomers for electrografting. In this study, the intensity of Peak I was observed to be dependent on the solvent properties. The authors explored the influence of the relative polarity and donor-acceptor properties of the monomer and solvent on the electrografting process. The Gutmann donor-acceptor approach to molecular interactions (Gutmann et al, 1978) was introduced to interpret the results.

The work showed that by increasing the donicity of the solvent, a range of poly-acrylates and poly-methylacrylates could be successfully electrografted for the first time namely poly-ethylacrylate (PEA), poly-methyl-methacrylate (PMMA) and poly-trimethyl-silyloxyethyl–methacrylate (PTMSOEMA). Several solvent/monomer pairs were investigated and the authors proposed that the competition between the solvent and monomer for localization in the double-layer and adsorption on the electrode could be controlled by the appropriate choice of solvent. The influence of the metal on monomer adsorption was also considered, nickel being the electrode of choice for this work.

The adsorption of the monomer is seen by the majority of authors as the prerequisite step for electrografting (Crispin et al 1999). References are made to theoretical models by Geskin et al (1996) and Crispin et al (1996) which propose that AN interacts with the surface copper, nickel and iron through the nitrile group and vinyl end, but does not interact with zinc.

Baute et al (1998) confirmed the usual electrochemical characteristics of the electrografting process i.e. the two peak regime and Peak I was taken as the electrografting signature. Thin PEA films were successfully electrografted in DMF and

IR spectra confirmed the structure to be like that of a free-radical polymerized sample. However attempts to electrograft in ACN only showed the 'diffusion' peak. The solvents have similar polarities but the Guttmann approach showed DMF to be a stronger donor/ poorer acceptor than ACN. The electroreduction of EA using different mixtures of DMF and ACN suggests that ACN competes with the monomer for adsorption. The authors explained the relevance of the donor- acceptor concept by comparing EA to AN. The ester group of EA is less efficient than the nitrile group at triggering electron delocalization, as they suggested that in the presence of the strong electron-withdrawing nitrile group, AN would orientate more effectively on the electrode under the influence of an electric field. The β carbon of the AN would then be in a good position to readily interact with a metal site. The monomer now has to compete for the metal site by displacing a number of solvent molecules.

Baute et al (1998) investigated a number of solvents; ACN, PC, DMF, PY and HMPA in a comparative reduction of AN. Smaller Peak I values were interpreted as the result of high local AN concentrations resulting in the faster formation of a film. Based on the changes to Peak I and concomitant film growth, the polarity of the solvent only had an effect if it was assessed to be a poor donor and a good acceptor. The selection of solvents for the work barely covered the donor and acceptor ranges. However the authors proposed criteria for the choice of solvent based on their findings. If the solvent is a better acceptor than the monomer, no electrografting will occur due to the preferential adsorption of solvent. When the solvent has similar donor acceptor values to the monomer, the adsorption of the monomer can be controlled by the solvent's relative polarity and, if the solvent is a better donor but poorer acceptor than the monomer, the tendency for monomer adsorption can be greatly increased. As regards the choice of monomer, a better acceptor and poorer donor than the solvent was recommended and suggested adjusting the monomer concentration to ensure visibility of the electrografting signature.

Following these predictive guidelines Baute et al attempted to electrograft a number of monomers. MMA assessed to be a poorer acceptor than AN due to the electron donating effect of the methyl group, was successfully electrografted in DMF, however it required high monomer concentrations and several scans to electrograft a reasonable film

The results from MMA were very similar to that of MAN (Tanguy et al, 1996) where successive cycles produced gel-like films consisting of a mixture of grafted and ungrafted polymer which, when rinsed in a good solvent, left only a strongly bound thin film. The authors were unclear as to why polymerization also occurred in solution at Peak I for MMA and MAN but not for AN.

2.18.2 Electrografting polymers with functionality

The monomer attracting most interest in the field of functional polymers was 2-hydroxyethyl-methacrylate (HEMA) because of possible applications as a biomaterial for implants. The monomer HEMA contains a hydroxyl group which has the potential to impart specific functionalization to grafted poly-HEMA enabling it to interact strongly with surrounding material. However the reactivity of this hydroxyl group needs to be protected during the electropolymerization process. Attempts to electrograft the monomers, 2-trimethylsilyloxyethyl-methacrylate (TMSOEMA) and 2-dimethylaminoethyl-methacrylate (DMAEMA) containing different protection groups were compared using the different solvents ACN and DMF. The electrografting signature was only observed for TMSOEMA in DMF a poorer acceptor/ better donor solvent. The PTMSOEMA films were similar to PMMA, a mixture of grafted and ungrafted polymer chains. Deprotection of the hydroxyl groups in PTMSOEMA was then expected to allow for the attachment of another phase e.g. biological material etc.

2.18.3 Alfrey Price Q e scheme

Based on the Alfrey Price Q e scheme which predicts monomer reactivity for co-polymerization, Baute et al (1998) proposed that the propensity of a monomer to electrograft depends on the electron deficiency of the β-carbon double bond and that their results could be explained by the shielding of the monomer vinyl β-carbon. MMA was observed to be less competitive than EA towards DMF due to the inductive effect of the α-methyl group counterbalancing the electron withdrawing effect of the ester group. This results in less delocalization of electrons and so the more shielded vinyl β-carbon is less likely to accept electrons.

2.18.4 Frumkin isotherm – predicting surface coverage

In an attempt to predict surface coverage Crispin et al (1999) undertook a theoretical study based on the density functional approach in which they modelled the interaction of the solvent (ACN, DMF and PY) and monomer (AN and EA) with a nickel (100) surface and then calculated the binding energy difference between the total energy of the complex and the sum of the energy of the isolated parts. Competition for the Ni surface was assessed by comparing these binding energies. The electropolymerization of the monomers AN and EA was then investigated using the different solvents. It was shown that if the calculated binding energy of the monomer was larger than that of the solvent, grafting was confirmed experimentally as in the case of the pair AN/ACN. If the solvent was calculated to be more strongly adsorbed as in the case of EA/ACN no electrografting occurred. A Frumkin type isotherm derived from the binding energy differences was then used to estimate the surface coverage and explain the experimental results. The isotherm predicted the high surface coverage of the strongly absorbed AN irrespective of what solvent or monomer concentration was used. The EA showed contrasting behaviour, the results demonstrating how the choice of solvent could significantly affect the coverage. The authors recommended high surface coverage for good adherence of the grafted polymer and when surface coverage was low suggested increasing the monomer concentration or decreasing the temperature to optimize the number of absorbed monomers to improve the density and hence adherence of films.

2.19 Stable chemisorbed reactive intermediate

Crispin et al (1999) confirmed the characteristic two peak voltammogram in relation to the electrografting process and observed how the monomer concentration affects the position and intensity of Peak I. Based on their QCM results Crispin et al proposed a new insight into the electrografting mechanism, that the essential step is the adsorption of neutral monomer onto the metal surface so that Peak I corresponds to the reduction of this monomer and not the adsorption of the product of an irreversible reduction occurring in solution as earlier proposed by Tanguy et al (1996). Adsorption of the monomer splits the LUMO into several levels which has the effect of significantly stabilizing the molecule so that when the cathodic potential is applied and the energy of

the electrons in the metal is increased to reach the acceptor level, the transfer of an electron is possible which can result in a stable radical anion remaining chemisorbed to the surface despite the electrostatic repulsion. This chemisorbed reactive intermediate can then initiate the polymerization.

2.19.1 Detection of a reaction intermediate

Crispin et al (2001) carried out a spectroscopic study of the polymer/metal interface to show that the grafted polymer is initiated from the electrode surface. Using the unique set up of an ultra high vacuum (UHV) chamber connected to an experimental reactor they were able to build the interface avoiding contamination and then transfer the electrodes to an electrochemical cell to study the pre-requisite step of the electrografting reaction under a controlled chemical environment. Surfaces were prepared using standard surface physics procedures under UHV then the vacuum was broken with highly purified helium protecting the surface from contamination before introducing the electrolyte. The procedure was tested for contamination using highly oxygen-sensitive thiols on nickel.

The adsorption of AN was studied on different oxide-free metal substrates; Pt, Ni and Cu. The XPS core level spectra showed two different absorption behaviours for AN. For Pt/Ni both the carbons from the double bond and the nitrogen interact with the metal atoms in a di-σ–adsorption. For Cu only one of the carbons and the nitrogen is involved in a di-σ–adsorption. The in-situ spectroscopic study also showed the motion of the nuclei to be far slower than the electrons suggesting that the charge transfer occurs at fixed nuclei: a reaction intermediate.

Bureau et al (2001) used a quantum chemical calculation to determine the lifetime of the chemisorbed radical anion, which they believed to have a critical influence on the grafting. The one dimensional model was based on the formation of an interface bond, the anion/metal image charge potential and the anion polarized surface electrostatic repulsion. Interestingly, the calculations showed the probable existence of metastable states of the adsorbed radical anion before it then desorbed. They concluded therefore that the grafting of a polymer is 'decided' during this very short period when an adsorbed

monomer has already been reduced, but has not yet desorbed from the polarized surface to polymerize in solution.

2.20 Permanent traveling concentration wave solutions.

Bureau et al (1999) devised a mathematical model for an electropolymerization reaction which demonstrated that Peak I was most probably due to the dynamic effect of the polymerization occurring in solution and not as previously thought the result of electrode passivation. The purpose of the model was to make use of the known facts to try and understand what was happening in solution. The outcome of this work was examined with respect to experimental observations of the double peak regime, the concentration range for which it occurs, the contrasting peak responses to scan rate and the fact that both peaks have an intensity which decreases as a function of monomer concentration. These experimental findings are fairly typical of the electrografting work to date; however there is some conflict over the latter feature as Mertens et al (1996) observed a contrasting peak dependency on the monomer concentration, where Peak II was observed to increase rather than decrease as a function of the monomer concentration.

Inconsistencies aside, Bureau et al considered the mechanism for the voltammetric response of a homogeneous polymerization occurring in solution as a radical - radical coupling initiated polymerization reaction coupled to an irreversible charge transfer (Bhadani et al, 1992). The model only considered the propagation and termination steps of the reaction and ignored any effects due to adsorption or hindered diffusion. The termination step depends on the availability of protons in the solution i.e. residual water content. A set of non-linear partial differential equations were derived which resolved into a family of permanent, travelling concentration wave solutions when a parameter defining the balance between the propagation and termination rates was greater than unity.

The concentration waves characterize the building of a polymer/solution interface as the polymer grows from the surface. Based on the model Bureau at al (1999) concluded that the double peak was due to the rapid consumption of monomer as a result of coupled polymerization at low potentials. The monomer reduced close to the surface

acted as the initiator for polymerization. The propagation was then sufficient for the coupled polymerization to consume monomer rather than for this to occur through charge transfer. Because the wave travels faster than diffusion can compensate, a depletion region develops behind the wave leaving behind a constant concentration of monomer. The voltammetric current is proportional to this concentration profile and as a result the current falls to zero yielding the shape of Peak I. Residual monomers trapped by the polymer can then be reduced giving rise to Peak II. The conditions are such that the reduction occurs as if no polymerization has occurred so that Peak II shows diffusion-like characteristics.

2.21 Precipitation and reoxidation of non-terminated chain ends.

Tanguy et al (2000) reviewed the work on the electropolymerization of MAN and AN. The complex behaviour observed from double-step chronoamperometry, EQCM and EIS experiments in conjunction with recent studies led to a revised interpretation of the results. The paper attributed Peak I to two processes; the formation of a monomer depleted zone as a result of a fast coupled polymerization reducing the current and the precipitation of the polymer which blocks the electrode. Tanguy et al maintains this view despite the recent work by Viel et al (1999) using a RDE. A comparison of QCM frequency changes with the amplitudes of forward and reverse current peaks for successive cycles shows the complex formation of a polymer layer. Tanguy et al describes a change in the polymer structure from pancake to brush to account for these findings.

An alternative grafting mechanism was proposed to account for this re-organisation. It was suggested that polymer chains bearing anionic ends are precipitated onto the electrode during the forward scan. These active extremities are then re-oxidised during the reverse scan to form radical ends which will readily graft to the metal surface forming a strong bond. A positive current recorded on reverse scans was seen as supporting evidence for this re-oxidation. The interplay of precipitation and desorption allows for the progressive change to a brush type structure as more chain ends graft to the surface.

2.22 Anodic polymerization – No Peak I ?

In a study by Bureau et al (1996) to investigate the interface structure of the anodic electropolymerization of MAN at a platinum electrode, experimental work was undertaken on the electroactivity of various monomers. It was found that even though no electroactivity was evident before the oxidation barrier of the perchlorate, polymer films were formed below this barrier but no Peak I was observed in the voltammograms. It therefore posed the question as to whether the interface bond formation and the electroactivity of the monomer are necessarily connected. However the polymer structure was dependent on the applied potential - a PMAN film comparable to a commercial sample was obtained at anodic polarization potentials of + 2.0V (Ag^+/Ag) but the polymer film formed at + 1.8V (Ag^+/Ag) had a different structure. UPS and XPS spectral characteristics of these polymer films support cationic polymerization of MAN through the nitrile groups. Two different mechanisms were proposed, the quasi conjugated poly-imine type $-(N=C)_n$ and the poly-cumulene type $-(N=C=C)_n$. A theoretical study of the reactants concluded that the poly-imine type was more favourable.

2.23 Electrografted PAN - a useful precursor for carbon fibre

The pyrolysis of PAN is an important method of producing carbon fibres. PAN is usually prepared by solution or suspension polymerization. Electrografting can produce PAN films of well defined chemical composition through the careful control of the electrochemical conditions. It has the potential of being a valuable technique for producing carbon fibres. A number of studies have followed the evolution of these films during heat treatment. Leroy et al (1985) used specular reflection infrared spectroscopy to understand the process. The study compared electropolymerized PAN films grown for different electropolymerization durations of 2 and 10 seconds, with PAN samples produced commercially through free-radical and an electroinitiated process. The thicknesses of their electropolymerized films (few μm) suggest they are possible precipitates and not electrografted films. However the absence of monomer and solvent in the spectra of the electropolymerized films suggests that during polymerization the

double-layer and supporting electrolyte are progressively and efficiently repelled from the electrode surface by a dense growing layer of PAN.

The spectra of the electropolymerized PAN films resembled the spectra of electroinitiated PAN and contained vinylic terminal bonds indicating some segmentation of the chains. Films grown for a shorter duration (2s) showed only cis-type bonds compared to the presence of both cis and trans in films for grown for a longer time (10s). This suggests that the cis is more probable in early stages of growth but as the process relaxes the formation of trans structures are more likely.

Heat treatments were applied under vacuum ranging from 200°C - 600°C for periods varying from 1 hour to several days. The spectra show the development of new structures. A broad weak band centered about 1575 cm^{-1} associated with conjugated imino groups was seen as evidence of intrachain cyclization as proposed by Funt et al (1964).

The width of the bands suggests many intermolecular bonds which is typical of a macromolecule in contrast to the sharp peak of the nitrile group attached to the polymer skeleton. The spectra follow the degradation of the nitrile group. The appearance of bands characteristic of nitrogenated unsaturated carbon rings and the increase of the C=C are evident as the carbon fibre evolves. The spectra of samples subjected to further heat treatment show only carbon fibre peaks.

Reynaud et al (1982) used metastable de-excitation spectroscopy (MDS) and ultraviolet photoemission spectroscopy (UPS) to study the transformation of an electrografted PAN layer subjected to heat treatment in the atmosphere. The combination of the two techniques gives information on surface homogeneity since the analysis depth is different. Films were also characterized by infrared multi-reflection spectroscopy. Heat treatments from 20 °C to 150 °C did not give rise to irreversible transformation. However samples subjected to 200 °C for 4 hours in air showed the characteristic absorptions associated with reticulation and a reduction in the nitrile peak. Oxygen accelerates the reticulation process.

UPS and MDS spectral shapes were modified by charging as a result of electron loss from the surface. When electrons are emitted from organic layers positive charges can appear at the surface giving rise to a temperature dependent electrostatic potential. As

the temperature was increased above 20 °C the potential decreased and vanished altogether for both treated and untreated films above 100 °C. It was also noted to be larger for untreated PAN samples. The phonon assisted hopping model of electrical conduction adapted to organic layers by (Doblhofer and Ulstrup, 1977 in Reynaud, 1982) was proposed by Reynaud to account for the behaviour in the untreated films. An increase in temperature enhances the chain vibrations making it more probable for an electron to hop from one nitrile group to another. However in the treated films the reticulation of structures and the conjugation of imine groups provide conduction paths for delocalized electrons. It was shown that treated thicker layers showed poorer conduction suggesting breaks/defects in chains. These results demonstrated the value of electrografting as a method of producing films of a reproducible purity and high quality.

Newton et al (1997) studied the topographic evolution of electrografted PAN thin films submitted to rapid thermal treatment. The main interest in such work was the potential for coating of electrical contacts for specific applications. AFM measurements of the film roughness when subjected to soft thermal treatments showed a significant levelling of the surface. The comparison of AFM data and IRRAS spectra showed that rapid thermal treatment induced a physical transformation of the film before the structure altered chemically. Samples heat treated at 350 °C for 10 s showed no change in the spectra compared to the significant changes measured by AFM. Only when heating the PAN film at 400 °C for 10 s are any structural changes in the spectra observed with complete transformation occurring after ~ 30 s. The authors proposed that softening of the film altered the kinetics for the chemical reaction thus allowing for a quicker chemical transformation.

2.24 Electrografting – New method producing isotactic PAN films

Calberg et al (1998) investigated the differences between electrografted and commercial solvent cast PAN films using dynamic mechanical thermal analysis (DMTA) and infrared spectroscopy. PAN films were electrografted on specially prepared copper electrodes using the optimised growing conditions established in the field. The copper showed similar behaviour to nickel. The temperature dependence of the viscoelastic properties showed the response of electrografted film to be very different to the solvent

cast samples. The electrografted films were found to be essentially amorphous and comparable to amorphous isotactic PAN prepared by the irradiation of the urea canal complex. In contrast the commercial spun-cast samples were assessed to be paracrystalline and syndiotactic.

The higher temperature transition was made possible for the first time due to the deposition of the PAN films on a metallic support. The unusual fast cyclization times at lower than expected temperatures of the electrografted PAN films led the authors to deduce a different configuration for these films in comparison to the commercial spun cast reference. A predominant isotactic structure was proposed based on the knowledge that polyimine formation occurs faster in isotactic structures as compared to syndiotactic types. The paper referred to Viel's XANES measurements for grafted PAN showing nitrile groups orientated parallel with the regularity deteriorating with thickness as supporting evidence. The DMTA was also used to investigate films electrografted under different conditions i.e. solvent, monomer concentration and grafting potential. Thicker films prepared in DMF or as a result of increasing the monomer concentration gave a more intense response as expected, encompassing the range of amorphous and paracrystalline phases.

Calberg et al (1998) in agreement with Viel et al (1993) proposed that the chain configuration initiates from the electrode surface as isotactic but as the chain grows the sterical and electrical influences controlling this placement become less effective and the thermodynamically driven syndiotactic placement prevails. The IR spectra of PAN films of varying thickness were analysed for isotactic trends by comparing the ratio of peak absorptions at 1230 and 1250 cm^{-1} which were known (Viel,1990)[1], to be proportional to the content of isotactic triads. Thin films were assessed to be predominantly isotactic. Thicker films were found to be comparable to the commercial sample.

Whitish films prepared in DMF at higher potentials were also analysed. The DMTA response showed transitions characteristic of both the grafted and the commercial PAN film. The authors proposed that the structure of the resultant PAN was dependent on the applied potential and that films electrografted at Peak I were amorphous and isotactic compared to films at Peak II which were mainly paracrystalline and atactic.

[1] in Calberg et al (1998)

Studies by Renschler et al (1988) of spin/solvent cast PAN films also show efficient carbonization. A thermal oxidative pre-treatment (220 °C in air for 16 hours) before carbonization gives a greater degree of unsaturation. UV, IR, Raman and XPS spectroscopy studies of different stages of film formation during heat treatment show that the degree of graphitic order and conductivity can be controlled by the temperature. Thickness loss measurements during film pre-treatment show only 1-3 Å/h in air up to 300 °C, making PAN a useful precursor for producing robust smooth continuous films that can be carbonized without loss of shape.

2.25 Non-linear optical properties

Pospisil et al (1998) investigated the optical properties of a pseudo – one dimensional ladder polymer obtained by the pyrolysis of spun-coated PAN films. Polymer films demonstrating high optical non-linearity have potential as photonic devices. Since conjugation is not restricted to a single carbon chain it can also occur in a ladder like structure. This type of conjugation can support structural excitations such as solitons in polymers with degenerate ground states and polarons and bipolarons in structures having non-degenerate ground states. Pospisil et al proposed that the conjugated structure formed in the pyrolysis of PAN is from ring closure involving nitrile side groups. The formation of the structure during pyrolysis was found to be dependent on the presence of air. Anaerobic conditions produced a chain of C-C bonds with a parallel strand of C=N bonds whereas aerobic conditions produce a carbon chain partially unsaturated and a fused aromatic structure. The work focused on the conjugated imine formed by heating PAN in air to 225 °C for 1- 3 hours.

The structural evolution of the films was studied using FTIR and UV-visible spectroscopy. No changes in structures were observed for temperatures below180 °C. However above this temperature, the colour was noted to change from yellow to brown at which point the film became insoluble in DMF. FTIR spectra showed a decrease in the nitrile absorption at 2240 cm^{-1} and a corresponding increase in imine absorption at 1650 $cm^{-1}$and 1360 cm^{-1} indicating polymer chain conjugation.

The UV-visible spectra of the heat treated PAN films show a significant change characteristic of a delocalized π-electron structure from conjugated C=C and C=N, with

peaks ~ 270 nm and ~ 400 nm. Electrical conductivity measurements taken at different stages during the pyrolysis showed that the conductivity of the PAN films increased as the degree of cyclization increased. Pospisil et al (1998) proposed that a change in the conjugation of the polymer chain increased the charge carrier mobility and that the formation of charges on the chain from spurious dopants would account for these measurements.

2.26 Surface electroinitiated emulsion polymerization (SEEP)

Electrografting is a costly, time consuming process, involving elaborate purification procedures. One of the main concerns is protecting the electrochemical cell from water and oxygen, the main inhibitors of the electrografting process. Considering the relative abundance of these atmospheric constituents chemical engineers are continually on the look out for more viable robust techniques. Deniau et al (2006) showed that by combining the 'grafting to' and 'grafting from' techniques in a process called surface electroinitiated emulsion polymerization (SEEP), hydrophobic polymers can be synthesized in aqueous solutions. 'Grafting to' is the bonding of a preformed end functionalized polymer to a reactive surface group on the substrate. 'Grafting from' is the immobilization of initiators onto a substrate which initiate the polymerization from the surface. The aim of the work was to graft polymers onto a conducting surface in a one-step process at room temperature using water as the supporting solvent. The growth of the grafted polymer is then a purely chemical process independent of the influence of the electrode. This helps overcome the sensitivity of the cathodic electrografting to the water content of the electrolyte. The technique depends on the propensity of diazonium salts to electrograft onto an electrode in aqueous conditions. A cathodic potential is applied to an aqueous emulsion containing the diazonium salt, a vinylic monomer and a surfactant. The 'grafting from' stage is the electroreduction of the nitro-benzenediazonium tetrafluoroborate salt to form a grafted layer of phenyl radicals for the surface initiation. The 'grafting to' stage is then the initiation of the radical polymerization of the monomer from the emulsion, then a final coating can be applied by grafting a growing macro radical onto the primer layer (Figure 2.15). Monomers of varying solubility in water were compared; acrylic acid (AA) (totally miscible), AN and butyl methacrylate (BMA). The

resulting film growth showed that solubility was not considered a problem. This low cost technique for preparing a stable covalently bonded organic coating offers great promise for a wider range of functional monomers without the problems of toxicity.

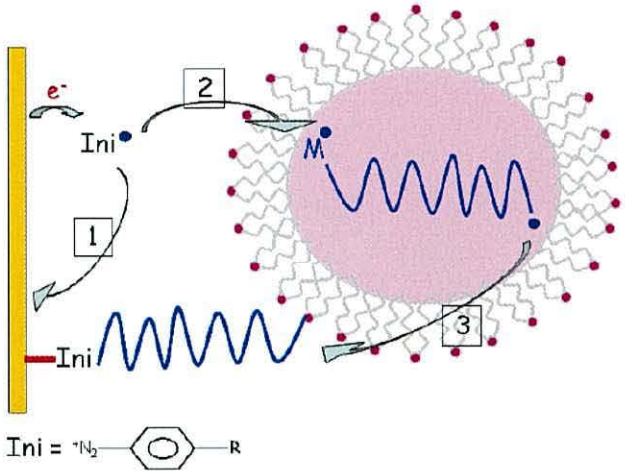

Figure 2.15 *The steps in the SEEP process (Deniau et al, 2006),*
1) Electrografting of the diazonium initiator.
2) Initiation of the radical poly-merization of the monomer M.
3) A termination reaction that grafts a growing chain to a poly-phenylene chain.

2.27 Conclusion

The electrografting process has been shown to be a valuable technique for producing quality polymer coatings covalently attached to a substrate, which are of good stability, controlled thickness and well defined structure. The thickness of the polymer coating can be controlled by the monomer concentration, type of monomer, solvent, salt, temperature and possible side reactions. The electrode provides the initial charge injection to initiate the reaction and a supporting field to enhance the monomer orientation. However cathodic electrografting has some major disadvantages; the need for strict anhydrous conditions and the limited choice of monomer. SEEP offers a solution, by combining the advantages of the cathodic electrografting process with polymerization in emulsion.

Insofar as the present study is concerned the key points to emerge from the literature survey are:

- the essential requirement for purity and dryness of the experimental conditions.
- limitations of cyclic voltammetry as a method for initiating and controlling the electrografting process.
- the critical effect of exceeding the grafting potential leading to structural changes to the polymer or straining and the eventual debonding of a grafted film.
- similar structural changes such as cyclization occur more efficiently when electrografted PAN films are heated compared with solution electropolymerized PAN.
- the need to activate the electrode surface by removal of the metal oxide.
- the solvent influence on the surface coverage and quality of films.
- electrografting can potentially influence the tactic nature of the polymer film, particularly the early growth of the structure.
- the chemisorption of AN depends on the electrode metal used.
- the influence of molecular structural differences when extending the technique to other monomers (steric and electrical).
- that altering the molecular structure will require an increase in monomer concentration to compensate for a reduction in the monomer competition and probably result in the formation of a mixture of grafted and ungrafted chains.
- the requirement for successive scans for less competitive monomers.

2.28 References

Bard, A. and Faulkner, L. *Electrochemical methods, Wiley, New York,* 2001

Baute, N., Teyssie, P., Martinot, L., Mertens, M., Dubois, P. and Jérôme, R., *Eur. J. Inorg. Chem.,* (1998), 1711.

Baute, N., Jérôme, C., Martinot, L., Mertens, M., Geskin, V.M., Lazzaroni, R., Brédas, J.L. and Jérôme, R., *Eur. J. Inorg. Chem.,* (2001), 1097.

Bhadani, S. N., Ansari, Q. and Gupta, S. K. S., *J. Appl. Polym. Sci.,* **44**, 1992, 121.

Boiziau, C., Leroy, S., Reynaud, C., Lécayon, G., Le Gressus, C. and Viel, P., *J. Adhesion,* **23,** (1987), 21.

Bouizem, C., Chao, F., Costa, M., Tadjedinne, A. and Lécayon, G., *J. Electroanal. Chem.,* **172**, (1984), 101.

Bureau, C., Deniau, G., Valin, F., Guittet, M. J., Lécayon, G. and Delhalle, J., *Surface Science,* **355**, (1996), 177.

Bureau, C., Deniau, G., Viel, P. and Lécayon, G., *Macromolecules,* **30**, (1997), 333.

Bureau, C., *J. Electroanal. Chem.,* **479**, (1999), 43.

Calberg, C., Mertens, M., Jérôme, R., Arys, X., Jonas, A.M. and Legras, R., *Thin Solid Films,* **310,**(1997), 145.

Calberg, C., Mertens, M., Baute, N., Jérôme, R., Carlier, V., Sclavons, M. and Legras, R., *J. Polymer Sci., Part B,* Vol **36**, (1998), 543.

Charlier, J., Bureau, C. and Lécayon, G., *J. Electroanal. Chem.,* **465**, (1999), 200.

Crispin, X., Lazzaroni, R., Geskin, V.M., Baute, N., Dubois, P., Jérôme, R. and Brédas, J. L., *J. Am. Chem. Soc.,***121**, (1999), 176.

Crispin, X., Lazzaroni, R., Crispin, A., Geskin, V.M., Brédas, J.L. and Salaneck, W.R., *J. Electroanal. Chem.,* **121**, (2001), 57.

Deniau, G., Lécayon, G. and Viel, P. *Langmuir*, **8**, (1992a), 267.

Deniau, G., Viel, P. and Lécayon, G. *Surf.Interface Anal.*, **18**, (1992b), 443.

Deniau, G., Viel, P., Bureau, C., Zalczer, G.,Lixon, P. and Palacin, S., *J. Electroanal. Chem.,* **505**, (2001), 33.

Deniau, G., Azoulay, L., Bougerolles, L. amd Palacin, S., *Chemistry of Materials,* **18,** (2006), 23.

Fredriksson, C., Lazzaroni, R., Brédas, J.L., Mertens, M. and Jérôme, R., *Chem. Phys. Lett.*, **258,** (1996), 356.

Funt, B.L. and Williams, F.D., *J. Polymer Sci., Part A,* **2**, (1964),865.

Grassie, N. and Hay, J.N., *J. Polymer Sci.*, **56**, (1962), 189.

Jérôme, R., Mertens, M. and Martinot, L. *Advanced Materials,* 7, **No 9,** (1995), 807.

Langmuir. I., *J. Am. Chem. Soc.* **39** (1917),1848.

Lécayon, G., Bouziem, Y., Le Gressus, C., Reynaud, C., Boiziau, C. and Juret, C., *Chem. Phys. Lett.*, **91** (1982), 506.

Lécayon, G., Viel, P., Le Gressus, C. and Boiziau, C., *Scanning Electron Microscopy*, **1**, (1987), 85.

Leroy, S., Boiziau, C., Perreau, J., Reynaud, C., Zalczer, G., Lécayon, G. and Le Gressus, C., *J. Molecular Structure*, **128**, (1985), 269.

G.Mengoli *Adv. Polym. Sci.,* **33**, (1979),2

Mertens, M., Calberg, C., Martinot, L. and Jérôme, R., *Macromolecules,* **29**, (1996), 4910.

Mertens, M., Calberg, C., Baute, N., Jérôme, R. and Martinot, L., *J. Electroanal. Chem.,* **441**, (1998), 237

Newton, P., Houzé, F., Guessab, S., Noel, S., Boyer, L., Lécayon, G. and Viel, P., *Thin Solid Films,* **303**, (1997), 200.

Palacin, S., Bureau, C., Charlier, J., Deniau, G., Mouanda, B. and Viel,P., *Chem. Phys. Chem.***5,** (2004), 1469.

Parent, Ph., Laffon, C. and Tourillon, G., *J. Phys. Chem.,* **99**, (1995), 5058.

Pospisil, J., Samoc, M. and Zieba, J., *Eur. Polym. J.,*Vol 34,**7**, (1998), 899.

Rault-Berthelot, J. and Granger, M. M., *J. Electroanal. Chem.,* **382**, (1995), 169.

Renschler, C.L., Sylwester, A.P. and Salgado, L.V., *J.Mater.Res.,* **4**, (1989), 452.

Reynaud, C., Boiziau, C.,Lecayon and Le Gressus, C., *Scanning Electron Microscopy* **111, (**1982), 961.

Sánchez-Soto, P.J., Avilés, M.A., del Río, J.C., Ginés, J.M., Pascual, J. and Pérez-Rodríguez, J.L. *J. Ana. App. Pyrolysis,* **58**, (2001), 155.

Southampton Electrochemistry Group, *Instrumental Methods in Electrochemistry*, Ellis Horwood Ltd., Chichester. (2001).

Tanguy, J., Viel, P., Deniau, G. and Lécayon, G., *Electrochimica Acta,* Vol 38, **11,** (1993), 1501.

Tanguy, J., Deniau, G., Augé, C., Zalczer, G. and Lécayon, G., *J. Electroanal. Chem.,* **377**, (1994), 115.

Tanguy, J., Deniau, G., Zalczer, G. and Lécayon, G., *J. Electroanal. Chem.,* **417**, (1996), 175.

Viel, P., de Cayeux, S. and Lécayon, G., *Surface. Interface Anal.,* **20,** (1993), 468.

Viel, P., Bureau, C., Deniau, G., Zalczer, G. and Lécayon, G., *J. Electroanal. Chem.,* **470**, (1999), 14.

Willard, H.H., Merritt,L.L., Dean, J.A. and Settle, F.A., *Instrumental Methods of Analysis,*(1988), ISBN 0-534-08142-8

Wopshall, R.H. and Shain, I., *Anal. Chem.* **39, (**1967), 39.

Chapter 3: Experimental Methods

3.1 Introduction

The objective of the experimental work was to develop electropolymerization as a useful technique in the preparation of well-defined macrostructures for a variety of applications.

This chapter describes the experimental procedures employed to investigate the electrografting process for the prototype electron deficient vinylic monomer, acrylonitrile, with the purpose of extending the technique to other more functional monomers. Various experimental parameters were explored to establish the optimum growing conditions; electrolyte, electrode preparation, working environment and potentiostat control. The effect of any changes was monitored electrochemically using cyclic voltammetry. The morphology and chemical structure of successful film growth was evaluated using a combination of Atomic Force Microscopy, Raman Microscopy, FTIR spectroscopy, ellipsometry and UV VIS spectroscopy. All film preparation described in this chapter was carried out in a class 10,000 clean room to minimize atmospheric contamination.

3.2 Health and safety

The substances used in this thesis are potentially extremely hazardous to the user and the environment. Material safety data sheets MSDS were consulted on each chemical, COSHH forms were filled out and the necessary precautions were taken. The handling of all hazardous solvents and monomers strictly took place in a certified fume cupboard. Protective clothing, eye-ware and chemical resistant gloves were used. Risk Assessments were drawn up for each aspect of the work; substances used, storage of chemicals, disposal of waste, preparation of solutions, transfer and measuring of air sensitive liquids, transfer and weighing of air sensitive solids, purging with nitrogen, electropolymerization and handling of the polymer films. Worst case scenarios were thought out and prepared for.

3.3 Cathodic/ anodic electropolymerization (Mills' technique)

Initially the experimental trials adopted a technique used by Mills et al (2000) from the work on the electropolymerization of polymeric macrostructures.

3.3.1 Electrochemical cell and electrode set up

The standard three electrode cell consisting of a working, counter and reference electrodes was assembled and connected to a potentiostat (*PAR EG + G Model 273A*). The potential of the working electrode (WE) was controlled relative to the reference electrode (RE), using the potentiostat (see Figure 3.1). The operational amplifier is the key component of the potentiostat, with the feedback circuit driving the current between the working and counter electrode (CE) and ensuring that none passes through the reference electrode circuit.

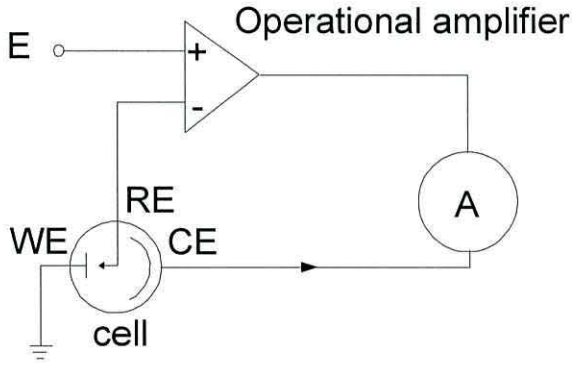

Figure 3.1. *Circuit and electrode arrangement used by the potentiostat.*

3.3.2 Electrode preparation

3.3.2.1 *Working electrode*

A blemish free microscope glass slide with polished, ground edges (*BDH Super premium*) was selected for the substrate base and scored using a glass cutter at approximately midway. Before depositing any metal the slide was thoroughly washed by first rinsing in cold, hot and ultra pure water (*Millipore Q system*), then applying *Decon 90* (*Scientific Services Ltd*) a bleach substitute to remove any traces of organic contaminants and finally repeating the rinse sequence. The glass surface was then examined under light and further washes were undertaken if necessary. Once clean, the

slide was then carefully dried in a stream of warm air and stored under vacuum. The working electrode was prepared by coating the clean slide with a thermally evaporated Ag film using a turbo pump vacuum system (*Balzer TSH170)* using the following procedure. The slide was securely clamped in place ~ 12 cm above the evaporating source set-up consisting of a molybdenum boat for the metal of choice (Ag,Au or Cu) and a Cr rod. In the initial experiments a 15mm length of pure Ag wire (*99.99% Advent Research Materials*) was coiled and placed in the boat. The chamber was then sealed and pumped down to $3x10^{-6}$ torr. To ensure good adhesion of the Ag film to the slide, a Cr keying layer of approximately 5-10 nm was applied by allowing 4 A to flow through the Cr rod (*Testbourne*) for approximately 2-3 s. The vacuum was then allowed time to recover before depositing the Ag by passing 4 A through the boat for about 30 s allowing the metal pool to completely evaporate forming a film approximately 100 nm thick over the 70 mm x 25 mm area of the slide.

3.3.2.2 ***Counter electrode***

The CE consisting of a Pt foil (*99.99% Advent Research Materials*) of approximate area 7 mm^2 welded to a Pt rod (*99.99% Advent Research Materials*) 0.5 mm diameter, concealed in a glass tube was prepared by flaming the foil to remove any impurities.

3.3.2.3 ***Reference electrode***

The potential of the cell was measured against a pseudo-reference electrode. A piece of Ag wire (*99.99% Advent Research Materials*) was used for this purpose. Using this type of electrode reduces the risk of contamination of the analyte but the disadvantage is that the reference potential is unknown, as it is dependent on the composition of the analyte solution. The tip of the wire was positioned close to the surface of the WE to minimize uncompensated resistance.

3.3.3 Electrolyte solution

Acrylonitrile (AN), acetonitrile (ACN) HPLC grade, and tetraethylammonium perchlorate (TEAP) were purchased from *Sigma–Aldrich* and used without further purification. The electrolyte solution consisted of AN (0.4 M) with the conducting salt, TEAP (5×10^{-2} M) diluted in ACN. Then 40 ml of this solution was placed in the

electrochemical cell, see Figure 3.2. Before each polymerization experiment, the cell solution was de-aerated by purging with nitrogen gas for 20 minutes to reduce any oxygen present. Oxygen is electroactive and can be reduced quite easily. A blanketing layer of inert gas maintained over the solution during experimentation prevented further contamination.

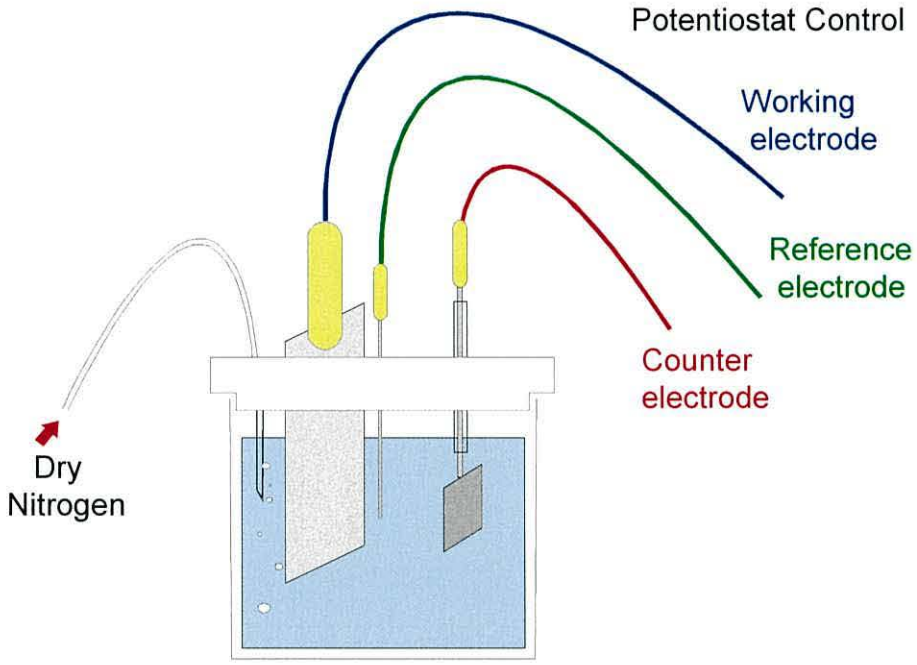

Figure 3.2 *Diagram of the electrochemical cell used by Mills et al (2000).*

3.3.4 Potentiostat control

The electropolymerization technique replicated from Mills et al's (2000) work is a two-step technique adapted from Taylor et al (1991) for the electropolymerization of poly-3-methylthiophene. A high potential was applied for a short duration to nucleate growth and then the potential was scanned to a lower potential for a longer period to support the main polymer growth (see Table 3.1). The current flowing through the cell was monitored using the potentiostat digital panel and a X-Y plotter (*Roland DXY*).

Table 3.1 *Electropolymerization steps.*

	Nucleation step		Growth step	
Type of electropolymerization	Applied potential/V	Time applied/s	Applied potential/V	Time applied/s
Cathodic	-2.8	10	-1.8	600
Anodic	2.8	10	1.8	1200

3.3.5 Rinsing and storage of films

At the end of the growth step the working electrode was removed from the cell and rinsed with acetonitrile then acetone to remove any residual solution and subsequently dried under a gentle stream of pure nitrogen gas. Before characterization the samples were stored under vacuum overnight.

3.4 Improvements to the Mills' technique

Exhaustive attempts to duplicate the Mills et al (2000) work failed to produce the characteristic electrografted PAN films reported in the references. Only pale yellowy crystalline precipitates were observed forming on the electrode at high almost constant currents during cathodic trials. These polymer films were not considered to be electrografted for a number of reasons such as; electrode passivation did not occur and films were easily removed during a 'peel test' (see below).

A thorough examination of the procedures involved identified water, oxygen and electrode contamination to be the main inhibitors to the cathodic electrografting process. The need for stringent conditions is emphasised throughout the review of the electrografting literature (see Chapter 2). A series of necessary modifications was undertaken to establish the essential experimental conditions for the successful growth of quality electrografted films. The following parameters were individually investigated; electrode preparation, cell design, electrolyte preparation, potentiostat control and film preparation for characterisation. Evaluation of successful film growth by cyclic voltammetry, AFM, Raman microscopy, FTIR and UV VIS spectroscopy provided the essential feedback to make these improvements.

3.4.1 Standard peel test

The adhesion of electropolymerized films to the metal substrate was measured using the peel test. The peel test is a common method for measuring polymer adhesion. A transparent adhesive tape (half an inch wide; *Scotch, 3M*) was carefully stuck to the film surface and then a peel test was performed according to ASTM D3359 'Standard methods for measuring adhesion by tape test'. This technique is good for detecting poor adhesion but is sensitive to the technique used. The tape should adhere well to the surface

and be pulled over a cut through the film since the edge allows the fracture to initiate at the interface otherwise the film can act like a 'drumhead' and not fail even though the bond is weak. The transparent tape was then viewed under magnification using an optical microscope and the adhesion was qualitatively measured by the amount of 'pull outs' of film released from the electrode surface. A disadvantage of this test is that the film is likely to be contaminated by residual adhesive and this needs to be considered if films are to be used or processed.

3.4.2 Electrode preparation

3.4.2.1 ***Working electrodes***

Precipitates of electropolymerized polyacrylonitrile formed using Ag coated microscope slides tended to be 'patchy' in appearance. This suggested that the area of the WE was too large compared to that of the platinum electrode thus leading to a non uniform current density at the WE. The first improvement was then to correct this. A shadow mask was produced in the shape of a 'lollipop' of circular diameter 12 mm and stem 2 mm, to reduce the area of the working electrode closer to that of the CE.

a) *Adhesion layers*

When the electrochemical cell was set up using a Cr/Ag coated slide as a working electrode as in Figure 3.2, an open circuit voltage (~ 0.25 V) was recorded and sometimes during the nucleation step, the Ag was observed to disappear from the slide. According to Ling et al (2003) if a similar bimetallic layer, Cr/Au, is exposed to the electrolyte it forms an electrochemical cell which interferes with the electrochemical measurements in such a way that the Cr dissolves allowing the Au layer to detach. The voltage observed in the present work before the potentiostat control was applied suggests that the bimetallic junction here was also exposed to the electrolyte causing corrosive galvanic currents. Exposing a slide coated only with Ag gave a zero voltage confirming the galvanic effect. However, without a keying layer the Ag readily peeled off.

An adhesion layer of Cr has also been shown by Gernet et al (1989) to diffuse through the surface metal and participate in electrochemical reactions thus producing additional peaks in cyclic voltammograms. Therefore an adhesion layer can seriously compromise the performance of an electrode. Thus it is essential that the Cr layer is not

exposed to the electrolyte. W/ Ti were recommended as a suitable less corrosible alternative but the evaporator system was unsuitable for such metals. In an attempt to remedy the problem the thickness of the electrode metal was increased from ~100 nm to ~250 nm while reducing the Cr layer from ~10 nm to ~3 nm. This change enhances the likelihood of the effective coverage of any exposed Cr edges and creates a significant barrier to diffusion. The diffusion of Cr was also investigated by evaporating a barrier layer of palladium sandwiched between the Cr and the metal e.g. Cr/Pd/Au in the ratio of 3/8/70 nm. The quality and thickness of the films and their corresponding electrochemical behaviour are presented in Section 4.18. Semi-transparent metal films to enable UV-visible spectra of deposited films were also prepared. In such cases ~10 nm of Au was deposited onto ~2 nm of Cr.

b) *Evaporating Cr/Metal using the Edwards 306 Turbo Evaporator*

The Edwards evaporator is a two source system and is generally reserved for Au and chrome films however an exception to include Ag and Cu was allowed for this work. The evaporator lid is designed to hold up to eight microscope slides for batch processing. Batches were useful to ensure consistency in WE preparation when investigating other parameters. For each slide a shadow mask was machined in brass to clamp over the top of the glass. The slides (*BK7*) were each washed and prepared as in Section 3.3.2.a. A measured amount of pure metal wire (99.99% Advent Research Materials) dependent on the thickness required was prepared by first washing in *Decon 90*, then rinsing with hot water and then finally ultra pure water. Before placing in the evaporator the wire was thoroughly dried in a hot air stream. Carefully using a pair of watchmaker tweezers, the metal wire was coiled and then placed in a dish at the bottom of the chamber. The chrome filament was then checked and replaced if insufficient. To assist monitoring of the deposition process a viewing port was provided by inserting a hole in the shrouding chamber foil. A quartz crystal microbalance was used to monitor deposition rates. The quartz crystal was replaced regularly to provide consistent results and especially if the deposition rate appeared to fluctuate during a controlled deposition. If the deposition rate is oscillating during a controlled deposition, it is a sign that the crystal needs to be replaced. The quartz deposition meter used to monitor the deposition was programmed for each material used. The Edwards evaporator can reach vacuums of below 8×10^{-6} mbar

in approximately 1 hour. Upon achieving this pressure the Cr was evaporated by applying a steady current of 1.8 A to achieve a deposition rate of 0.1 nm/second. The required Cr thickness of 2.5 nm took about 25 seconds. Evaporating the Au required a higher steady current of 2.5-3 A and thicknesses of 250 nm took several minutes to obtain. The system was allowed to cool for a few minutes before letting air into the chamber.

c) *Comparing different working electrodes*

Surface enhanced Raman spectroscopy (SERS) was used by Xue et al (1994) to show that Ag can catalyse certain structural changes in PAN that are normally seen during heat treatment. In order to consider this influence a range of different electrode metals was tested and compared. Ag, Au and Cu were selected as all three can be prepared by the same evaporation process allowing for more consistent comparisons. Pt was also used but in foil form only.

SERS is a relatively recent technique used to enhance Raman signals (see Section 3.7.1.2.b). This Raman enhancement effect is generally strongest for Ag but has also been observed using Cu and Au. When the wavelength of incident light is close to the plasma wavelength of the metal, conduction electrons in the metal surface are excited into an extended surface electronic resonance called a surface plasmon. The intensity of this resonance is dependent on many factors i.e.the wavelength of the incident light and the nanostructure morphology of the metal surface. The wavelength should match the plasma wavelength of the metal. According to Muniz-Miranda et al (2007) Cu and Au have a plasma wavelength between 600 nm and 700 nm whereas Ag can be as low as 380 nm for 5 μm particles. The subsequent use of different electrode metals of similar morphologies, excited by different laser wavelengths would therefore allow for an assessment of this effect.

d) *Electrochemical cleaning of metal surfaces*

The condition of the surface of working electrodes can have a significant effect on the current response of voltammetric experiments. The fundamental process in the required electrografting reaction is the transfer of electrons between the electrode surface and the monomer adsorbed at the surface. The kinetics of this process can be significantly affected by the structure of the surface and the blocking of active sites by absorbed impurities. It was therefore considered important to develop methods to remove this

contamination and activate the surface for the preferred adsorption and subsequent reduction of the monomer.

Ag, Au, Cu and Pt surfaces if exposed to the ambient atmosphere will rapidly adsorb a number of potential contaminants. Ag in particular is known for its propensity to adsorb atomic oxygen and is used to great effect in the catalytic epoxidation of ethylene to form ethylene oxide. Schoenfisch et al (2000) developed an electrochemical cleaning protocol to effectively remove carbonaceous contamination from Ag and Au surfaces prior to depositing self-assembed monolayers. This method requires the use of a standard reference electrode.

A typical electrochemical cleaning protocol for Au usually involves cycling between a positive and negative voltage for the formation, and then subsequent reductive desorption of the Au oxide. However the electrochemical cleaning of Ag is not so straightforward. Schoenfisch et al refers to an in-situ Raman study by Mahoney et al (1980) which demonstrates the reversibility of Ag oxides rather than the desired desorption. Oxidation–reduction cycling (ORC) is a standard electrochemical method used in SERS experiments to clean and roughen surfaces. Tian et al (1997) showed that Pt surfaces not normally used for SERS can be effectively activated using just such a technique.

e) *Electrochemical cleaning procedure.*

Based on the work of Schoenfisch et al (2000) the electrochemical cleaning of the electrode surface of the different metals used was investigated. Various conditioning potentials were applied in an attempt to free the different metal surfaces of oxides, hydroxides and organic contaminants. Care was taken not to decompose the electrolyte and poison the electrode surface. This meant working within a potential window where the solvent, salt and metal remained electroinactive, the only electroactivity being that of absorbed impurities. A cell design was developed with siphoning access and a drainage tap (see Figure 3.3), so that the WE could be electrochemically cleaned in a monomer free solution of solvent and salt then flushed ready for the monomer solution to be introduced. The cell was assembled as shown in the Figure. The monomer free electrolyte consisting of the solvent, dry *N, N*-dimethylformamide, DMF (Fluka, puriss, absolute, over molecular sieve < 50ppm water) and the salt TEAP (Fluka, puriss, electrochemical

grade) was then siphoned in. A blanket of dry nitrogen was carefully maintained in the cell to provide protection from further contamination and assisted drainage. The electrodes were then connected to the potentiostat and the appropriate cyclic voltammetry (CV) potentials using manual control were applied (see Section 3.4.7 for potentiostat control). Scans were repeated until reproducible cyclic voltammograms were obtained. The effectiveness of the electrochemical cleaning process was assessed by the degree of success in growing good quality films. AFM measurements were taken before and after cleaning to investigate any structural changes to the metal surface.

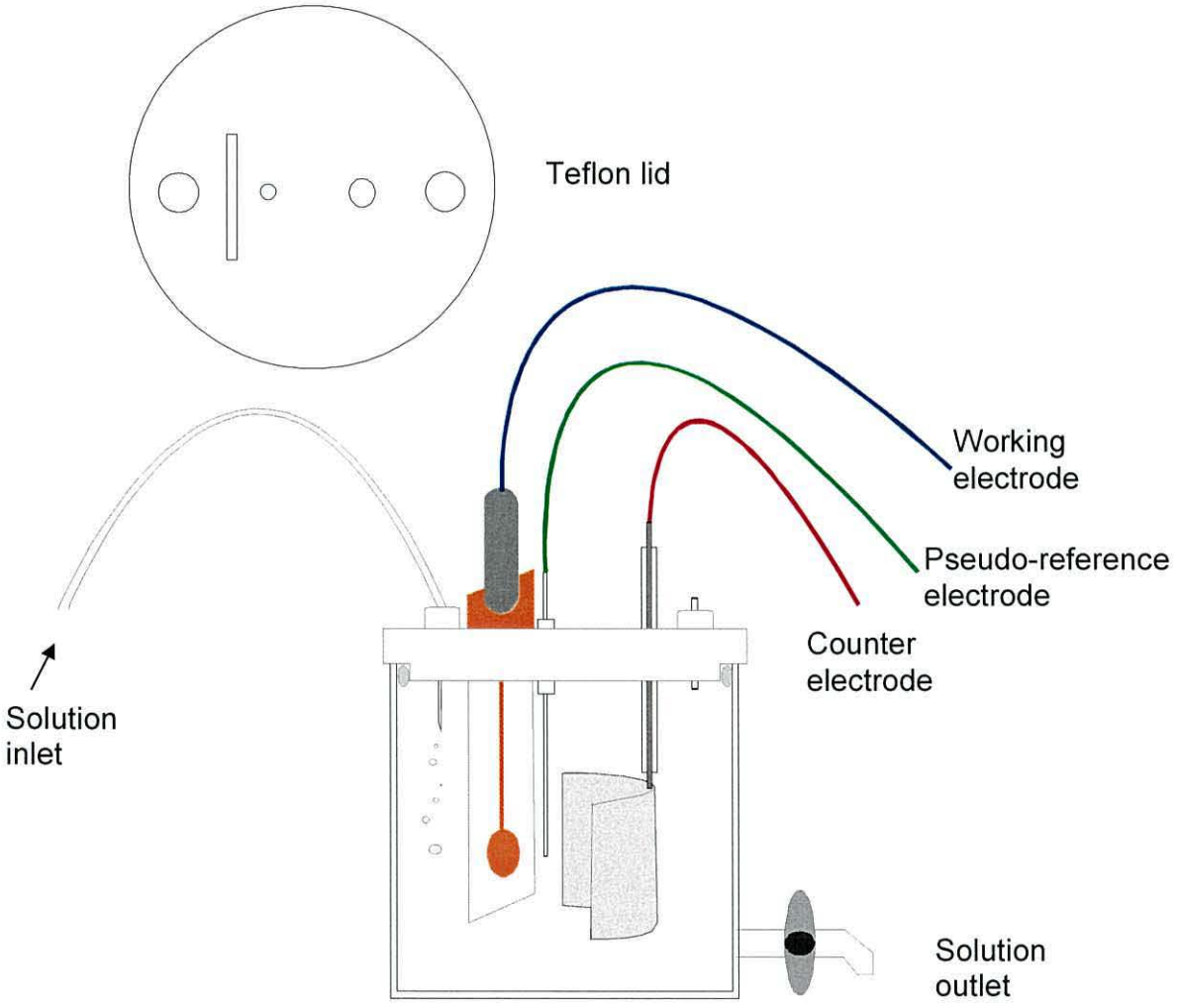

Figure 3.3 *Diagram of the improved electrochemical cell design.*

3.4.2.2 *Counter electrode*

Mills et al (2000) used a platinum counter electrode of area 7mm x 7mm. In order to support the current generated at the working electrode, the surface area of the counter electrode must be equal to or larger than that of the working electrode. Therefore the CE was fabricated using a platinum foil (*Goodfellow, High purity 99.99 + %, 0.25 mm thick)* 25 mm x 25 mm in area which was spot welded to a platinum rod 0.5 mm in diameter which was then sealed and mounted in a glass tube. The glass tube provided a better sealing surface for inserting into the cell lid (see Figure 3.3). Before using the electrode it was thoroughly washed and rinsed to remove any surface impurities. The foil was then carefully cleaned by flame treatment and then stored in a vacuum chamber.

3.4.2.3 *Reference electrode*

Pseudo- reference electrodes are simply metal wires such as platinum and silver, immersed in the electrolyte solution. Although such electrodes provide a constant potential the reference potential is unknown and depends on the composition of the solution. Advantages of using this type of reference are minimal contamination, low impedance and good stability. Platinum wire (*99.99% Advent Research Materials*) was selected due its stability in the potential range considered and because the wire can easily be reproducibly flame-cleaned for each experiment.

3.4.3 Electrochemical cell design

The cell was designed to protect the carefully prepared electrolyte and electrodes from contamination. Earlier trials had involved the use of an *atmosbag* i.e. a specially designed plastic bag as an alternative to a glove box. But the work was too hazardous and the bag was found to be too cumbersome to use. The cell set-up and cannula lines allowed for liquids to be siphoned in and drained out for cleaning, electropolymerization and rinsing. The siphon inlet point also provided and maintained a blanket of nitrogen during these processes. A Teflon lid with Teflon O-ring provided adequate seals to support the set up. The components of the experimental set up minus the electrodes (see electrode preparation) were all thoroughly washed in *Decon 90*, rinsed in ultra pure water, dried and stored in a drying oven. Prior to use, the cell plus electrodes were carefully assembled and stored in a vacuum dessicator. Care was taken with the positioning of the

electrodes. The reference electrode was placed as close as possible to the working electrode to reduce resistance but not so close as to interfere with film growth.

3.4.4 Electrolyte preparation

3.4.4.1 ***Monomer***

a) *Removal of inhibitors*

AN (*Fluka, puriss*) when purchased contains a stabilizer, hydroquinone monomethyl ether, which acts as an inhibitor to prevent free radical polymerization during transit. This stabilizer can be removed from the AN by passing the monomer through a disposable inhibitor removal column (*Aldrich*). The pre-packed glass column was first pre-washed with a small amount of the AN. Then the monomer was introduced to an addition funnel which was secured above the column. Care was taken to maintain and monitor a drop-wise rate of addition to prevent overflow of the column. The AN was then collected using an appropriate flask containing molecular sieves and sealed with a suitable chemical resistant septum. However this process proved to be both time-consuming and hazardous and unfortunately failed to remove water, an additional inhibitor that was found to be present. Therefore further purification was required and distillation under reduced pressure was used as the preferred alternative.

b) *Distillation under reduced pressure*

All glassware (*Chemistry labs*) was washed, rinsed and dried thoroughly by baking in a drying oven before use. The vacuum distillation was set up carefully in a fume cupboard. AN was vapourized under reduced pressure, condensed and then collected in a flask seated in a cooling bath of liquid nitrogen. A diaphragm pump (*Divac*) provided the necessary vacuum. When sufficient monomer had been obtained the flask was then quickly and carefully sealed with a blanket of nitrogen and a chemical resistant septum, which allowed for measured dispensing of the monomer using glass syringes and transfer needles.

c) *Other monomers*

After establishing and developing the essential growing conditions for the model monomer AN, attempts were made to electrograft a range of other monomers.

Some of these monomers were readily purchased from *Aldrich,* others needed to be synthesized at the Department of Chemistry at Hull University. The objective was to investigate in a systematic manner, the structure of alkenes that will undergo both anodic and cathodic electropolymerization.

The majority of monomers used had the same basic structure (Compound 1).

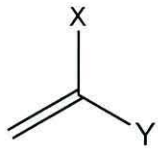

(Compound 1)

The X and Y substituents for the different monomers was varied. If the X group is either H or CH_3 very little chemistry can be done on these groups after polymerisation. So it was decided that the X group used should be either CN or $CO_2CH_2CH_3$. When using Y as CH_2OH (compounds 1 and 2, see below), it was found that it decomposed during the electropolymeristion process so the use of different protection groups was explored (compound 3, 4-nitrobenzyl and compound 4, tetrahydropyran). The following monomers were tested:

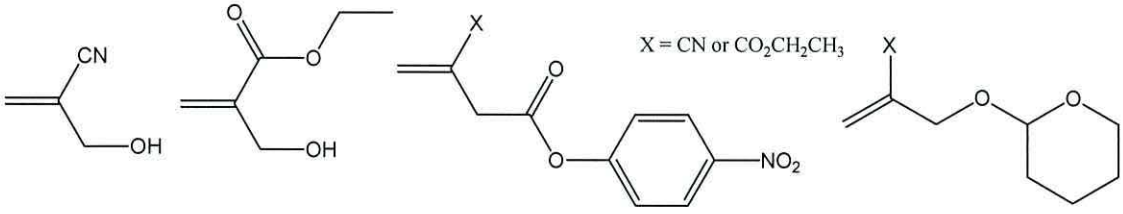

1 **2** **3** **4**

The choice of substituent was not simple. According to Baute et al (1998) the relative donor acceptor properties and polarity of the solvent with respect to the monomer influence the competition process for being absorbed on the electrode. From their results they found that the solvent should have a weaker acceptor character but a higher donicity than the monomer. Therefore it was important to select substituents that increased the acceptor capacity of the vinyl monomer with respect to the solvent to increase the monomer competition for the electrode. However if the monomer competition is weak as in the case of methylmethacrylate and DMF an increase in its relative abundance was observed to be effective by the authors.

As a result of these findings DMF was chosen as the solvent for the electropolymerization trials due to its high donicity and monomer concentrations of 2M were used where possible to encourage the preferred adsorption of the monomer at the electrode. However this was not always possible as the synthesis and purification of the more sophisticated monomers limited the sample sizes. Cu or Au films were selected as suitable working electrodes.

3.4.4.2 ***Electrolyte salt***

Electrochemical grade tetraethylammonium perchlorate, TEAP was purchased from *Aldrich*. According to good electrochemistry practice this hygroscopic compound needs to be dried before use to remove water. A vacuum drying oven (*Buchi*) was used to dry the salt overnight (minimum 12 hours) at 80°C with a dessicant to assist the process. After drying the salt was then stored in a vacuum dessicator.

3.4.4.3 ***Solvent***

N,N-dimethylformamide (DMF) and acetonitrile (ACN) were initially purchased from *Sigma–Aldrich* as HPLC grade and used without further purification. According to the *Aldrich* data sheets the water contents of these solvents before opening were 300 ppm and 50 ppm respectively. The solvents do not come protected over molecular sieves with septum for dispensing which makes handling them difficult as both solvents are extremely hygroscopic and once exposed to the atmosphere will rapidly absorb water. Experiments using these solvents were unsuccessful and the corresponding CV's were difficult to interpret. Water was identified to be the main problem.

Molecular traps (*Prime Synthesis*) which are highly activated molecular sieve packets designed specifically to provide and maintain extremely low water levels in ultra-pure solvents and solutions were used to try and compensate for this problem. They can generally be used in any application where molecular sieves are utilized such as to dehydrate or maintain anhydrous solvents through repeated air exposures. A Karl Fischer instrument was used to assess the dynamic scavenging effect of these traps by measuring the water content of made up solutions see Section 3.4.4.4. Different concentrations of monomer with DMF and 0.05M TEAP were investigated to identify the main contributor of water contamination. Experimental electropolymerization trials were also carried out to assess the impact the water content has on the electrografting procedure.

Electropolymerization attempts using solutions dried with molecular traps showed a strong current signal at -700 mV on the cyclic voltammogram suggestive of the reduction of water. This response swamped any voltammogram indication of monomer reduction.

Films grown in solutions contaminated with water were inspected with an optical microscope. Even at low levels of water contamination there was a significant number of film defects i.e. pin holes which noticeably increased in quantity when the levels of water increased. Molecular traps were found to be effective in reducing the water content but this was not nearly sufficient for our requirement of producing quality films. According to the experimental findings of Mertens et al (1998) water concentration levels above 400 ppm ACN and 1000 ppm in DMF prevent the electrografting of PAN with levels below seriously affecting the quality of the films. Therefore anhydrous solvents (<50 ppm) over molecular sieves with dispensing septa were purchased from *Aldrich* in small amounts. Solvent dryness and protective handling were identified as essential.

3.4.4.4 ***Karl Fischer measurements***

A moisture titrator *MKC-510* (coulometric method) was employed to measure the water content of samples. In the Karl Fischer reaction, if water is present in a sample, it will react with iodine and sulphur dioxide quantitatively in the presence of a base and alcohol. As soon as the detector of the titrator senses a drop in iodine levels electrolysis will start to generate iodine to restore its equilibrium. The amount of water present is calculated from the current flow during the electrolysis. The instrument can measure water content from 10 μg to 100 mg. This was converted to parts per million for comparison. Moisture levels were found to be greater than 100 ppm and to be particularly sensitive to exposure during the sampling for testing. Changing the monomer concentration had little impact on the water content suggesting the solvent was the main contributor.

3.4.5 Prevention of further contamination

One of the main concerns when making up an electrolyte solution before an electropolymerization experiment is contamination from the atmosphere. A cannula technique needed to be developed whereby all three components; anhydrous solvent, distilled monomer and vacuum dried salt could be introduced without exposing it to the

contaminant. A set up of conical flasks, septa, double-ended steel needles, glass syringes needles and balloon were used to maintain the high levels of purity acquired.

For each experiment two solutions were made up; one without the monomer for the electrochemical cleaning of the working electrode and the other with monomer for the electrografting. All glassware and needles had previously been washed, rinsed and dried thoroughly overnight in a drying cupboard. Two conical measuring flasks were placed in an *atmosbag* (*Aldrich*) along with a balance, septa and desiccator containing the dried salt. Before opening the desiccator, the bag was evacuated then filled with dry nitrogen twice. The salt was then carefully weighed out, transferred to a dried flask and sealed with dry nitrogen using a septum. The flasks were then removed from the bag and placed in a fume cupboard. A cannula transfer line was then set up using a double ended steel needle inserted in the flask septum at one end and the required solvent bottle septum at the other. Care was then taken to introduce dry nitrogen via a needle into the solvent bottle and then a release needle was quickly placed in the flask to prevent a build up of pressure. By lowering the transfer needle carefully into the solvent the required amount was then transferred. Care was taken to remove the needles in the appropriate sequence so as to provide a blanket of nitrogen to prevent exposure of the vessel to air. The monomer was added by using a syringe and needle. A balloon inserted in the flask septum compensated for the change in pressure when the syringe was emptied. Prior to use, both flasks of solutions were purged by bubbling with dry nitrogen for twenty minutes to remove any oxygen present in the electrolyte.

3.4.6 Electrochemical cell set up and procedure.

When required the cell was extracted from the desiccator and secured in place in the fume cupboard using clamps. A dry nitrogen line was introduced to the cell to maintain protection and the potentiostat contacts were attached to the relevant electrodes. The appropriate solution was then siphoned in and the relevant potentiostat measurements were made. The potentiostat was isolated before the cell was drained and refilled for the next stage. The blanket of dry nitrogen was maintained throughout (see Figure 3.3).

3.4.7 Potentiostat control

The potentiostat used for the voltammetry experiments was a *PAR EG + G Model 273A*. Waveforms for the cyclic voltammetry were programmed into the unit. A start voltage E_1, delay d_1, scan rate s_1, peak voltage E_2, delay d_2, return scan rate s_2 and final voltage E_3 were entered in sequence. A XY plotter was connected to the outputs to monitor the voltammograms. The potentiostat was calibrated using a standard resistor. The integrity of a vapour deposited gold working electrode was tested using a series of cyclic voltammograms for the reversible one-electron oxidation of ferrocene. The voltammograms were recorded over a range of potential scan rates with the potential settings remaining the same for each scan. Analysis of the data was considered for diagnostic purposes.

The electrochemical active area of the electrode was calculated using the gradient of the plot of the current peak height against the square root of the potential scan rate, and the *Randles-Sevcik equation*. The obtained value compared well to a geometric estimate of the electrode area. However this was used as an exercise of familiarity with the potentiostat set up. The geometric calculation assumes a flat projection of the surface and only a slight variation in the surface roughness of the electrode would increase the electrochemical area significantly.

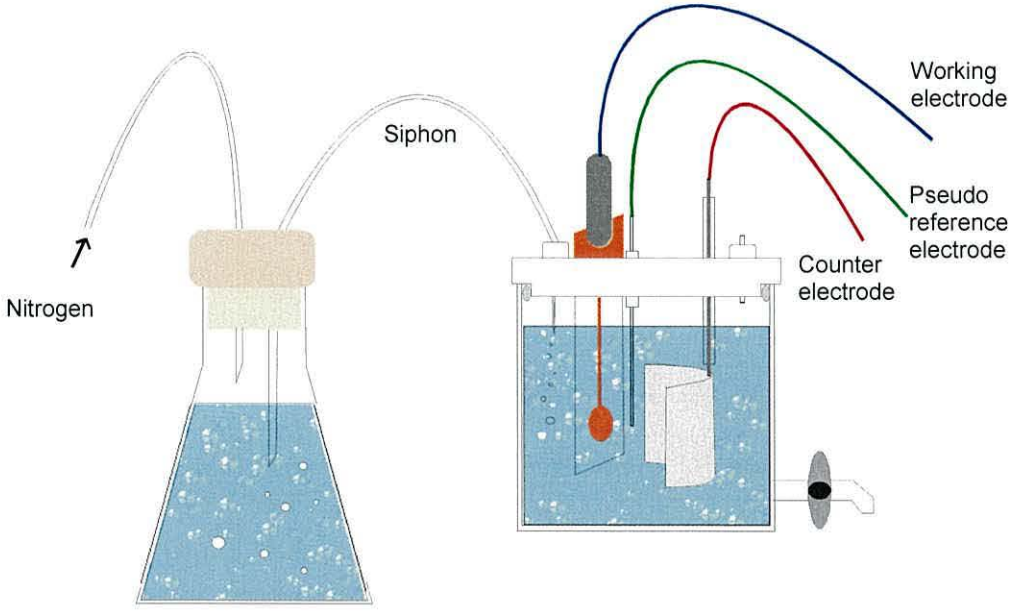

Figure 3.3 *A diagram showing the experimental improvements to the electrochemical cell and procedure.*

3.4.7.1 *Electrochemical cleaning protocols*

Different waveform protocols for a range of potentials were applied and compared. For each protocol the cell was filled with a monomer free solution (solvent + TEAP).

Protocol 1 involved the application of a positive oxidation voltage E_2 (500 mV). This method was recommended by Jerome et al (1995) based on their experience of electrochemically cleaning the oxide from nickel electrodes prior to electrografting. For metals which readily oxidize at positive potentials protocol 2 was used where a negative reduction voltage E_2 (-1.5 to -2.0 V) was applied to activate the surface. Finally protocol 3 based on the ORC method used the combination of both these protocols in sequence, an oxidation (500 mV) followed by a reduction cycle (-1.5 V). E_2 was reprogrammed at the end of the positive cycle. The magnitude of the peak voltage in each case depended on the working electrode metal. The waveform was repeated until a reproducible form was evident. Then the cell was drained maintaining the blanket of nitrogen and refilled with the electrolyte containing the monomer.

3.4.7.2 *Electropolymerization*

a) *Cathodic*

Table 3.2 is an example of a typical waveform which was programmed into the potentiostat for cathodic electropolymerization:

Table 3.2 *Cathodic waveform.*

E_1	Delay1	Scan1	E_2	Delay2	Scan2	E_3
0 volts	5 secs	50mV/s	- 2 volts	5 secs	50mV/s	0 volts

The voltage E_2 and the scan rates s_1 and s_2 were the main experimental parameters and were changed as required. During electropolymerization it was necessary to monitor the current during the voltage sweep from E_1 to E_2. According to Mertens et al (1998), Baute et al (1998) and others electrografting was supposed to occur at Peak I. A manual control option on the potentiostat allowed the user to over-ride the program if a peak was observed and start the return scan. Care was taken not to exceed voltages yielding a peak as debonding and film damage to films occurred. The position of the peak was difficult to predict and a number of factors affected the intensity and position. Current peaks and

visible film formation were often found to be unreliable indicators of electrografting. The concentration of the monomer in the electrolyte was a contributing factor. Low concentrations of monomer e.g. 0.2M produced thin films which were difficult to detect with the naked eye whereas higher concentrations failed to show significant current intensities. However successful film growth was confirmed by a passivation test. This involved repeating the previous scan. Untreated PAN is an insulator; if an electrografted film has formed the electrode should exhibit a level of passivation depending on the surface coverage of the film. Cyclic voltammograms were recorded and compared.

b) *Anodic*

Anodic electropolymerization trials using Ag working electrodes were unsuccessful. On application of a positive voltage sweep the Ag was observed to dissolve into the supporting electrolyte and the experiment was terminated. According to Skothiem et al (1986) Ag is not a good choice of anode as it oxidizes more readily than the monomer. The anode needs to be inert under the conditions used. So no further studies of anodic electropolymerization were undertaken.

3.4.8 Preparation of films for characterization.

After rinsing in a suitable solvent the working electrode was carefully removed for drying. Acetone a more volatile solvent and known for its drying capability was compared in a trial rinse to DMF and ACN. The film was then placed under a gentle stream of dry nitrogen to remove any excess solvent from the surface. According to Sánchez-Soto et al (2001) the amide molecules are difficult to completely eliminate from PAN films and can remain trapped even after prolonged drying. For more efficient removal of any remaining solvent the films were left overnight in a vacuum drying oven at 80°C (see Figure 3.4). The films were then ready for characterization.

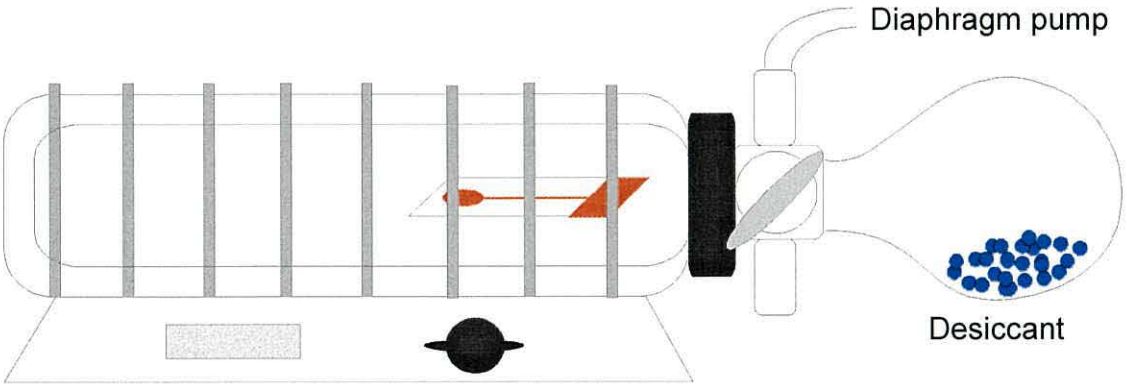

Figure 3.4 *Vacuum drying oven used to assist the removal of trapped solvent in films before characterization.*

3.5 Commercial polyacrylonitrile

Commercial PAN powder, average molecular weight of 150,000, was purchased from *Aldrich* for comparison and confirmation of electropolymerization. 10% PAN by weight was dissolved in DMF by heating gently in a hot water bath (glass transition temperature, T_g of PAN is 85°C). Thin films on different substrates were prepared by spin coating at 3000 rpm for 30 s on glass slides coated with different metals: Au, Ag and blank. The slides were then placed in a vacuum desiccator overnight to eliminate the solvent. Film thicknesses of approximately 200 nm were measured using an AFM. Both FTIR and Raman spectra were recorded.

3.6 Electropolymerization experiments.

The experiments listed below were carried out using the above techniques. In each case cyclic voltammograms, FTIR, Raman, UV vis spectra, AFM images and ellipsometry measurements were recorded and are presented in Chapter 4.

1. Confirmation of polymerization - electrografted films were compared to spun coated commercial samples.
2. Confirmation of electrografting - the adhesion of an electropolymerized film to the metal substrate was assessed for evidence of electrografting.
3. Films electrografted on different metal substrates; Au, Ag, Cu and Pt, for different monomer concentrations were compared.

4. Electrochemical cleaning protocols. Different electrochemical pretreatments of the different metal substrates were assessed by comparing the resulting film qualities.
5. Investigating the effect of electrochemical pretreatment on the surface morphology of the metal substrates. The surface roughness of vapour deposited metal films; Au, Ag and Cu, was measured before and after the application of an electrochemical pretreatment using an AFM.
6. The influence of the thickness of the keying layer of chromium was assessed.
7. Solvent effect on the quality of electrografted films. Cyclic voltammograms, spectra and AFM measurements of polyacrylonitrile films grown in different supporting solvents; DMF a solvent of the polymer and ACN a non-solvent were compared.
8. Thickness control, the influence of the monomer concentration, solvent and metal substrate was investigated using AFM and ellipsometry measurements.
9. Attempts to eliminate the solvent trapped in electrografted films grown in different solvents were compared by analyzing the spectra of films rinsed in acetone, a volatile solvent or drying overnight in a vacuum drying oven at 80°C.
10. Raman investigation into electronic transitions. Films grown on different pretreated metal substrates were excited using lasers of different wavelengths and the corresponding Raman spectra were compared.
11. Investigation of heat treated PAN films using UV vis, FTIR, Raman spectroscopy. Films were prepared by electrografting a thin polymer film (1M AN, DMF, 0.05M TEAP) onto a transparent 10nm thick Au vapour deposited substrate. The films were then heated to 225°C in a vacuum drying oven. Spectra of the films were taken before and after the heat treatment and analysed for any structural changes.
12. Investigation into the heating effect of the Raman laser intensity. Spectra of electrografted PAN films using the laser at different intensities and duration were analysed for any transformations.
13. Monomer trials – water content measurements

3.7 Film characterization

The effect of changing the growing conditions was monitored by investigating film morphology and chemical structure using a combination of Raman Microscopy, Atomic Force Microscopy, FTIR spectroscopy, UV VIS spectroscopy and Ellipsometry.

3.7.1 Fourier transform infra red (FTIR) and Raman spectroscopy

FTIR and Raman spectroscopy were used to characterize and identify the chemical structure of the electropolymerized polymer films. Both techniques involve shining light on a sample and recording the frequency of molecular vibrations energised by the incident light. However the mechanisms underpinning the techniques are different and provide complimentary spectral information. The spectra are complex and are characteristic of the entire molecule. This complexity allows the user to match an unknown against reference spectra through peak by peak correlation. The position, intensity and shape of the different bands give clues to the identification of the polymer structure. Reference charts were used to recognize the characteristic bands of different molecular substituents. The structure of the polymer was proposed after a detailed study of the different bands in the different spectra which were characteristic of particular functional groups and their relative environment.

3.7.1.1 *Infrared spectroscopy.*

Infrared spectra are obtained when a sample absorbs radiation from the infrared region of the electromagnetic spectrum 4000 – 40 cm^{-1}. The absorbed radiation is converted by the molecule into energy of molecular vibration. In quantum mechanical terms a transition occurs between two vibrational energy levels E_1 and E_2. The difference in these energy levels ΔE is equal to the energy of the adsorbed photon hf i.e.

$$\Delta E = E_1 - E_2 = hf \qquad (3.1)$$

The frequency of the infrared radiation absorbed directly translates to the frequency of the vibration. The absorption appears as a band due to accompanying changes in rotational energy. The frequency of absorption depends on the relative masses of the atoms, the force constants of the bonds and the geometry of the structure. The band positions are presented as wavenumbers and intensities can be expressed as transmittance or absorbance. Transmittance is the ratio of radiant intensity transmitted to the incident

intensity. Absorbance is the logarithm of the reciprocal of the transmittance. The intensity of absorption A can be directly related to the concentration and pathlength l using the Beer- Lambert law (Lambert et al, Organic structural spectroscopy, 1998).

$$A = \varepsilon Cl \qquad (3.2)$$

where ε is the molar absorption coefficient.

There are two types of molecular vibrations; stretching and bending. Stretching vibrations are rhythmical movements along the bond axis and can be either symmetrical or antisymmetrical. Bending vibrations involve changes in bond angles between bonds with a common atom or the movement of a group of atoms with respect to the rest of the molecule without movement of the atoms in the group with respect to one another. Examples of bending vibrations are twisting, wagging, rocking, scissoring etc. Only vibrations resulting in a change in dipole moment are observed using FTIR spectroscopy. The changing charge distribution from the vibration produces an alternating electric field which couples with the oscillating field of the infrared radiation. Generally functional groups with a strong dipole give rise to strong absorptions in the infrared. Fundamental vibrations where there is no change in the centre of gravity are generally the strongest absorption bands. However overtones (multiples of the frequency) and combinations (the sum of two other vibrations) can add to the background complexity of spectra.

a) *FTIR instrument and method*

The FTIR spectra of the electropolymerized polymer samples were recorded on a *Bomem Michelson MB-100* Fourier transform infra-red spectrophotometer, equipped with SiC internal source. Depending on the film thickness the instrument was set for different scan accumulations at 4 cm^{-1}resolution in the Mid IR region, (4000 - 400 cm^{-1}) using *Win Bomem Easy* (*version 3.04*). The spectra were obtained in reflection mode at incident grazing angles of 60° and 80°. The sample holder was open to the atmosphere. Prior to the recording of a polymer spectrum, a subtraction spectrum was taken of a blank evaporated metal-coated slide.

3.7.1.2 *Raman spectroscopy*

When light is scattered by a molecule most of the photons are scattered elastically. However a small fraction (1×10^{-7}) are inelastically scattered at an optical frequency usually lower than the frequency of the incident photons. This is known as the

Raman effect. This can occur when there is a change in the vibrational energy of a molecule. The difference in energy between the incident photon and the Raman scattered photon is equal to the vibration of the scattering molecule. This vibrational energy is dissipated as heat in the sample. A Raman spectrum is a plot of the intensity of the scattered light versus the energy difference. Zero on the abscissa corresponds to the frequency of the laser line used to excite the spectra. Positions of peaks are shifts between the laser frequency and observed frequency. These are converted to wavenumbers due to the large range of frequencies. At room temperature the majority of molecules are in the ground state and the scattered photon will have a lower energy than the incident exciting photon resulting in the usually observed Stokes shift. However according to the Boltzmann population of states a few will be in an excited state. When a Raman scattered photon leaves these molecules in a ground state an Anti- Stokes shift can be observed. These photons will have a higher energy. Stokes and Anti-Stokes shifts give the same frequency information. Raman and Infrared spectra are directly comparable.

Strong Raman scatterers are functional groups with de-localised electron clouds such as the carbon-carbon double bond which are easily polarized in the electric field of the incident photon. The bending or stretching of such a group causes a large change in the dipole moment. In contrast, a molecular vibration will be infrared active when the incident radiation causes a net change of permanent dipole moment during the vibration. Hence, vibrations in molecules with a centre of symmetry will be Raman active and infrared inactive.

Intensities in Raman are less quantitative. The height of a band depends on a number of factors namely the laser power, wavelength of the exciting radiation, detector and amplification system used. However quantitative results can be obtained if an internal standard is used. In Raman the intensity is a linear function of the concentration whereas with infrared the intensity dependency is logarithmic. Therefore doubling the concentration for the same settings in Raman will double the peak size in contrast to infrared where the relative change will depend on the initial peak intensity .i.e. weaker bands showing a bigger increase.

a) *Resonance enhanced Raman scattering (RERS)*

Raman spectroscopy is generally performed using a helium neon (632.8 nm) or argon ion (514.5 nm) laser. The wavelength of these lasers is usually lower than the first electronic transition of most molecules. However if the excitation wavelength falls within the spectrum of a molecule the intensity of some Raman-active vibrations can be enhanced by a factor of 10^2-10^4. There are different types of mechanism to enhanced Raman scattering (RERS). Franck-Condon enhancement is when the vibration is in a direction in which the molecule expands during an electronic excitation; the bigger the expansion the greater the enhancement. Another is vibronic enhancement where a vibration couples together two electronic transitions. In both cases enhancement factors roughly follow the intensities of the absorption spectrum. Resonance enhancement does not begin at a sharply defined wavelength. If the exciting laser is within a few hundred wave numbers below the electronic transition of a molecule, sometimes enhancements of 5 to 10 x can be seen.

b) *Surface enhanced Raman scattering (SERS)*

Enhancements of 10^3-10^6 can be obtained for molecules either adsorbed on or lying within a few angstrom of a structured metal surface. The specially prepared metal surface is usually Ag, Au or Cu. Surface enhanced Raman scattering (SERS) is generally stronger for Ag. There are two mechanisms contributing to this enhancement. The electromagnetic field mechanism occurs when the wavelength of the incident light is close to the plasma wavelength of the metal, resulting in conducting electrons being excited to an extended surface electronic excited state known as surface plasmon resonance. Molecules at the surface will be subjected to an exceptionally large local electromagnetic field with molecular vibration modes normal to the surface being enhanced the most.

SERS is strongest for molecules with lone pairs of electrons and π electron clouds. The intensity of the surface plasmon resonance is dependent on the wavelength of the laser and the morphology of the metal surface. The coin metals are generally used because their plasma wavelengths are within the visible spectrum. Schatz et al (2002) has compiled a diagram showing the plasma wavelength response of a variety of metals (see

Figure 3.5). Ag has a broad spectrum spanning the visible range in comparison to Au and Cu which are confined to the 600 nm region.

A variety of morphologies have been explored. A review of SERS by Campion et al (1998) found that electrochemically roughened surfaces of 10-100 nm gave the largest enhancement. Emory et al (1998) has shown that different sized Ag particles are responsive to different wavelengths, suggesting morphologies can be tuned to certain wavelengths. According to Brolo et al (1997) bumps in a rough surface provide the additional momentum for the photon to excite surface plasmon resonance. The other less dominant mechanism is due to the formation of a charge transfer complex between the absorbate and the surface (Schatz et al, 2002).

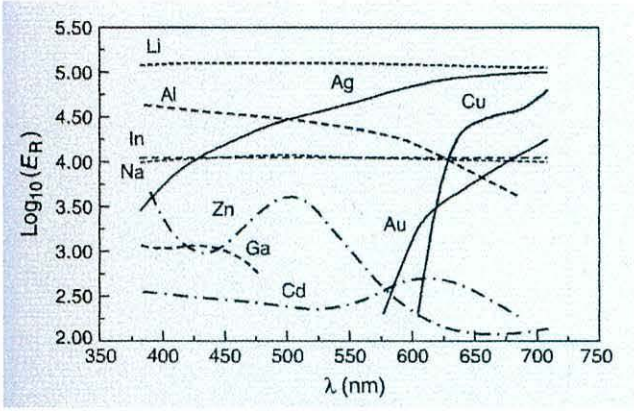

Figure 3.5 *Fully optimized Raman enhancement versus wavelength λ (optimized with respect to size and shape). The diagram compiled by Schatz et al (2002) is a useful guide in quantifying the EM for a variety of metals.*

c) *Raman microscopy and procedures*

Spectra were recorded with a Renishaw Ramanscope 1000 fitted with a 50x 0.75 NA objective. This was done in the backscatter geometry, that is the light collected was scattered back along the path of the laser. A helium/neon red light emitting laser of wavelength 632.8 nm was used for the majority of the work with an additional argon ion green laser 514.5 nm used in a comparative investigation into RERS and SERS effects. The laser light enters the spectrometer (see Figure 3.6) via a set of alignment mirrors and attenuation filters. Attenuation of the laser power is achieved using an attenuation filter wheel containing neutral density filters of transmittance percentages 10, 25, 50 and 100. Mirror alignment ensures a uniform intensity profile. The laser light is collimated via a lens into a parallel beam and reflected onto a holographic notch filter. The beam is then

reflected into the optical path of the microscope to illuminate the sample which is positioned using a motorized x-y stage. The amount of sample illuminated is dependent on the spot focus. The 25 mW laser was focused to spot size diameter of approximately 5 μm or less. A beam splitter allows the sample to be illuminated with white light to aid effective focusing and positioning of the sample. On the return path the 180° backscattered light is passed through the holographic notch filters to remove the Rayleigh elastic back-scattered component. The remaining Raman scattered light is re-collimated and reflected onto a diffraction grating dispersing the content for detection using a charge coupled device array detector (CCD).

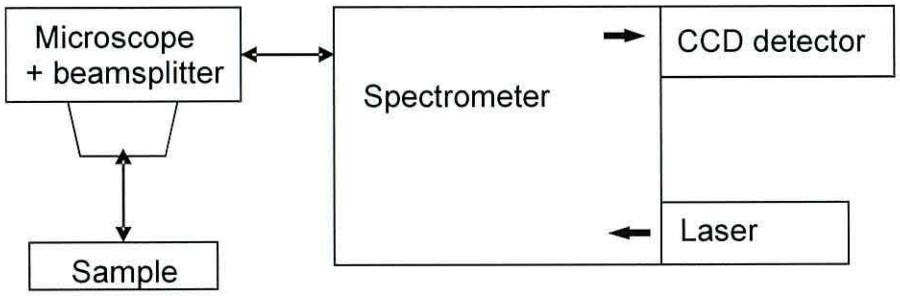

Figure 3.6 *A schematic diagram for the Raman optical system*

Good spectral resolution and signal strength were maintained by carrying out a performance verification and optimization routine each time the Ramanscope was used. Using the 50x objective a static spectrum of a Si wafer was taken using a 1 s exposure time. Si has a characteristic sharp band at 520 cm^{-1} which can be used to achieve optimum intensity by adjusting the pre-slit lens and slit position.

One of the main disadvantages of using Raman is the problem of fluorescence obscuring the spectral information from the polymer films. This was thought to be due to impurities fluorescing at the metal surface. Quenching was one suggested method. This involves leaving the laser incident on the sample for a while then running the analysis to burn off the impurities. However this method was used with caution as the chemical structure of PAN films subjected to prolonged radiation can be transformed. Alternatively using the green laser provided improved efficiency and a reduction in surface penetration ensuring that only the polymer film was analysed.

The procedure used to collect a spectrum depended on the thickness and quality of the films. A variety of exposure durations and accumulations were used to optimize

the spectral intensities and improve the signal to noise ratio. Thin films up to 200 nm need the signal to be built up. The CCD detector is shot-noise limited, so that long scans were found to give better signal-to-noise ratio than obtained in a series of short accumulations i.e. a single 100 s scan is better than 10 x 10 s scans.

3.7.2 UV-VIS spectroscopy

UV-VIS absorption spectra were measured using a *Hitachi U2000* spectrophotometer in the wavelength range 350–700 nm. The aim of the experiment was to investigate the structural transformations that occur when an electrografted PAN film is heat treated. Absorption peaks between 200 nm and 700 nm can indicate the presence of unsaturated bonds based on electron transitions from π bonding orbital to the π^* anti-bonding orbital. For these measurements electrografted films were grown on 10 nm thick semi-transparent Au electrodes and a blank Au coated slide was used as a reference. A spectrum of the PAN film was taken before and after heat treatment for comparison.

3.7.3 Atomic force microscopy (AFM)

A *Digital Instrument Nanoscope IIIA* multimode scanning probe microscope was used to analyse the surface topography of the electropolymerized polymer films and the electrochemically cleaned metal substrates.

The AFM builds up an electronic image of the surface by raster scanning the surface of a sample with a sharp probe or tip. The tip is on the end of a cantilever which bends in response to any changes in surface topography. A light reflecting off the top of this cantilever transfers any changes on to a split photodiode. For small displacements the cantilever obeys Hooke's law and therefore allows the interaction between the tip and surface to be measured. An extremely precise positioning device made from piezo-electric ceramics controls the movement of the tip or sample. The positioning device uses electronic feedback to respond to any changes in force which are detected, changing the tip to sample separation to restore the force to a pre-set value (see Figure 3.7)

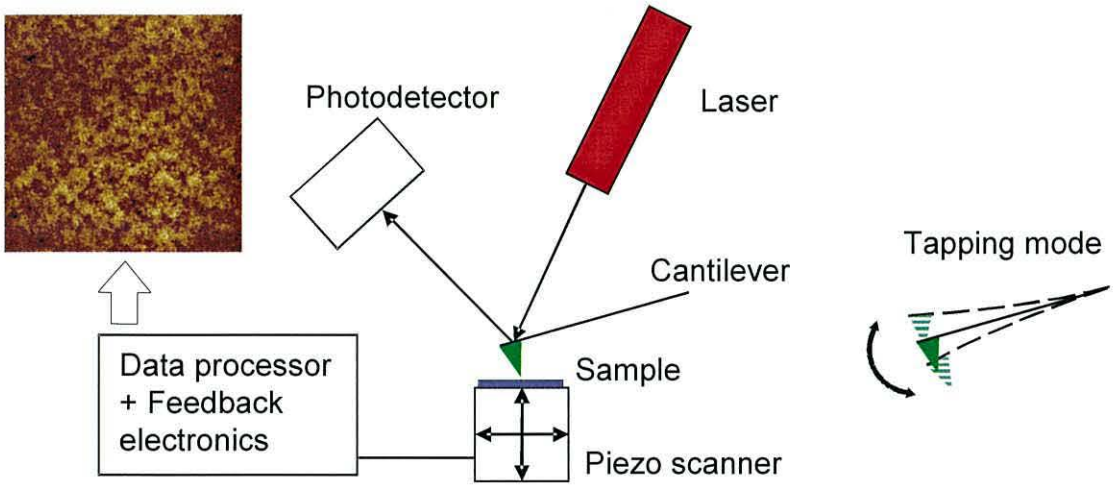

Figure 3.7 *Schematic diagram of an atomic force microscope interaction between tip and sample.*

Images of the films / metal substrates were obtained using either contact mode or tapping mode. In contact mode the tip (Si_3N_4) and sample remain in close contact as the scanning proceeds, within the repulsive regime of the inter-molecular force. A disadvantage of remaining in contact with the sample is that there exist large lateral forces on the sample as the tip is "dragged" over the surface. In tapping mode the cantilever is oscillated at its resonant frequency and positioned above the surface so that it only taps the surface for a very small fraction of its oscillation period. The very short contact times dramatically reduces the drag on the tip (Si) as it scans the surface. Tapping mode was the preferred choice when raster scanning soft samples. A surface roughness analysis was carried out by recording and comparing the image statistics; root mean square roughness, average roughness etc, for sample areas of 5 μm x 5 μm Thickness measurements involved the careful scoring of the polymer film using a scalpel blade and raster scanning the step using tapping mode. This was a difficult procedure to execute accurately as the cut often strayed into the metal substrate. Tips were also prone to fracture if the step was too large.

3.7.4 Ellipsometry

Electropolymerized PAN films grown on Ag, Au, and Cu substrates from 2M AN concentrations were sent to Hull University for ellipsometry measurements. The

instrument used for the work was the Philips SD 2000 ellipsometer, with a 633 nm wavelength laser. This machine is capable of measuring thicknesses of 0.1 to 1000 nm much smaller than the wavelength of the incident light used. Ellipsometry is a non-destructive specular optical method of probing thin transparent films absorbed on reflective substrates. By using the change in polarization of light reflected from the surface, the film thickness and refractive index can be determined. The electric field of the light incident on a reflective surface is the vector sum of two components; the s component oscillating perpendicular and the p component parallel to the plane of incidence. When light is incident on a reflective substrate with a thin transparent film adsorbed at the surface both these s and p components will undergo a phase and amplitude shift upon reflection. These shifts are different for each component. This results in a change of polarization for the reflected beam to that of the known polarization state of the incident beam which is usually either linear or circular. Both the path length through the film and its refractive index can determine the magnitude of this change. The reflected beam is generally elliptically polarised, hence the name 'ellipsometry'.

The amplitudes of the *s* and *p* components, after reflection and normalized to their initial value, are denoted by r_s and r_p, respectively. Ellipsometry measures the ratio of r_s to r_p, which is described by the fundamental equation of ellipsometry.

$$\frac{r_p}{r_s} = \tan \Psi e^{i\Delta} \tag{3.3}$$

Where $\tan\Psi$ is the amplitude ratio upon reflection, and Δ is the phase shift (difference). Ellipsometry is an indirect method, i.e. the measured Ψ and Δ cannot be converted directly into the film thickness (h) and complex refractive index (n). A complex model analysis must be performed. A three-layer model (Figure 3.8) was used to describe the PAN film absorbed onto the metal substrate. It was assumed the film and substrate had a uniform composition and the reflecting surface was perfectly smooth.

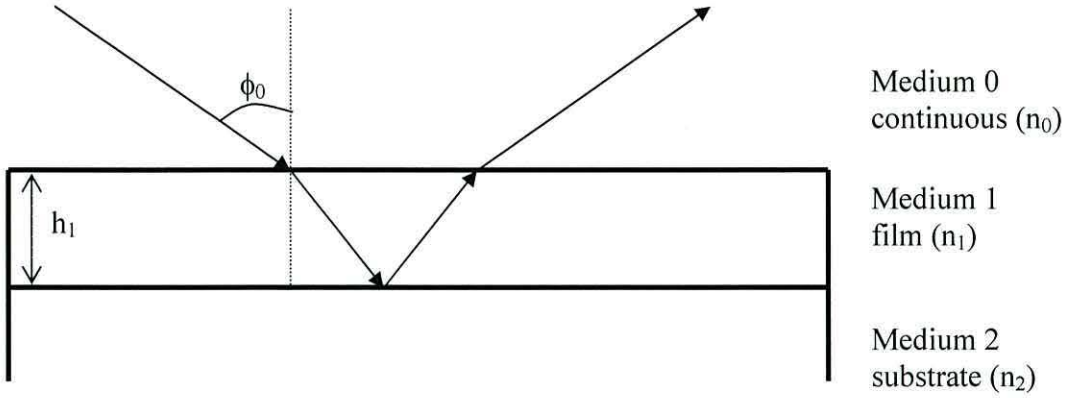

Figure 3.8 *The three layer model representing the PAN film absorbed on to the metal substrate.*

To calculate Ψ and Δ for this system knowledge of the complex refractive indices, the thickness and the incidence angle for each layer is required. The optical model is built up from as much information as possible leaving the three unknowns; the film thickness and the real and imaginary parts of the refractive index (McCrackin, 1969). Using an iterative procedure these unknown parameters are varied, and Ψ and Δ values are calculated using the Fresnel equations. The calculated Ψ and Δ values, which best fit the experimental data provide the refractive indices and thickness of the PAN film.The resulting film thicknesses were then compared to those obtained using the AFM. As ellipsometry measures the ratio or difference of two values rather than the absolute values it can potentially produce accurate and reproducible results. Advantages of using this method are its insensitivity to scatter and non-requirement of a reference sample (Tomkins, 1993).

3.8 References

ASTM D3359 *Test methods for measuring adhesion by tape test- annual book of ASTM standards* Vol 6.01 ASTM Philedelphia PA (1994).

Baute, N., Teyssié, P., Martinot, L., Mertens, M., Dubois, P. and Jérôme, R. *Eur. J. Inorg. Chem.* (1998), 1711.

Brolo, A.G., Irish, D.E. and Smith, B.D., *J. Mol. Science,* **405**, (1997), 29

Campion, A. and Kambhampati, *Chem. Soc. Reviews.* **27**, (1998), 241.

Emery, S.R., Haskin, W.E. and Nie, S., *J. Am. Chem . Soc.,* **120**, (1998), 8009.

Gernet, S., Koudelka, M. and de Rooij, N., *Sensors and Actuators B,* **18**, (1989), 59.

Jérôme, R., Mertens, M. and Martinot, L. *Advanced Materials,* 7, **No 9,** (1995), 807.

Lambert, B.L., Shurvell, H.B., Lightner, D.A. and Cooks, R.G., *Organic structural spectroscopy, Prentice Hall,* (1998).

Ling, T.G.I., Beck, M., Bunk, R., Forsén, E., Tegenfeldt, J.O., Zakharov, A.A. and Montelius, L., *Microelectronic Engineering,* **67, (**2003), 887.

McCrackin, F.L., Natl. Bur. Stand. (U.S.) Tech note, 479, (1969).

Mertens, M., Calberg, C., Baute, N., Jérôme, R. and Martinot, L., *J. Electro. Chem.* **441**, (1998), 237.

Mills, C.A., Lacey, D., Stevenson, G. and Taylor, D.M., *J. Mater. Chem.,* **10**, (2000), 1551.

Muniz-Miranda, M., Pergolese, B., Bigotto, A., Giusti, A and Innocenti, M., *Materials Science and Engineering* C **27, (**2007),1295.

Sánchez-Soto, P.J., Avíles, M.A., del Río, J.C., Ginés, J.M., Pascual, J. and Pérez-Rodríguez, J.L., *J. Anal. App. Pyrolysis*, **58**, (2001), 155.

Schatz, G. C. and Van Dyne, R.P., *Handbook of Vibrational Spectroscopy,* Wiley (2002).

Schoenfisch, M.H., Ross, A.M. and Pemberton, J.E. *Langmuir,* **16**, (2000),2907.

Taylor, D.M., Gomes, H.L., Underhill, A.E., Edge, S. and Clemenson, P.I., *J. Phys. D: Appl. Phys.,* **24**, (1991), 2032.

Skotheim, T.A., *Handbook of Conducting Polymers;* Marcel Dekker; New York, (1986); Chapter 8, p268.

Tian, Z.Q., Ren, B. and Mao, B.W.,*J. Phys. Chem. B,* **101**, (1997), 1338.

Tomkins, H.G.,*A user's guide to ellipsometry, Academic Press, London*, (1993).

Xue, G., Dong, J. and Zhang, J., *Polymer,* **35**, (1994), 723.

Chapter 4: Results obtained during the study of PAN.

4.1 Introduction

This chapter gives an evolutionary account of the results obtained from the different stages in the development of the electrografting technique. The aim of the experiments was to investigate and identify the necessary experimental conditions for the electrografting of good quality PAN films suitable for surface functionalization. Once established these conditions were then to be applied to more interesting monomers with a greater functional group potential. At different stages during the above process various attempts were made to electrograft a range of such vinyl monomers. However poor film growth emphasized the sensitivity to the experimental conditions.

Where possible the results are given in chronological order to emphasize the rationale underlying certain experimental parameter changes. Unexpectedly, the Raman spectroscopy characterization of the PAN films revealed some unique spectral peaks not seen before in FTIR spectra of this polymer. This finding motivated the dedication of a large proportion of the experimental work to investigating the cause of this feature. This, in conjunction with the irregularities seen in the corresponding cyclic voltammograms and the limited success with alternative monomers justified this experimental commitment.

4.2 Electropolymerization – confirmation of polymerization.

Following a series of necessary modifications to the Mills' technique namely dry solvents protected with molecular traps, the electrolyte salt dried overnight in a desiccator, the removal of the monomer inhibitor using a column and an improved electrochemical cell design, the first PAN films were successfully grown on Ag working electrodes. However potentiostat control proved difficult. The Peak I referred to by Mertens et al (1998) was not observed. Cyclic voltammograms were difficult to interpret. The voltage scan was halted and reversed as soon as visible signs of film growth were observed, despite evidence of further electroactivity. Attempts to scan to higher negative voltages only resulted in the debonding of the film. Electroactivity occurred at a lower than expected negative potential for the electroreduction of AN suggesting a significant quantity of water was still present (see Figure 4.1).

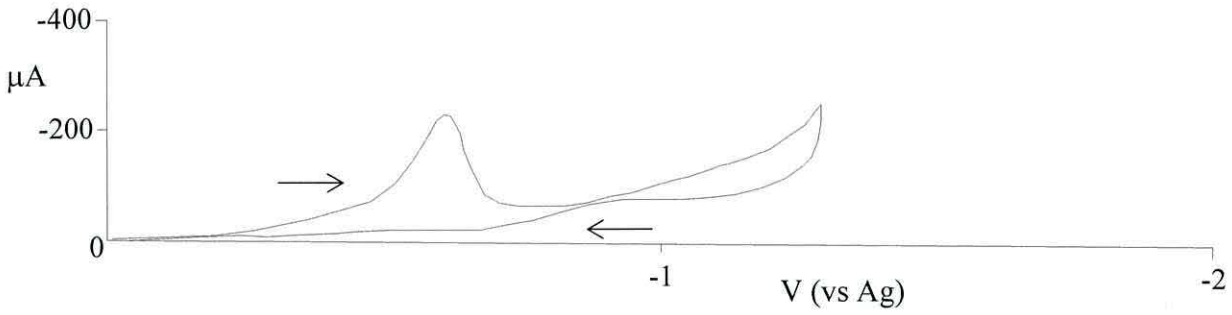

Figure 4.1 *Cyclic voltammogram of the electrografting of PAN showing clearly the effect of water at ~ -600 mV, (AN 0.5M, DMF, TEAP 0.05M, Ag slide electrode, 20 mV/ s scan rate).*

The films were characterized using Raman and FTIR spectroscopy. A comparison of the respective spectra with those of the monomer and a spun coated sample of the commercial PAN confirmed polymerization (see Figure 4.2 and 4.3). Table 4.1 gives the characteristic FTIR and Raman frequencies of the monomer and polymer for reference.

Table 4.1 *Characteristic IR / Raman frequencies (cm^{-1})*

Acrylonitrile	**Polyacrylonitrile**
ν **=C-H** (unsaturated) above 3000	ν **-C-H** (saturated) below 3000
ν **C=C** 1608	disappears
ν **C≡N** 2228	ν **C≡N** 2243
δ **CH_2** 1412	δ **$-CH_2-$** 1455
C-H rocking 1288	δ **=CH-** 1386
C-H_2 rocking 1094	δ (- **CH_2-** & **=CH-**) conjugated 1093
H_2C=C wagging 970	
C=C-C bending 568	

4.2.1 FTIR spectral comparison

A comparison of the FTIR spectra in Figure 4.2 corresponding to the electropolymerized PAN film and the commercial spun-coated sample shows strong peak correlation both in the wavenumber and relative intensity of the absorption bands. The characteristic FTIR peaks for PAN are evident. The spectral similarity extends even to

the presence of trapped DMF solvent as evidenced by the strong peak at 1665 cm^{-1} attributed to the C=O carbonyl FTIR active stretch which is not present in the NIST library spectrum for PAN. Further confirmation that electropolymerization has occurred is provided by the non-appearance of the characteristic peaks associated with the monomer i.e. the C=C at 1608 cm^{-1} and the unsaturated =C-H stretch above 3000 cm^{-1}.

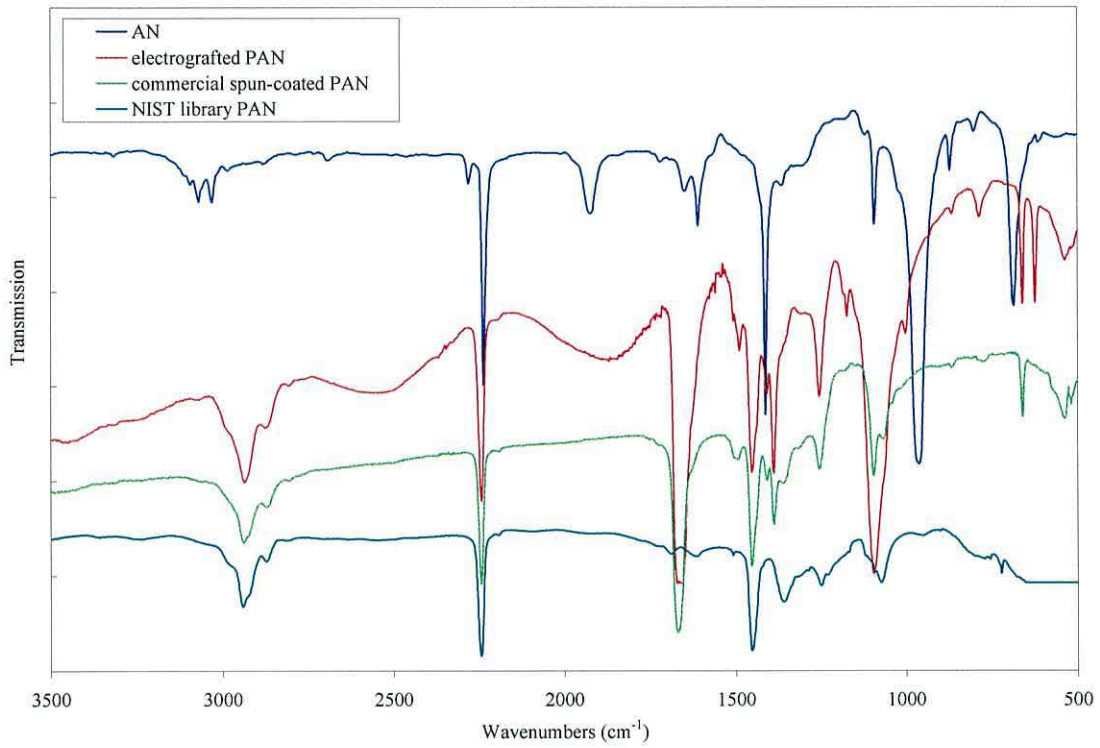

Figure 4.2 *FTIR spectra confirming electropolymerization of AN (AN 0.5M, DMF, TEAP 0.05M, Ag WE).*

4.2.2 Raman spectral comparison

Similarly the Raman spectra of the electropolymerized PAN correlate well with that of the spun-coated commercial sample of PAN. The characteristic peaks of PAN are clearly evident and like the FTIR results there is no indication of any monomer trapped in the film and a weak peak at 1660 cm^{-1} (a vibration not as active in Raman) also shows trapped solvent. However there are two unexpected peaks at ~1525 cm^{-1} and 1580 cm^{-1}. These anomalies were initially considered to be due to inadequacies in the experimental procedures e.g. contamination, poor potentiostat control etc, which proved not to be the case.

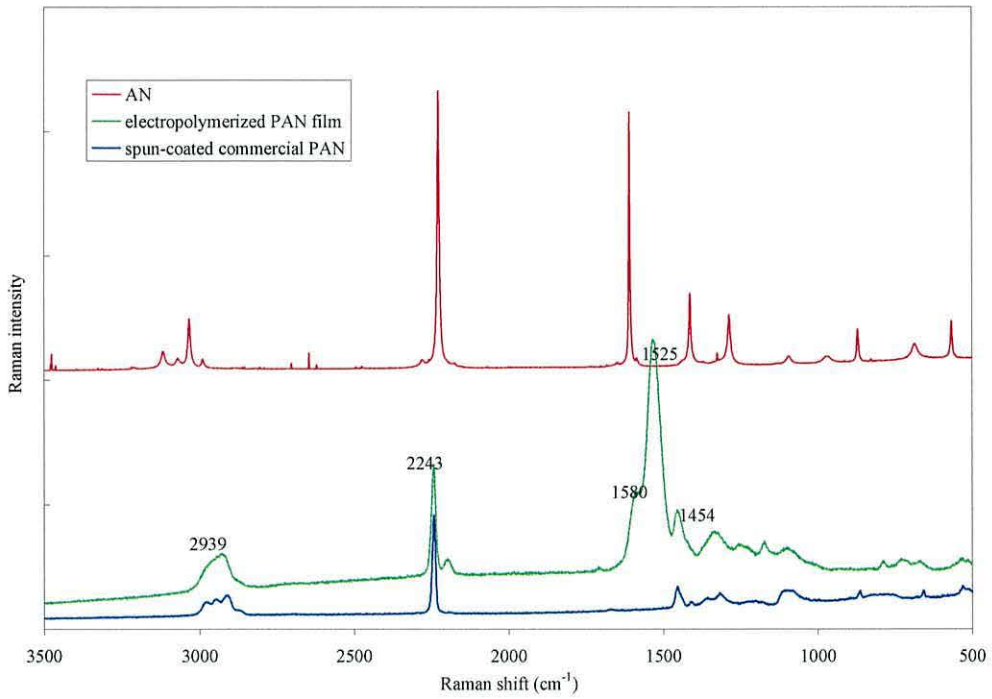

Figure 4.3 Raman spectra confirming the electropolymerization of AN
AN 0.5M, DMF, TEAP 0.05M, Ag WE.

4.3 Confirmation of electrografting

A number of points were considered when evaluating whether the PAN films were electrografted rather than precipitated onto the electrode.

- A standard peel test applied to a film/electrode edge failed to remove any PAN confirming a strong polymer-metal bond.
- PAN films resisted sonication in a solvent (DMF) bath.
- Films grown from the electrode surface in a solvent (DMF) for PAN provided strong evidence particularly as both the FTIR and Raman spectra showed no reasonable evidence of cross-linking of the polymer structure.
- AFM thickness measurements of PAN films grown in different solvents and monomer concentrations (see Section 4.18) were comparable to the findings of Calberg et al (1997).

4.4 Improvements in potentiostat control

Spectra of PAN films grown at different stages in the development of the electrografting technique (A to C) were recorded and compared, see Figure 4.4. Attempts to reduce the water content of the electrolyte and improve the potentiostat control resulted in visible improvements in film quality and their respective spectra. Comparison of the Raman spectra of the PAN films shows a sequential reduction of the non-characteristic PAN peaks of ~ 1525 cm^{-1} and 1580 cm^{-1} (peak values red shift to lower intensities). All other parameters remained constant i.e. monomer concentration, working electrode metal etc. However the voltammograms were inconsistent and difficult to interpret. The reduction peak appeared too low for the reduction of AN. There were no clear signs of electrode passivation from a repeat scan.

A microscopic inspection of the films showed non-uniformity of film growth and an abundance of holes which appeared to penetrate the whole film, suggesting insufficient current density supplied by the counter electrode for the former and a competing reaction at the electrode e.g. water reduction and the subsequent release of hydrogen gas to explain the latter. These holes probably allowed for continued electroactivity at the electrode and explained why no signs of passivation were observed. An AFM 3D image of the PAN film clearly shows these micro-structures (see Figure 4.5).

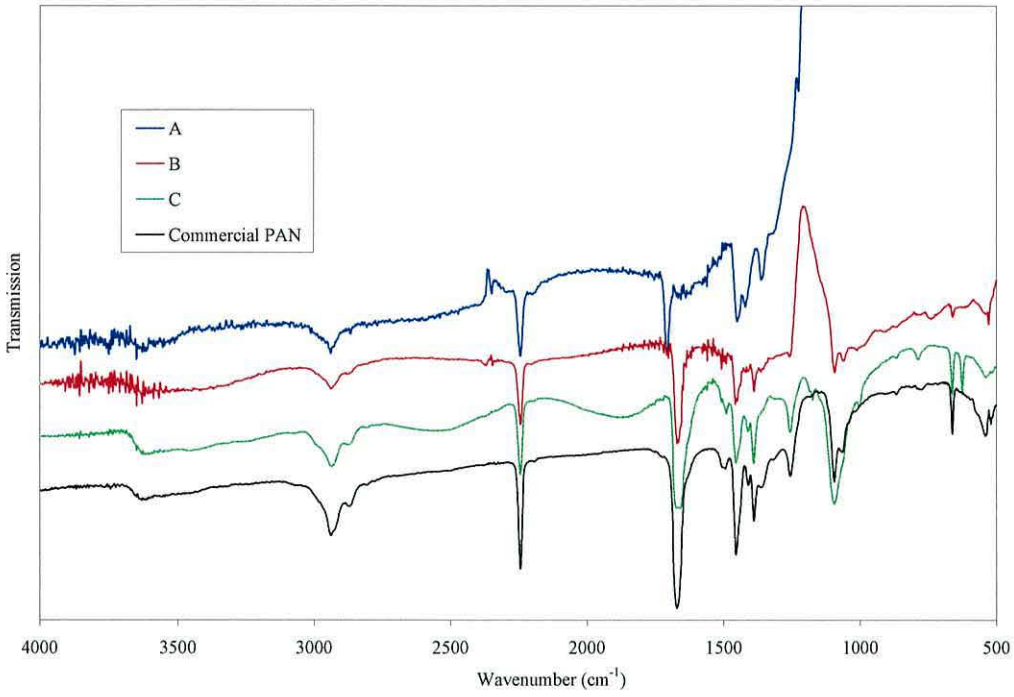

a)

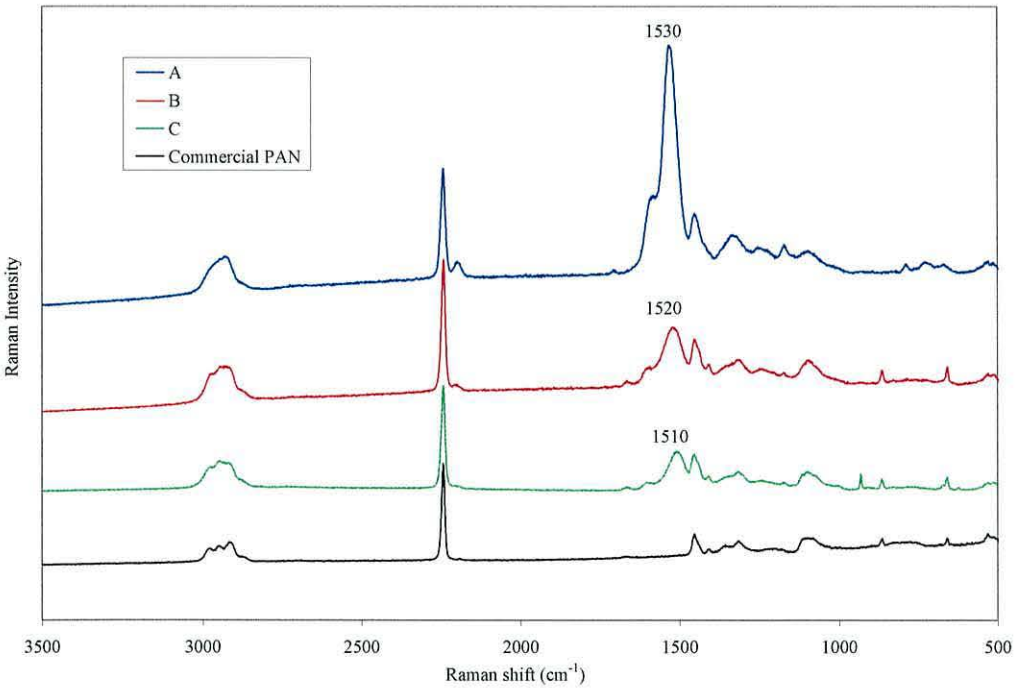

b)

Figure 4.4 a) *FTIR and b)Raman spectra of a range of electrografted PAN films showing the effect of improving potentiostat control from PAN film A to C (AN 0.5M, DMF, TEAP 0.05M, Ag WE)*

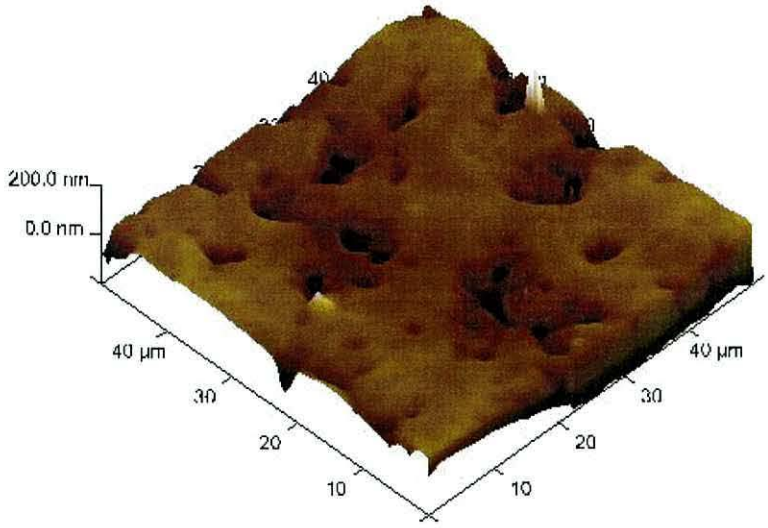

Figure 4.5 *AFM 3D image of an electrografted PAN film showing deep holes probably caused by the release of hydrogen gas from the competing reduction of water (AN 0.5M, DMF, TEAP 0.05M, WE Ag).*

4.5 Comparing different electrolyte solvents

PAN films electrografted in different solvents namely ACN and DMF were compared. In these measurements, water contamination was reduced further by the use of molecular traps, distillation of the monomer and the drying of the electrolyte salt TEAP in a vacuum oven overnight. A smaller working electrode was employed to encourage uniform film growth. Figure 4.6 compare the FTIR and Raman spectra. AFM micrographs of PAN films grown in the different solvents were also recorded and are shown in Figure 4.7.

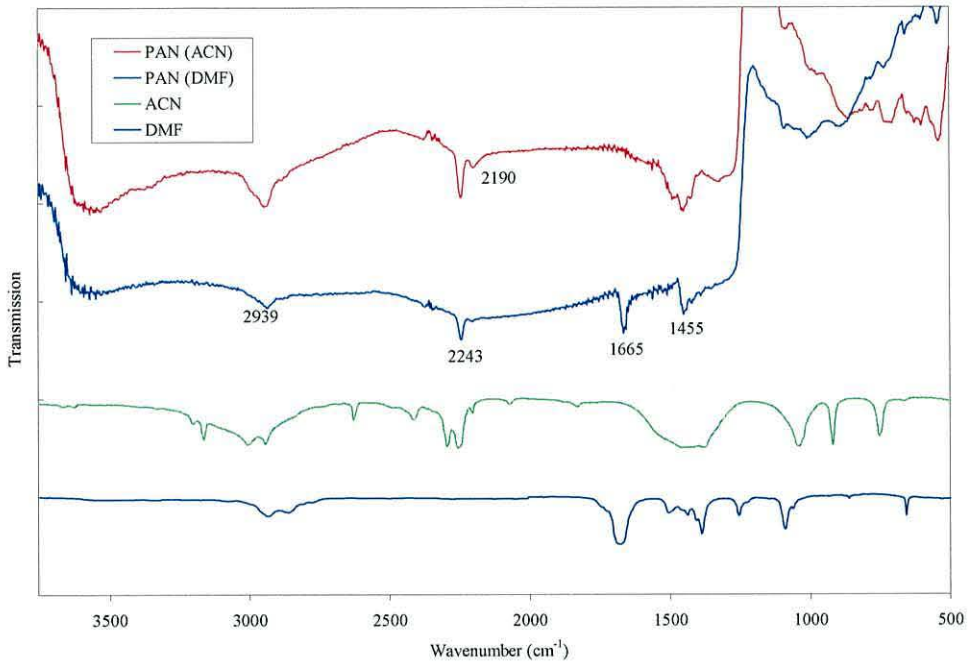

a)

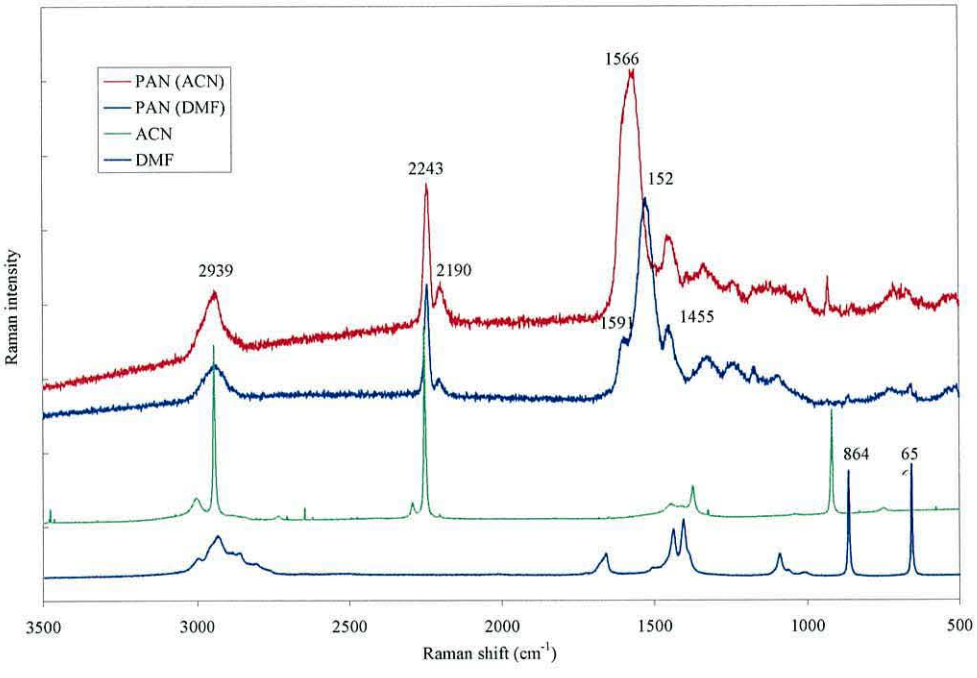

b)

Figure 4.6 *FTIR and Raman spectra of PAN films electrografted in different solvents together with the solvent spectra for comparison a) FTIR spectra b) Raman spectra (AN 0.5M, TEAP 0.05M, Ag WE).*

4.5.1 FTIR spectral observations

The FTIR spectra show some significant differences between films grown in ACN and DMF. The three characteristic PAN peaks at 2939, 2241 and 1455 $cm^{-1}$are evident for both samples. However the additional peaks clearly show the influence of the solvent. The peak at 1665 cm^{-1} for the PAN grown in DMF suggests some solvent remains trapped in this film as there are no signs of other peaks associated with PAN structural transformations, whereas the PAN films grown in ACN suggest the solvent has a structural effect. The peak at 2190 cm^{-1} is not characteristic of ACN and suggests some deterioration of the nitrile group and the subsequent formation of enamonitrile groups Newton et al (1997) observed such a structural transformation during the pyrolysis of electrografted PAN films. The peaks at 3345 and 1566 cm^{-1} associated with ν (N-H) and ν (C=N), although weak support these structural changes.

4.5.2 Raman spectral observations

Similarly, a study of the Raman spectra also reveals distinctive differences between the two PAN films. Both show the occurrence of unusual peak(s) between 1600 and 1500 cm^{-1}. However they vary in the position and number of these peak(s). For ACN this anomaly appears as a slightly broader peak at a higher frequency of 1566 cm^{-1}.

The most noticeable difference between the two PAN films was their outward appearance. PAN films grown in DMF appeared yellow, smoother, more uniform and transparent, whereas the films grown in ACN appeared whiter and more powder-like in consistency. This is not surprising since DMF had already been identified as the preferred solvent. According to Calberg et al (1997) it offers the greater range of thicknesses, (Calberg et al, 1998) a greater degree of isotacticity and it provides the experimenter with some indication of successful electrografting. A much closer inspection of these films using AFM confirmed the PAN films grown in DMF were smoother, as shown in Figure 4.7.

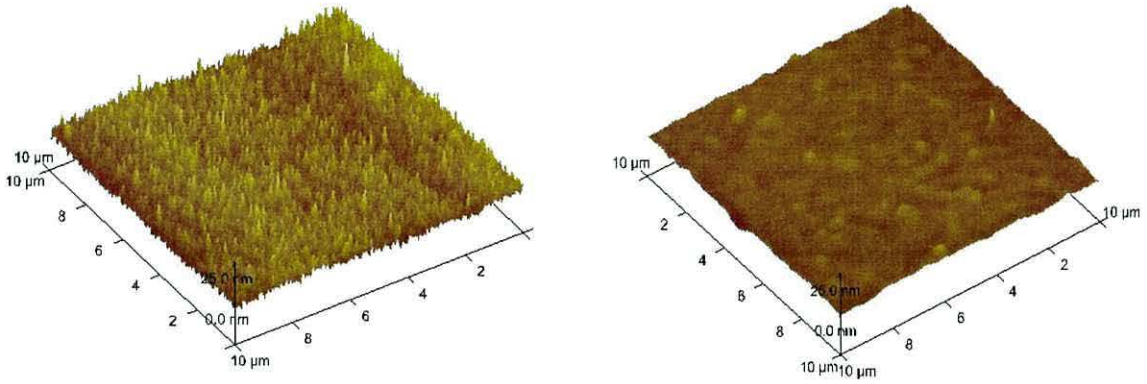

a) b)

Figure 4.7 *AFM 3D images of PAN films electrografted in a) ACN and b) DMF.*

AFM 3D images of PAN films electrografted in the different solvents show quite different surface topographies see Figure 4.7 above. The AFM measurements were performed in contact mode and at least 3 regions were analyzed for each sample. The root mean square (rms) roughness was computed using the Nanoscope software. PAN films grown in DMF gave a rms value of 0.68 nm compared to 2.47 nm for ACN.

4.6 Trapped Solvent

The FTIR and Raman spectra of PAN films electrografted in DMF both showed some evidence of DMF remaining trapped in the film. Acetone, a more volatile solvent and known for its drying capability, was compared in a trial rinse to DMF and ACN. Sánchez-Soto et al (2001) found that amide molecules are difficult to completely eliminate from PAN films and can remain trapped even after prolonged drying. The FTIR and Raman spectra of PAN films rinsed in acetone in Figure 4.8 show a marked reduction in the peaks associated with DMF. However no reduction was noted for the Raman anomalies. The main characteristic peaks associated with DMF and PAN are shown. Library spectra for DMF are given in Figure 4.9 for reference.

Acetone is an aggressive solvent and tended to crack the thinner PAN films during evaporation, as a result films were rinsed in DMF to remove any ungrafted PAN then left to dry overnight in a vacuum oven.

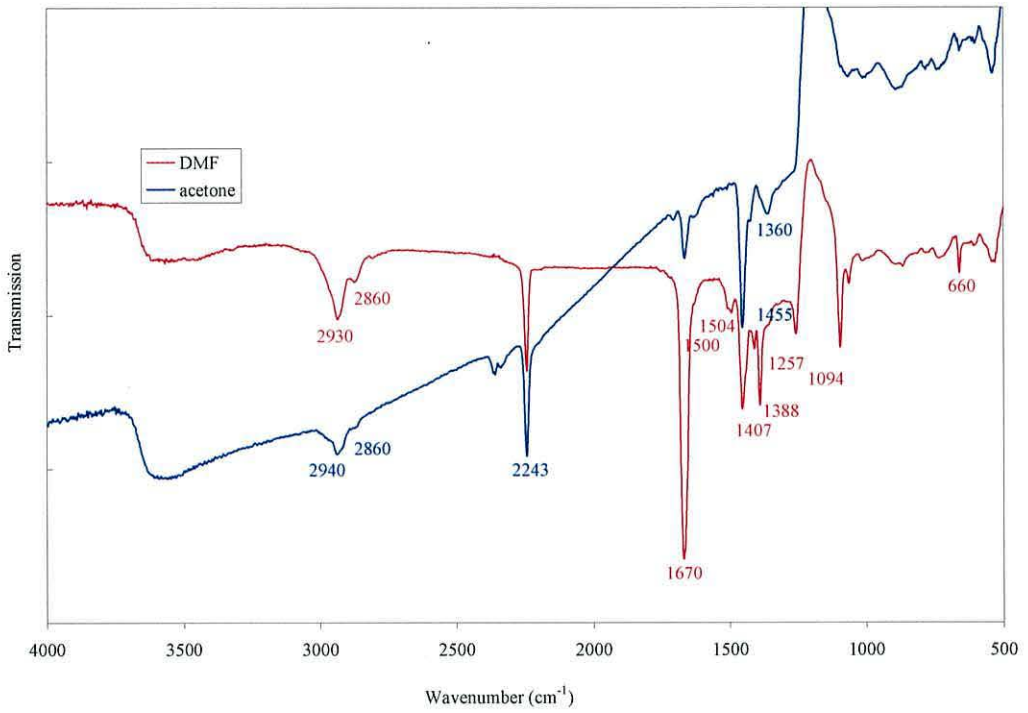

a)

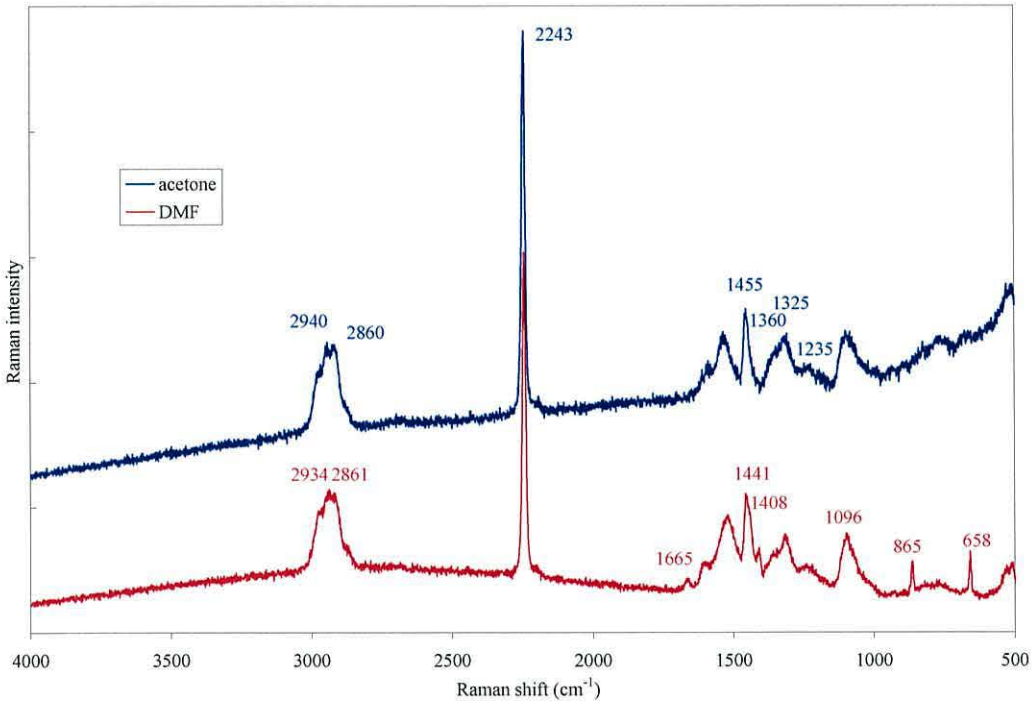

b)

Figure 4.8 a) *FTIR and b) Raman spectra of PAN films rinsed in different solvents then dried in oven prior to characterization, (AN 1M, DMF, 0.05M TEAP, Ag WE).*

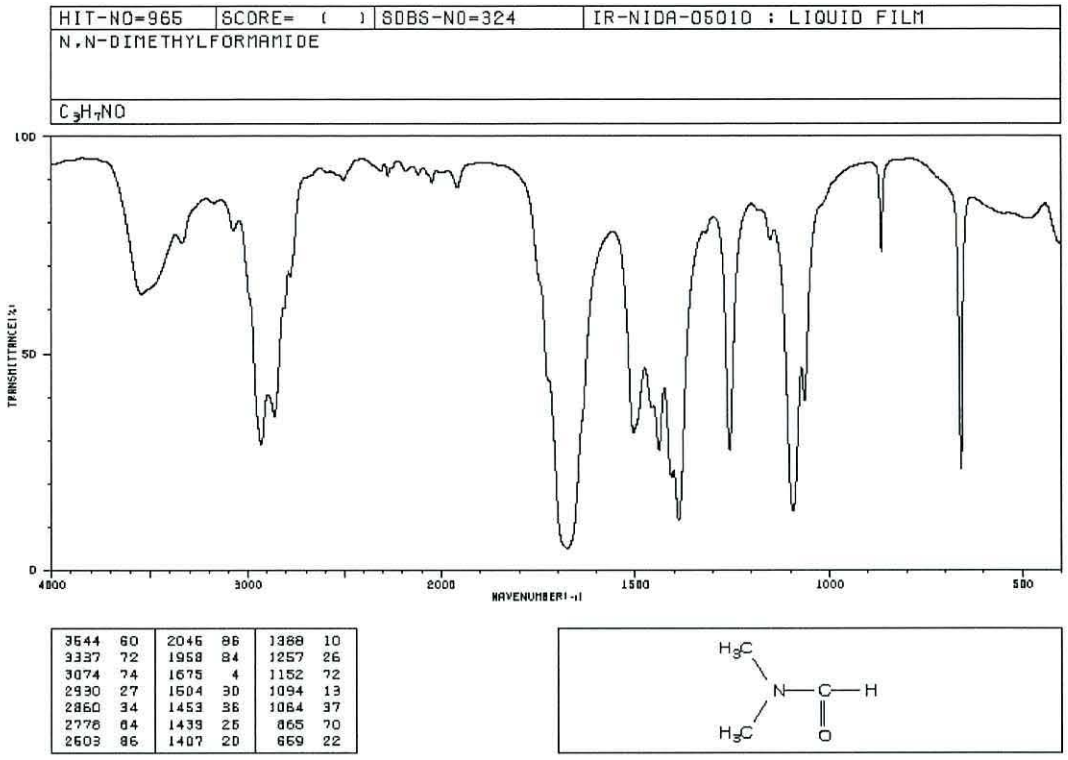

a)

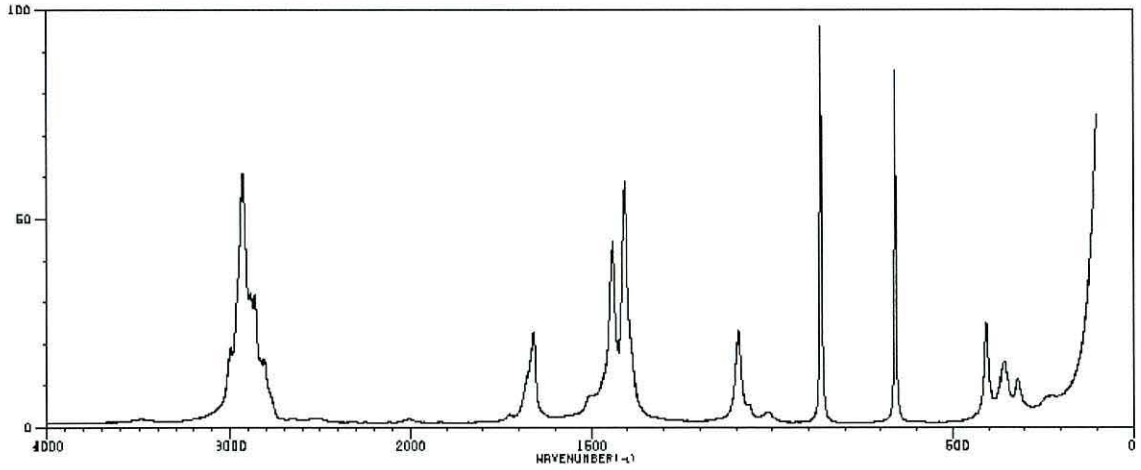

N,N-DIMETHYLFORMAMIDE
SDBSNO = 324 C_3H_7NO RM-01-00024 : 4880A.150M.LIQUID

2934	60
2861	31
1661	22
1441	43
1408	68
1086	22
867	95
660	85
407	23
319	11

b)

Figure 4.9 *FTIR and Raman library spectra for DMF (Spectral database for organic compounds, AIST, Japan).*

4.7 Monomer concentrations

In an attempt to improve the potentiostat control different monomer concentrations were used. Mertens et al (1998) showed the peak resolution i.e. the difference between Peak I and II, could be increased by increasing the AN concentration. Voltammograms recorded for different monomer concentrations show a marked reduction in the current peak as the concentration was increased. Some improvement was observed but further work on contamination reduction was required. The FTIR and Raman spectra (Figure 4.10) of the PAN films electrografted at the different AN concentrations gave some interesting results.

4.7.1 FTIR and Raman spectral observations

Looking at the FTIR spectra there is little difference between the PAN films apart from an overall increase in intensity across the spectral range. The peaks associated with DMF are approximately proportional to the PAN peaks in each case suggesting uniform entrapment of the solvent. However the Raman spectra show a marked contrast between the PAN films. The peaks at 1520 and 1596 cm^{-1} show a monomer concentration dependence. According to Calberg et al (1997) the thickness of electrografted PAN films can be controlled by adjusting the AN concentration. This suggests that the Raman anomalies are more pronounced the thinner the film pointing towards surface or interface related effects. Hence the removal of surface impurities became the next consideration.

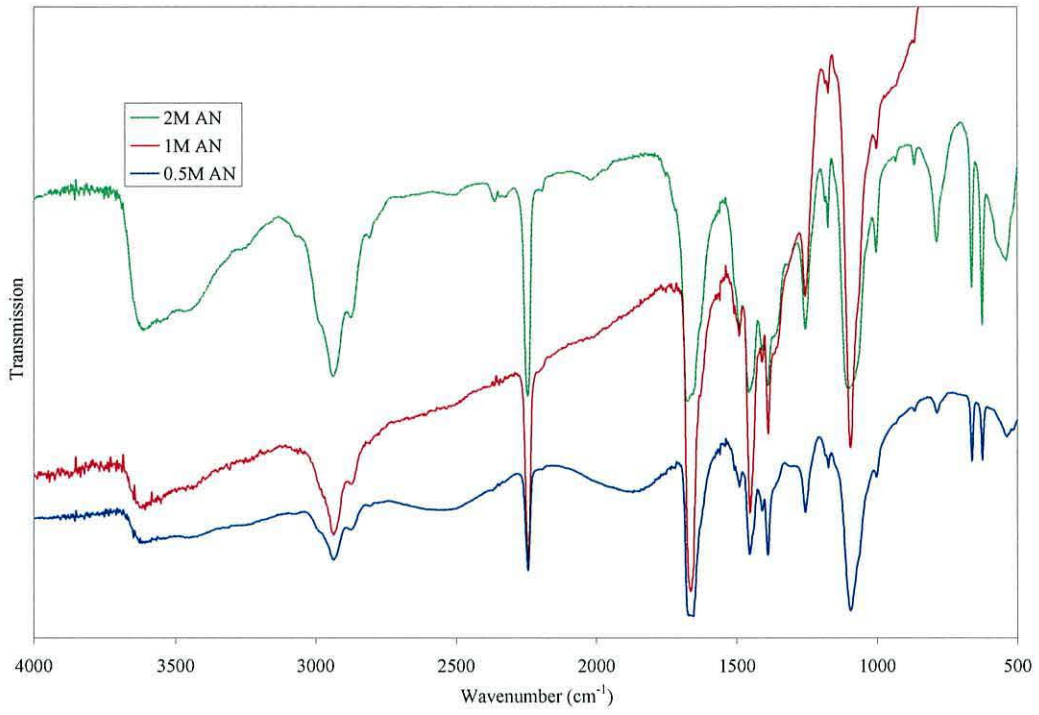

a)

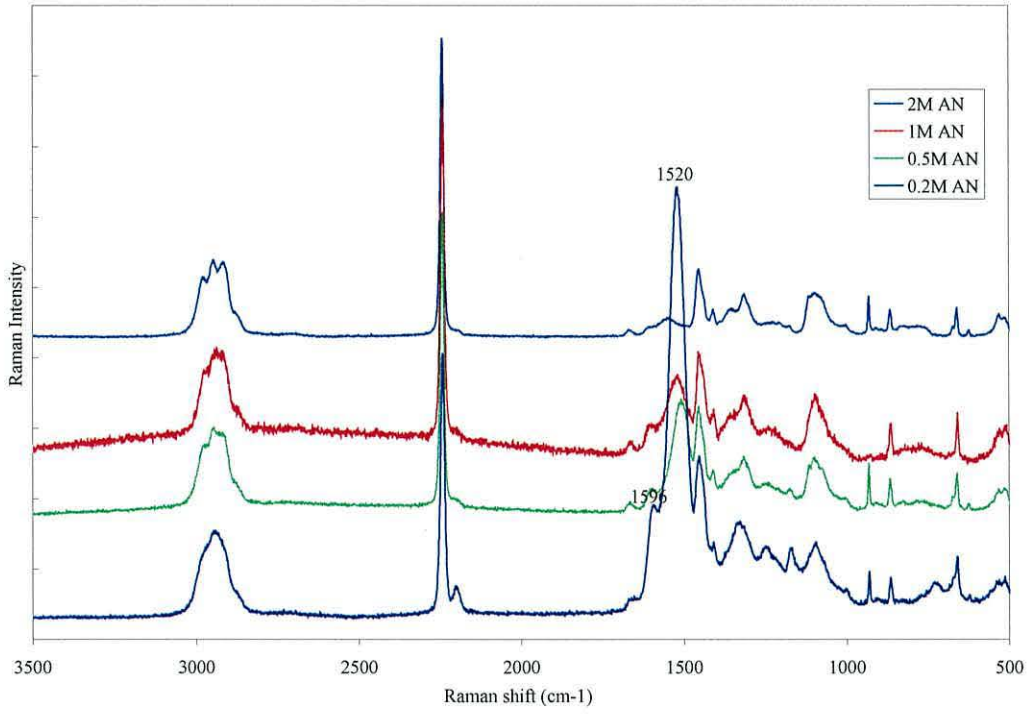

b)

Figure 4.10 a) *FTIR and b) Raman spectra of PAN films electrografted from different monomer concentrations, (DMF, TEAP 0.05M, Ag WE).*

4.8 Pretreatment of working electrode

The most likely source of 'contamination' was deemed to be the electrode surface. Thus various electrochemical cleaning protocols were applied to Ag WE's in a monomer free solution before the electrografting of AN. Figure 4.11 shows the FTIR and Raman spectra of the resulting PAN films. An AN concentration of 0.5M was selected to assess the affect on the Raman spectra. A siphoning technique was introduced for this experiment to protect the electrolyte (DMF < 50 ppm, vacuum oven dried TEAP) and cell components from further contamination (see Chapter 3).

4.8.1 FTIR and Raman spectral observations

FTIR spectra of a PAN film electrografted onto an Ag WE subjected to an oxidation then reduction cycle shows a new peak at 1725 cm^{-1}. Uncharacteristic of PAN or the electrolyte, the presence of the peak suggests the presence of an unwanted oxidized species. Possibly a carboxylic C=O stretch which normally absorbs at around these frequencies. This was to be expected as Ag is known for the reversibility of its Ag oxides rather than their desired desorption see Chapter 3. Nitrile groups can be turned into carbonyl groups as a result of nucleophilic attack by O^{2-} anions which are formed during the electrochemical cleaning of the metal see Chapter 2. In contrast the Raman spectra of the corresponding PAN film showed the complete disappearance of the 1525/1596 cm^{-1} peaks. This supports it being a surface effect. It was decided not to encourage the formation of the oxidized species, as its presence would interfere with the initiation of the electrografting process and bring into question the integrity of the PAN/metal bond. However the Raman spectra of the film grown on the Ag WE only subjected to the negative cycle shows only a slight attenuation of these absorption bands. An assessment of the spectra resulted in the negative pre-treatment being the preferred choice.

4.9 Efficient passivation and improved film quality

The most noticeable improvement and one of the main arguments for adopting the negative cycle pre-treatment for the WE was seen in the cyclic voltammograms. For the first time using a Ag WE when the electrode had been subjected to a negative cycle pretreatment, signs of electrode passivation were observed. A microscopic inspection of the films showed a marked reduction in defects such as holes. Figures 4.12 and 4.14 show the pre-treatment and electrografting cyclic voltammograms respectively.

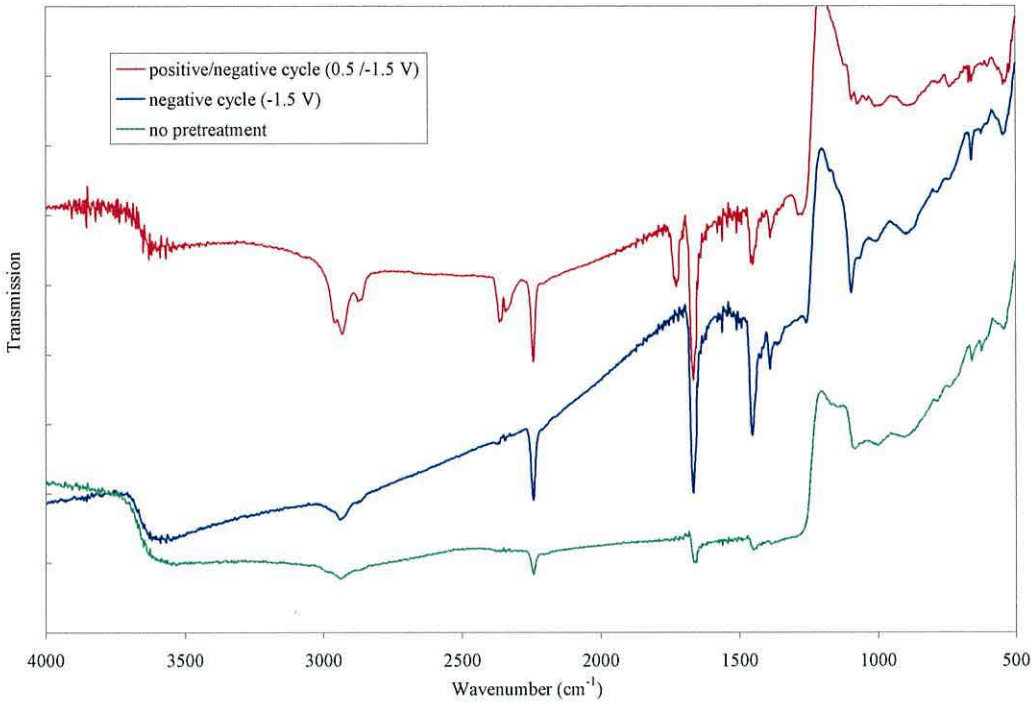

a)

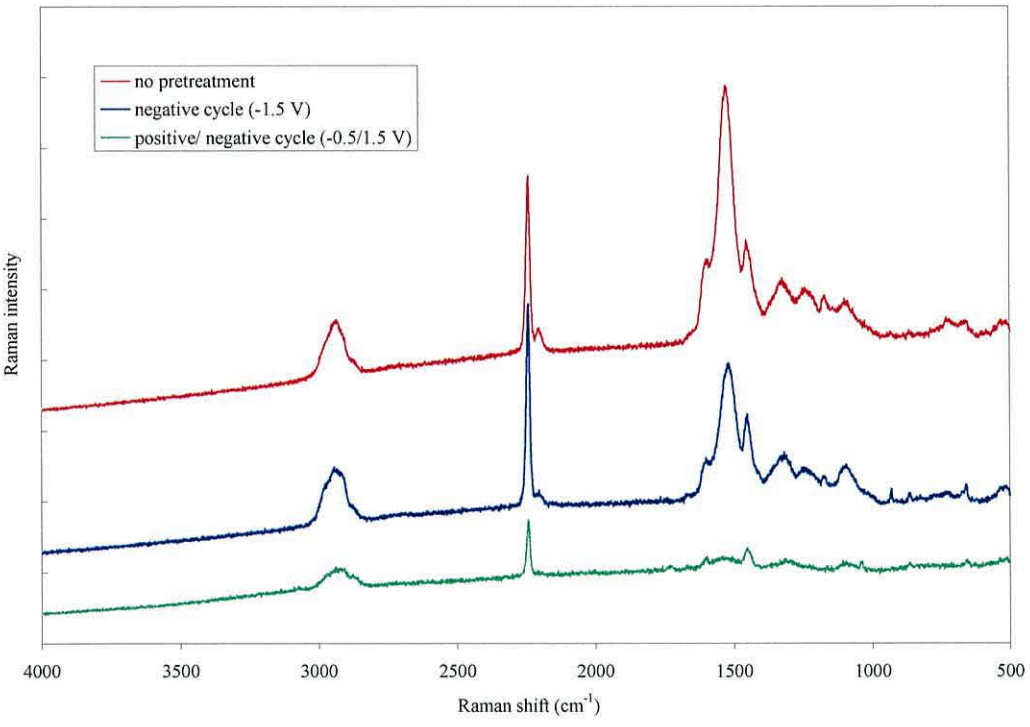

b)

Figure 4.11 a) *FTIR and b) Raman spectra of PAN films electrografted onto Ag WE, pretreated using different cleaning protocols, (AN 0.5M, DMF, TEAP 0.05M).*

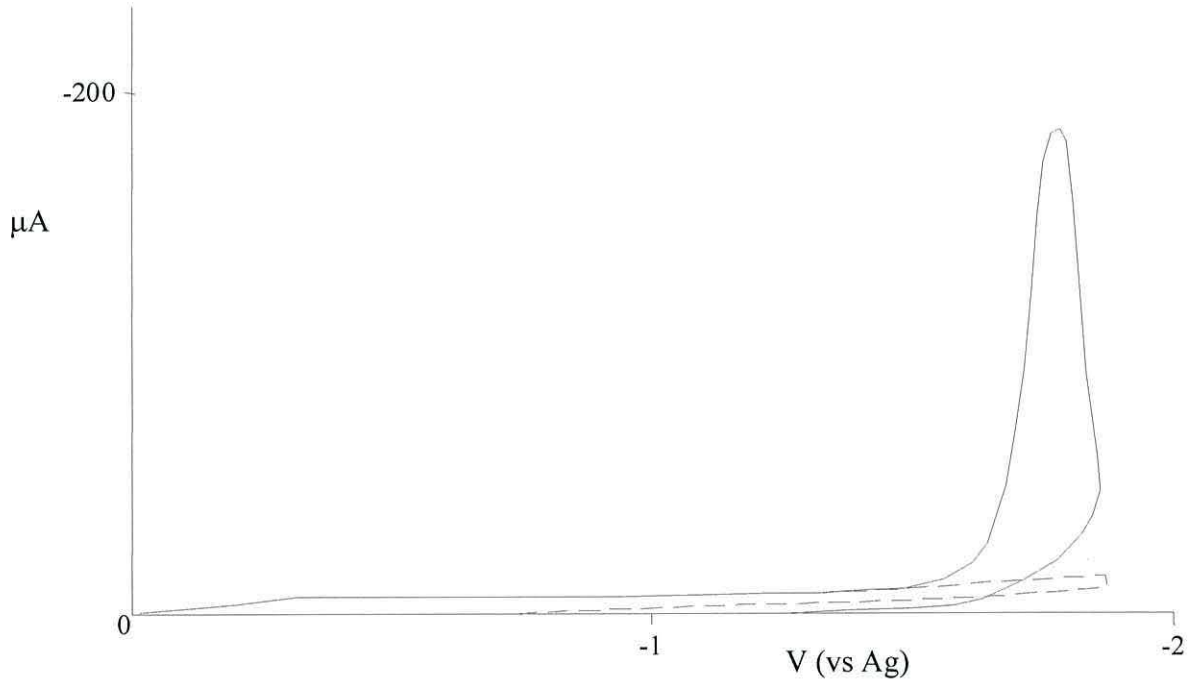

Figure 4.12 *Cyclic voltammogram of the electrografting of PAN. Repeat scan (- -) shows electrode passivation when the Ag WE is first pretreated by subjecting it to a negative voltage scan (AN 0.2M, DMF, TEAP 0.05M, 20 mV / s scan rate).*

4.10 Comparison of different working electrodes pretreated with a negative cycle

Ag is renowned for its catalytic effect on PAN. Xue et al (1994) showed using specially prepared Ag surfaces that structural transformations normally observed during the pyrolysis of PAN can be catalysed by Ag without being subjected to heat. However in this case the PAN was spun-coated. So for interest PAN films were electrografted onto pretreated Ag and Au WE and compared. Figure 4.13 shows the FTIR and Raman spectra.

A comparison of the FTIR spectra show a stronger contribution from the DMF solvent when PAN is electrografted onto Ag in contrast to a Au working electrode (WE), which mainly shows the characteristic peaks of PAN. Possibly the film on Ag is thicker or more porous thus trapping more solvent. However the FTIR spectra suggest that the PAN on Ag is a similar thickness if comparing the C-H stretch region whereas the Raman spectra definitely show a thicker film on Ag assuming the same beam intensity. Despite these conflicting observations even if the film thicknesses were of a similar order a comparison of the non-characteristic peaks relative to the characteristic PAN peaks in the Raman spectrum suggests the solvent is not responsible for these Raman anomalies.

Is the Surface enhanced Raman scattering (SERS) effect responsible? Oxidation and reduction cycling (ORC) can be used to prepare the nano-structured surfaces needed for SERS. However these anomalous Raman peaks were present for PAN films grown on non-treated electrodes. Possibly the evaporation deposition of the metal creates a nano-structure sensitive to this effect. Comparing the Raman spectrum for the PAN film grown on Ag in Figure 4.13 with the spectrum for the corresponding monomer concentration as seen in Figure 4.10, we see that the peaks are stronger after pretreatment. However the comparison must also consider the other changes that have been implemented, namely a drier electrolyte and the improvement in potentiostat control.

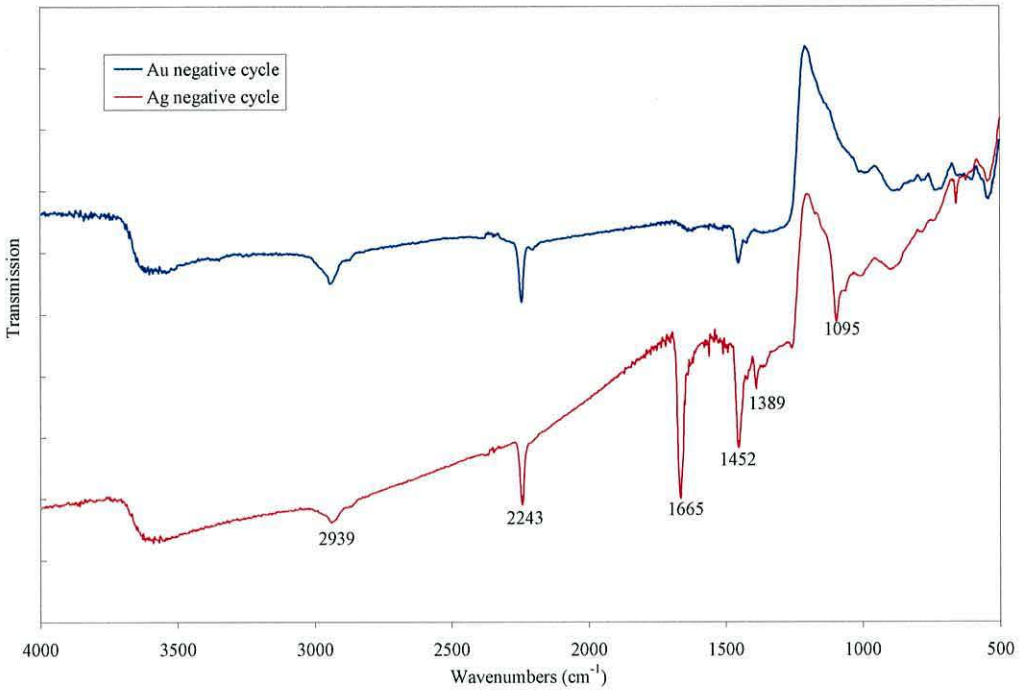

a)

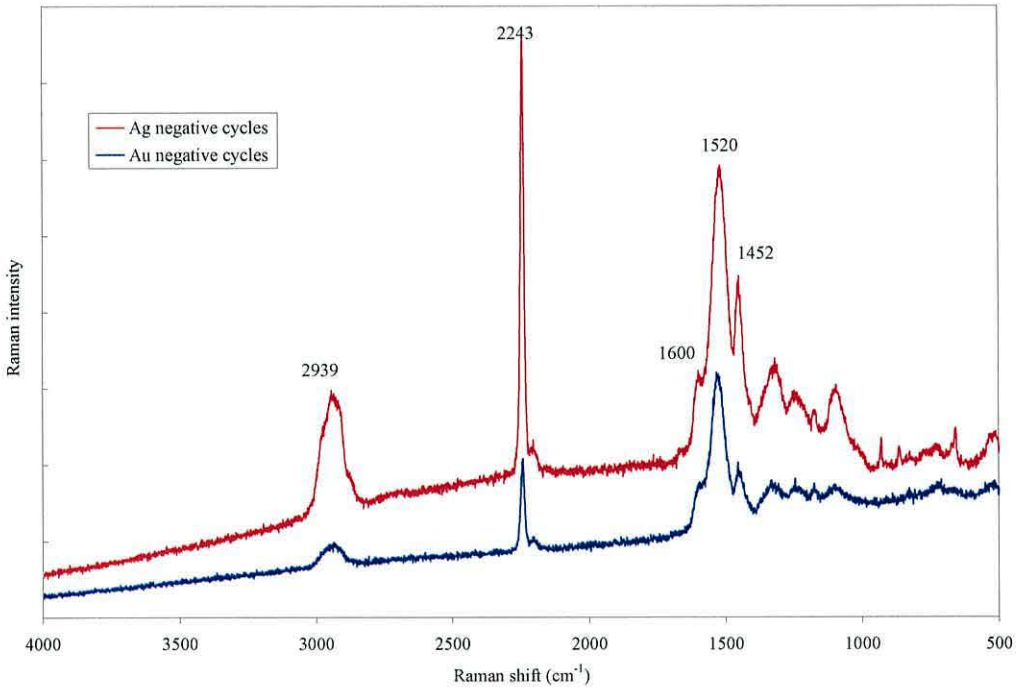

b)

Figure 4.13 a) *FTIR and b) Raman spectra of PAN films electrografted onto different WE, pretreated with negative cycles , maxima - 2 V, (AN 0.5M, DMF, TEAP 0.05M).*

4.11 Comparing the cyclic voltammograms of different working electrodes pretreated with negative cycles.

Figure 4.14 shows the voltammograms for the pretreatment of Ag, Au and Cu. The pretreatment involved repeated scanning from 0 volts to -1.8 V until the voltammogram was reproducible. A typical scan is given for each metal. The voltammograms vary according to the working electrode. All other conditions e.g. electrolyte were the same.

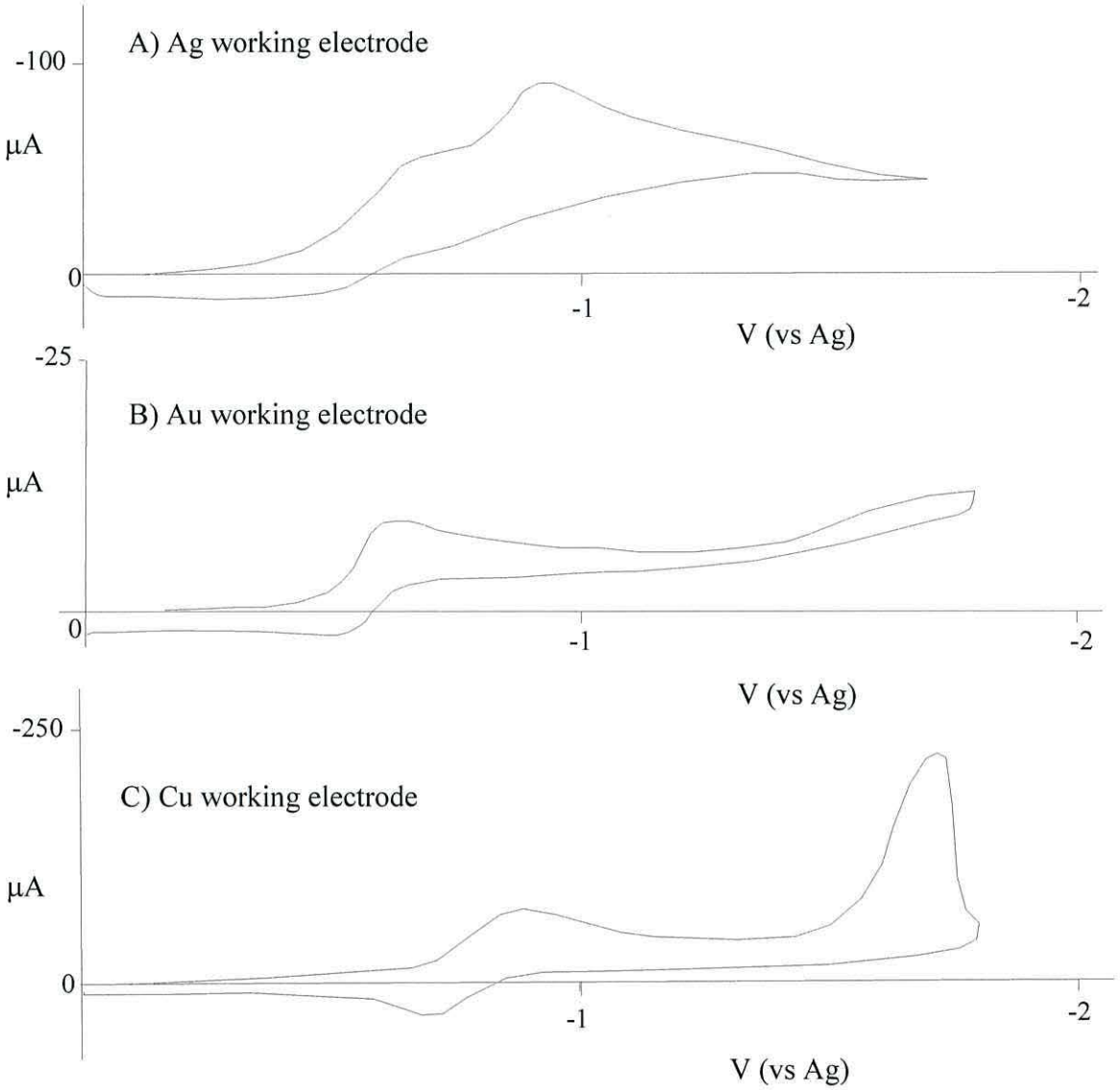

Figure 4.14 *Pretreatment of different working electrode in a monomer free solution. Cycles were repeated until a reproducible scan was obtained, typically 5 times, (DMF, TEAP 0.05M, 50 mV/s scan rate).*

A study of the surface topography of an evaporated Ag electrode before and after a negative cycle pretreatment was carried out using an AFM. The surface roughness was analyzed using a power spectral density (PSD) function. The function reveals periodic surface features that might otherwise appear random and provides a graphic representation of how they are distributed. A two dimensional isotropic PSD analysis was carried out on the surfaces. This is isotropic in the sense that it is an average taken over all directions of the data. Figure 4.15 gives the resulting PSD histograms for the three different Ag surfaces. An RMS roughness analysis was also undertaken and the results are given in Table 4.3.

From this investigation it is concluded that there is little difference in the structure of the three surfaces to justify the observed changes in the Raman spectra.

a)

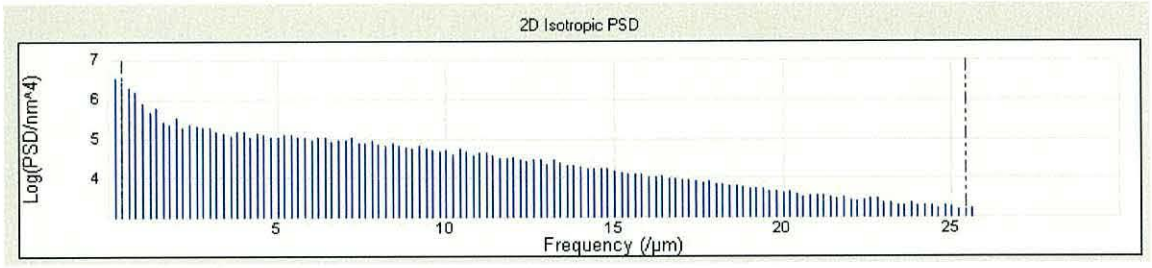

b)

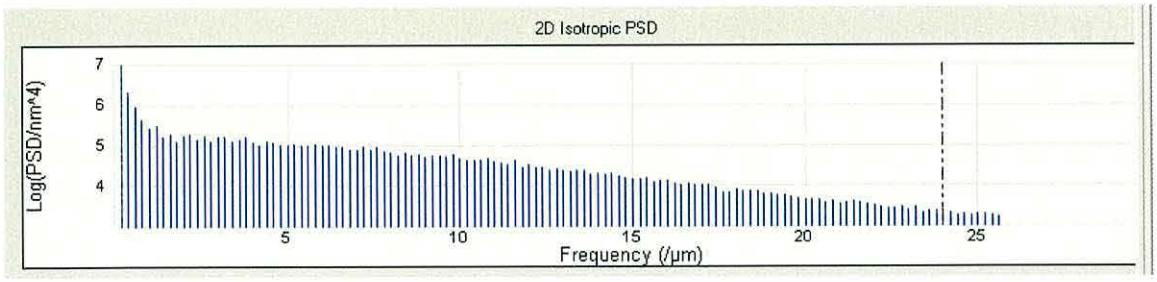

c)

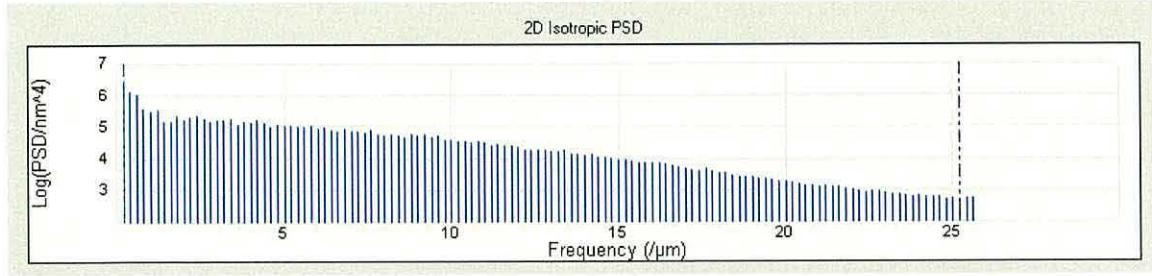

Figure 4.15 *AFM 2D isotropic PSD histograms of Ag surfaces; a) before pretreatment and after pretreatment with a negative cycle to b) -1.75 V and c) – 2 V.*

Table 4.3 *RMS roughness analysis of Ag surfaces*

Surface treatment	RMS roughness (5 x 5 μm)
No treatment	1.77nm
-1.75 V negative cycle	1.75nm
-2.00 V negative cycle	1.48nm

4.12 Comparison of PAN films electrografted onto Ag WE's pretreated with different negative cycles (-1.75 V, -2.0 V)

The cyclic voltammograms and Raman spectra of PAN films electrografted from 0.2 M AN onto Ag WE pretreated with different negative cycles were recorded and compared. The study was undertaken to see whether applying a harsher pretreatment to the WE influenced the Raman spectra of the PAN films. Figure 4.16 compares the Raman spectra of PAN films electrografted onto Ag WE pretreated with negative cycles extending to – 1.75 V and -2 V.

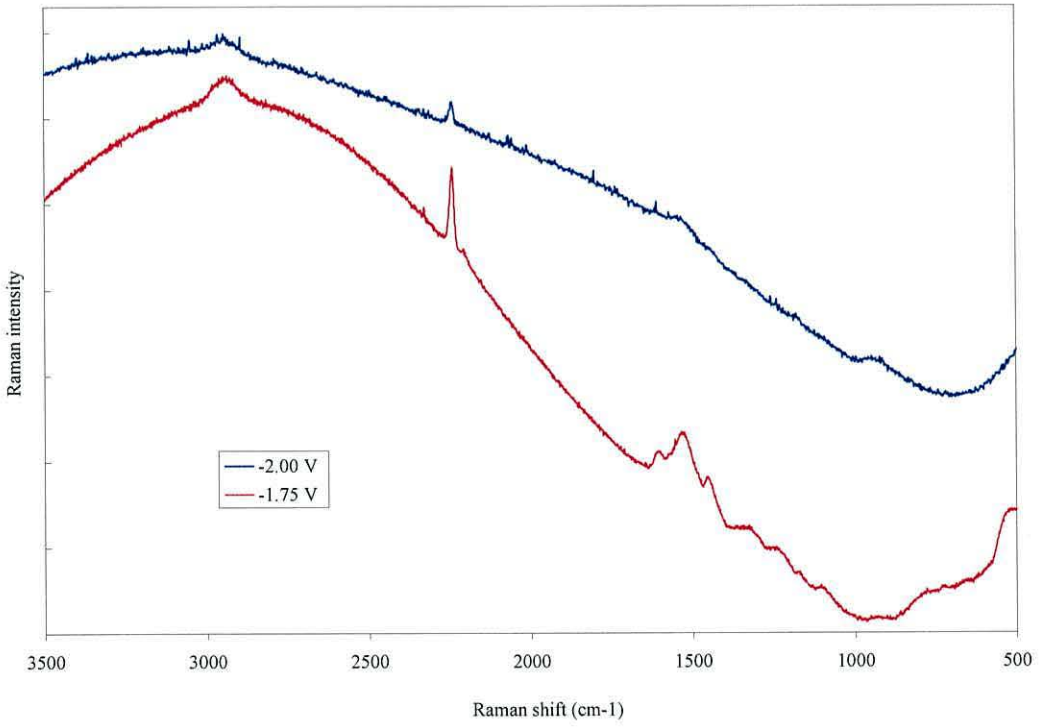

Figure 4.16 *Raman spectra of PAN films electrografted onto Ag WE, pretreated to negative cycle maxima of – 1.75 V and – 2.00 V (AN 0.2M, DMF, TEAP 0.05M).*

4.13 Fluorescence

A major drawback of the improving film quality i.e. reduction of film defects, was the deterioration in the ability to obtain spectral information, particularly for the thinner films electrografted from low monomer concentrations. The regular appearance of fluorescence in spectra masked the spectral detail. Figure 4.16 illustrates the problem. The Raman signal appears as sharp bands on top of the highly elevated sloping baseline. Fluorescence is considered to be due to surface impurities. It is a more efficient process than Raman scattering. Even if the analyte is present in much higher concentrations than the fluorescing impurity, the fluorescence can be overwhelming. The recommended method of reducing this influence is 'photobleaching' the sample with prolonged exposure to the laser prior to analysis. Chemicals which fluoresce tend to thermally degrade on continued exposure. Unfortunately so is the tendency of PAN to undergo structural transformation on heat treatment, the laser being a source of heat. As prolonged laser exposure was not an option, it was necessary to build the signal by increasing the scan duration and number of accumulations to improve the signal to noise ratio. Noting that since the CCD detector is shot-noise limited long scans will give a better signal to noise ratio than for the same total time in shorter accumulations. The fluorescence signal was then removed with an appropriate fitting and subtraction function to leave a reasonable Raman spectrum. However it is not possible to remove from the spectrum the shot noise inherently associated with the presence of fluorescence which can be of significant intensity masking Raman spectral information.

An alternative option would have been to limit the collection volume of the sample by exploiting the selective capability of the true confocal configuration. Closing the confocal hole would define a smaller collection volume. However due to the sensitive alignment of the instrument this was not explored.

4.14 Essential electrografting conditions

The following conditions were recognized as essential in order to produce good quality electrografted PAN films.

- Small Ag WE pretreated with a negative voltage cycle in monomer free solution to remove oxide.
- AN distilled to remove inhibitor
- Water in DMF < 50 ppm
- TEAP 12 hours in vacuum drying oven at 80°C
- Siphoning and transfer lines to protect and maintain dryness of electrolyte cell.

A PAN film was electrografted using the above conditions and compared to that of the commercial spun coated PAN sample. Figure 4.17 shows the resulting FTIR and Raman spectra.

While the spectra for the two types of film are very similar it appears from the relative intensity of the 1665 cm^{-1} C=O stretch in the FTIR that there is slightly more DMF trapped in the electrografted PAN sample. The reduction in the Raman peaks at 1520 and 1600 cm^{-1} for a PAN film produced from a lower concentration, see Figure 4.13, suggests the use of a higher monomer concentration produces a thicker film whose signal swamps any surface effects.

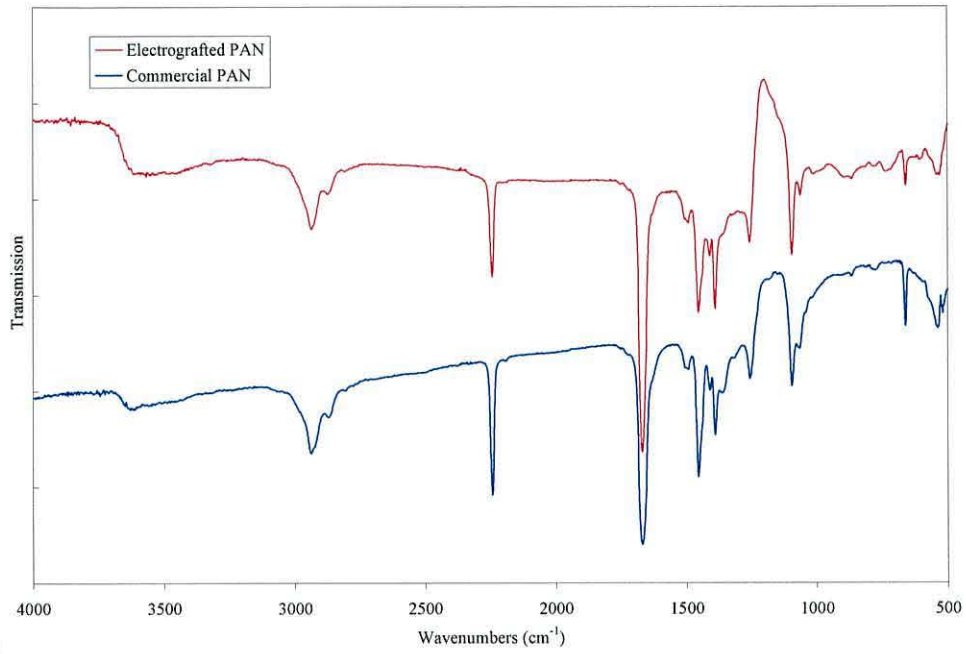

a)

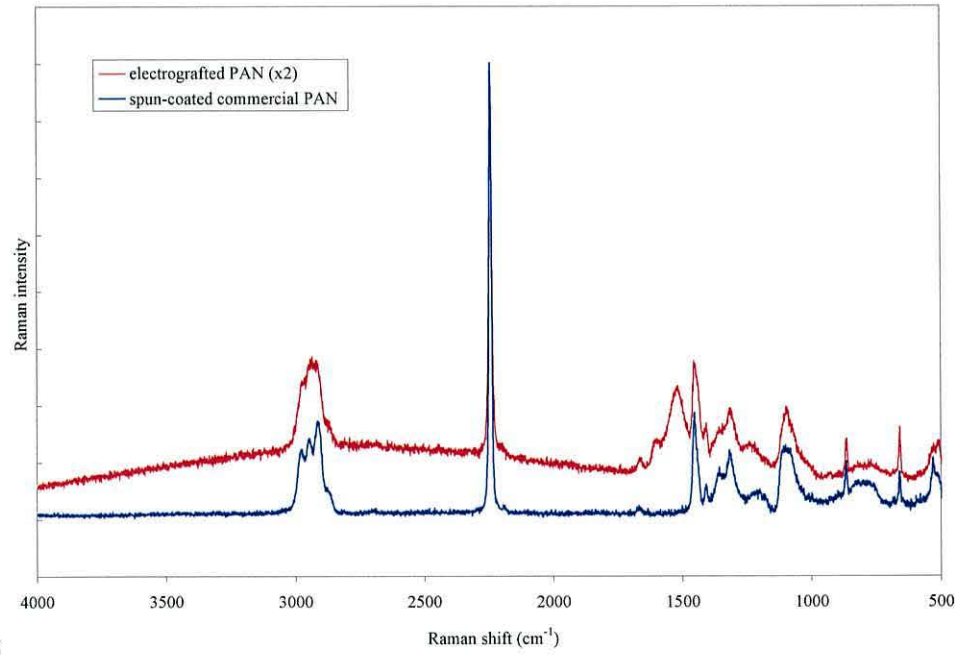

b)

Figure 4.17 *Comparison of a) FTIR spectra and b) Raman spectra of an electrografted PAN film produced under improved conditions with a spun-coated commercial PAN sample (AN 1M, DMF, TEAP 0.05M, Ag WE pretreated negative cycles).*

4.15 Influence of the working electrode

To investigate the influence of the WE material the study was extended to include Cu. Using the conditions described in Section 4.14, a PAN film was electrografted onto a pretreated Cu electrode (negative cycle to – 2 V in a monomer free solution). The cyclic voltammogram is given in Figure 4.18 FTIR and Raman spectra were recorded and compared to the spun-coated commercial PAN sample, see Figure 4.19.

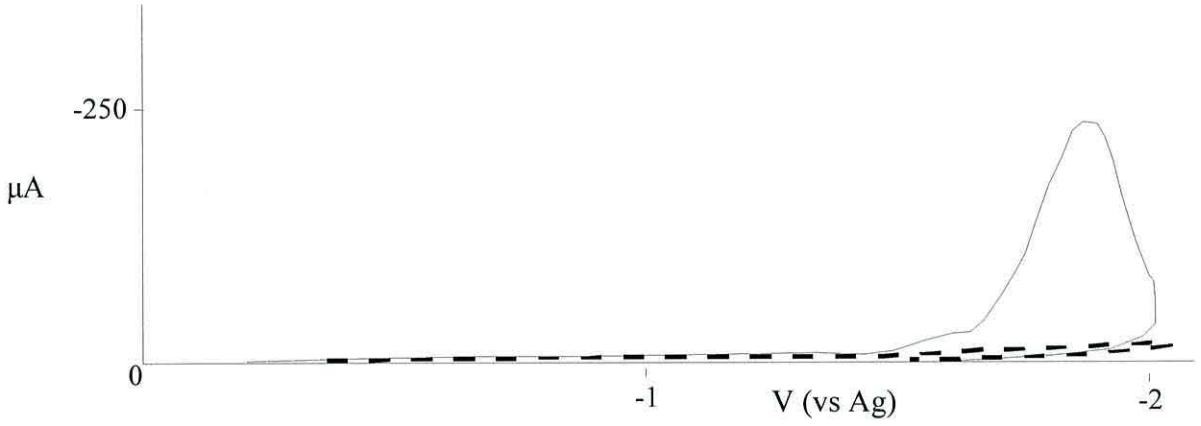

Figure 4.18 *Cyclic voltammogram of the electrografting of PAN* using a *Cu WE pretreated to negative cycles (- 2 V) (AN 1M, DMF, TEAP 0.05M).*

4.15.1 FTIR and Raman spectral observations

Both the FTIR and Raman spectra show good correlation between the electrografted and the spun-coated commercial PAN sample, particularly the FTIR spectra.. There appears to be little influence on the Raman peaks. The peaks in the 1525 - 1600 cm^{-1} range have a similar relative intensity to those seen in Figure 4.17 for a film produced on a Ag WE at the same AN concentration. The Raman spectrum of the electrografted PAN is very noisy probably due to fluorescence. A background correction was carried out but this subtraction fails to remove the shot-noise inherent to the fluorescence (see Section 4.13).

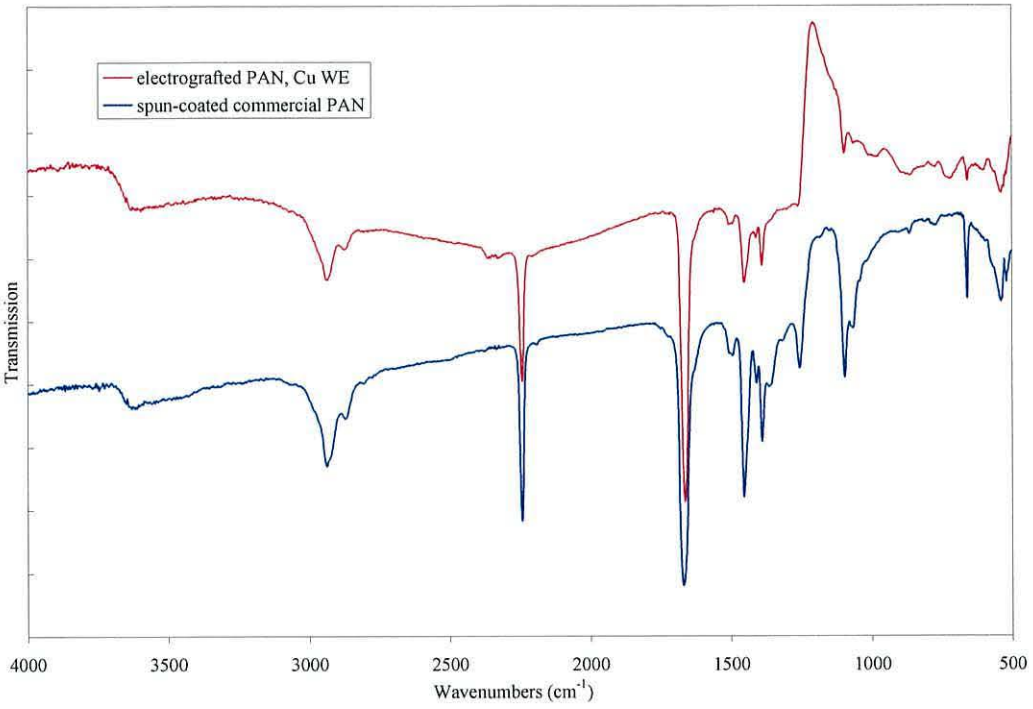

a)

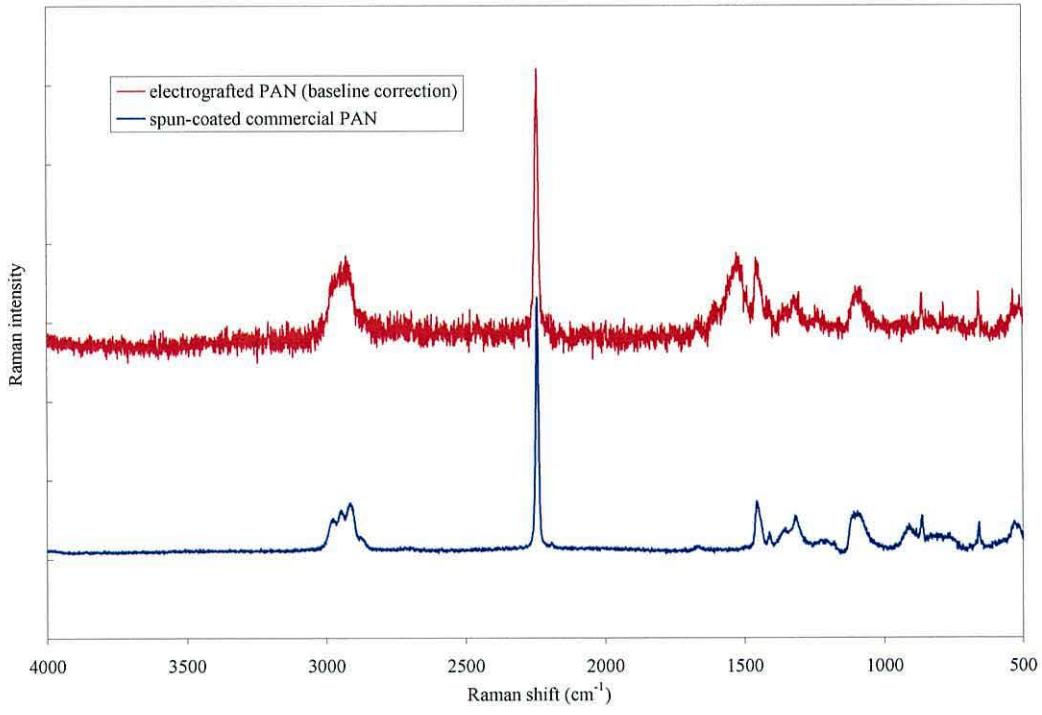

b)

Figure 4.19 *a) FTIR and b) Raman spectra of PAN film electrografted on to Cu WE pretreated with negative cycles to -2 V, (AN 1M, DMF, TEAP 0.05M).*

4.16 The influence of different WE on PAN film electrografted at different monomer concentrations.

In order to explore the influence of the WE more fully, a series of PAN films were electrografted onto different metals; Au, Ag and Cu, using different monomer concentrations and their properties compared. Two monomer concentrations were selected for comparison; 2M and 0.5M. The initial choice of 0.2M AN concentration was found experimentally to be too low for spectral analysis. In addition a Pt foil WE was included in the measurements at 0.5M in order to assess the influence of the Cr keying layer under the evaporated metal films. All four metals were subjected to a similar pre-treatment of negative voltage cycles in a monomer free solution. Figure 4.20 and 4.21 give the Raman spectra of PAN films grown at 2M and 0.5M AN concentrations respectively. Figure 4.22 gives the FTIR spectra for the 0.5M AN concentration only. The Raman and FTIR spectra for the PAN films grown in 0.5M have been normalized with reference to the intensity of the nitrile stretch, so that changes to the other peaks are easier to assess.

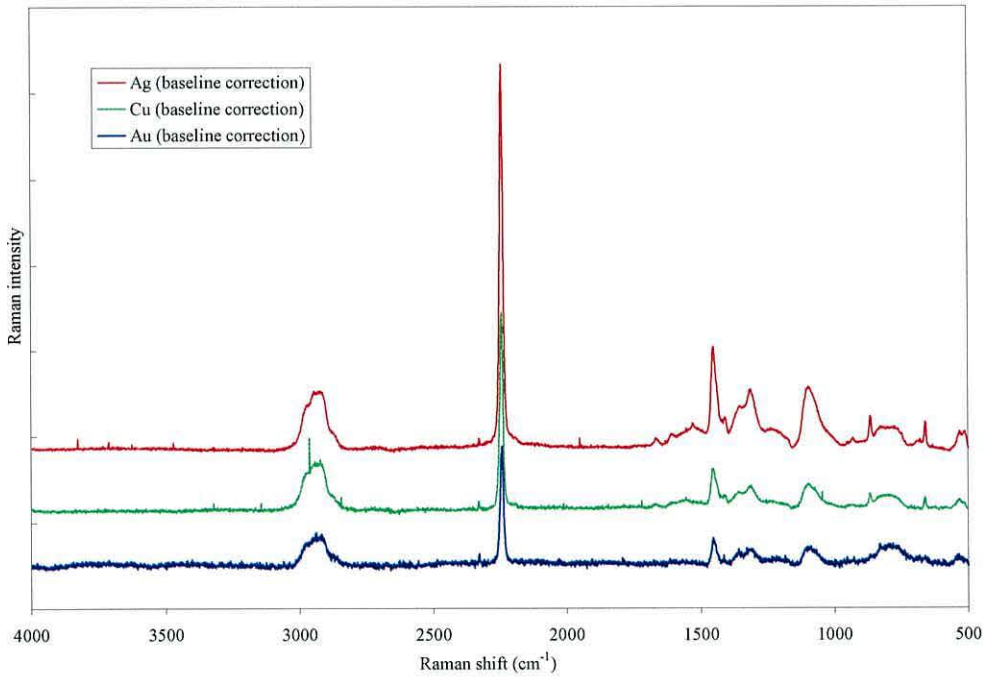

Figure 4.20 *Raman spectra of PAN films grown from 2M AN solution under improved conditions on different WE (DMF, TEAP 0.05M, WE pretreated with negative cycles > -1.75).*

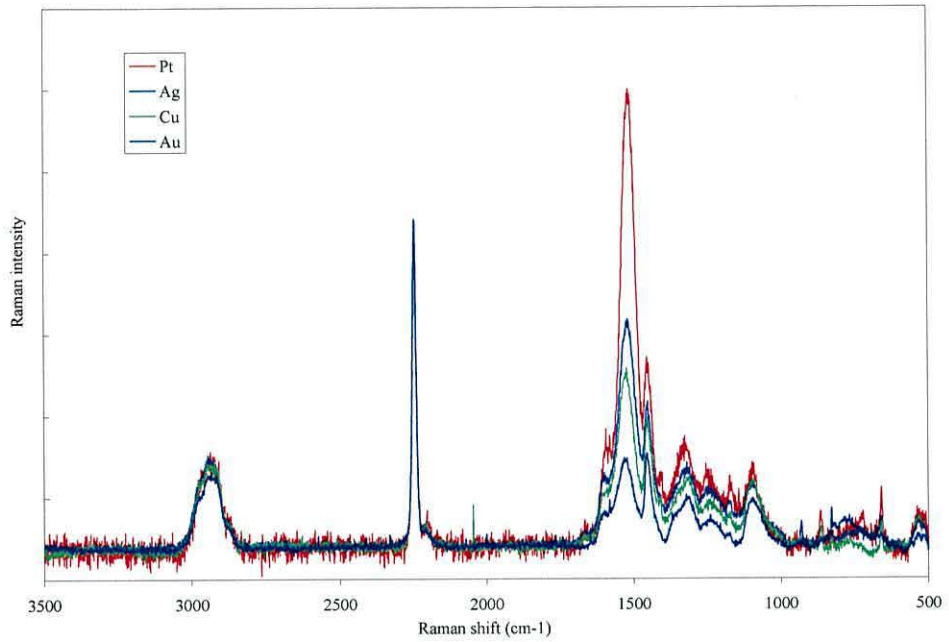

Figure 4.21 *Raman spectra of PAN films grown from 0.5M AN solution on different WE. All spectra are baseline corrected and normalized to the intensity of the nitrile band at 2243 cm^{-1} (DMF, TEAP 0.05M, WE pretreated negative cycles > -1.75.)*

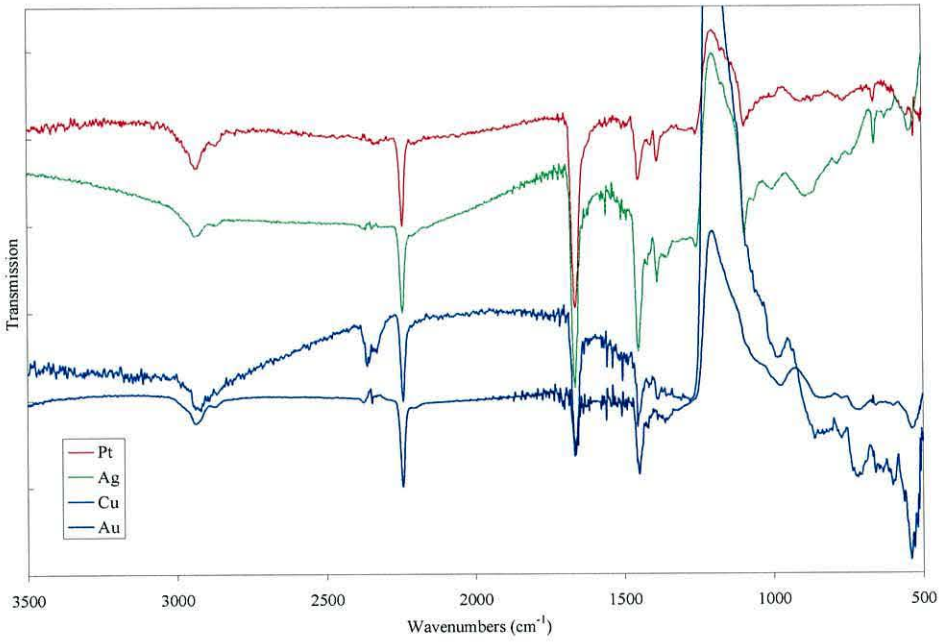

Figure 4.22 *FTIR spectra of PAN films grown from 0.5M AN solution on different WE. All spectra have baseline corrections (DMF, TEAP 0.05M, WE pretreated negative cycles > -1.75).*

4.16.1 FTIR and Raman spectral observations

The Raman spectra of the PAN films electrografted from a 2M AN solution (Figure 4.20) confirm previous findings. The anomalous PAN peaks between 1520 and 1600 cm^{-1} seen for lower concentrations are barely evident in any of the three metals. The spectra of PAN grown on Ag show peaks of a very weak intensity at 1525 and 1605 cm^{-1}, whereas Cu shows an even weaker peak appearing blue shifted and centered at approximately 1550 cm^{-1}. The baseline correction may well be responsible for this as no such shift is detected for Cu at lower concentrations (see Figures 4.19 and 4.21).

In contrast the Raman spectra from the PAN films grown at 0.5M (Figure 4.21) show a significant increase in the intensity of these peaks supporting the suggestion that they are due to some surface-related feature. The spectra in Figure 4.21 show that the anomalous PAN peaks occur at the same wavenumber but differ in the peak intensities. The intensity of the two uncharacteristic PAN peaks varies considerably according to the WE metal. Of interest, the spectra of PAN films electrografted on Pt show the strongest intensity for the 1520/1600 cm^{-1}peaks. This therefore eliminates Cr as the cause of the Raman anomalies. Also to be considered are the differences in the intensity of the fingerprint region below 1500 cm^{-1} relative to the increase in the peaks. However as all the Raman spectra required baseline corrections the differences can be attributed to the problems of curve fitting. Interestingly as the quality of the PAN film improves i.e. number of defects are reduced etc, the fluorescence presented more of a problem.

4.17 Comparison of electrografted PAN films before and after the experimental improvements

A comparison of the Raman spectra of PAN films electrografted on different WE from 2M monomer concentrations before and after the experimental improvements (in particular after reducing the electrode area) show very little change in the intensity of the very weak peaks at 1520/1600 cm^{-1} for Ag whereas in contrast these unique peaks are no longer evident for Au (see Figures 4.23 and 4.24). This raises the question as to whether the pretreatment of the Au WE has improved the density of the PAN film so that a stronger bulk swamps surface effects.

The main differences to the electrografting technique were; the working and counter electrode size, the purity of electrolyte (reduction of water and oxygen), pretreatment of WE and potentiostat control.

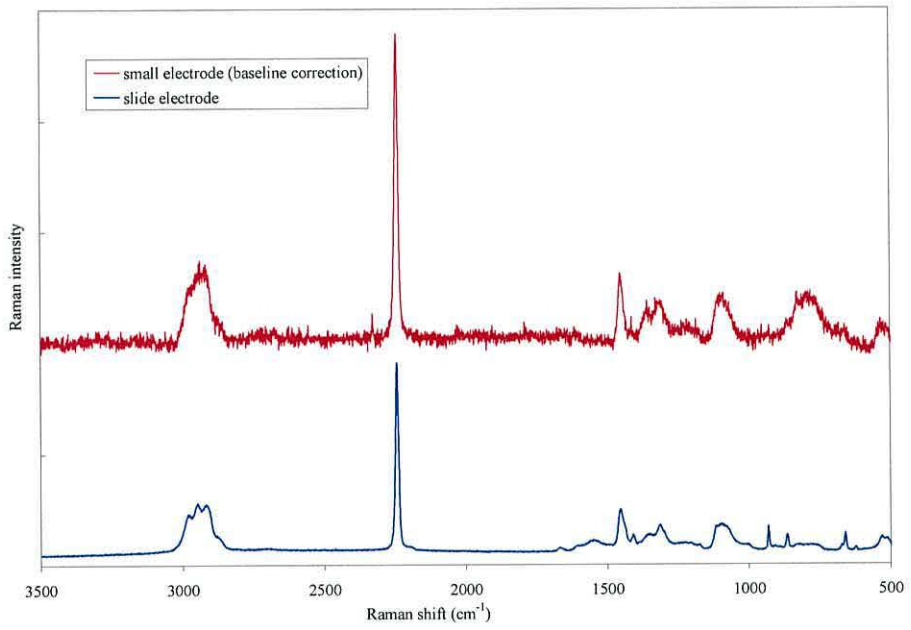

Figure 4.23 *Raman spectra comparing PAN films electrografted on Au WE under improved conditions (AN 2M, DMF, TEAP 0.05M).*

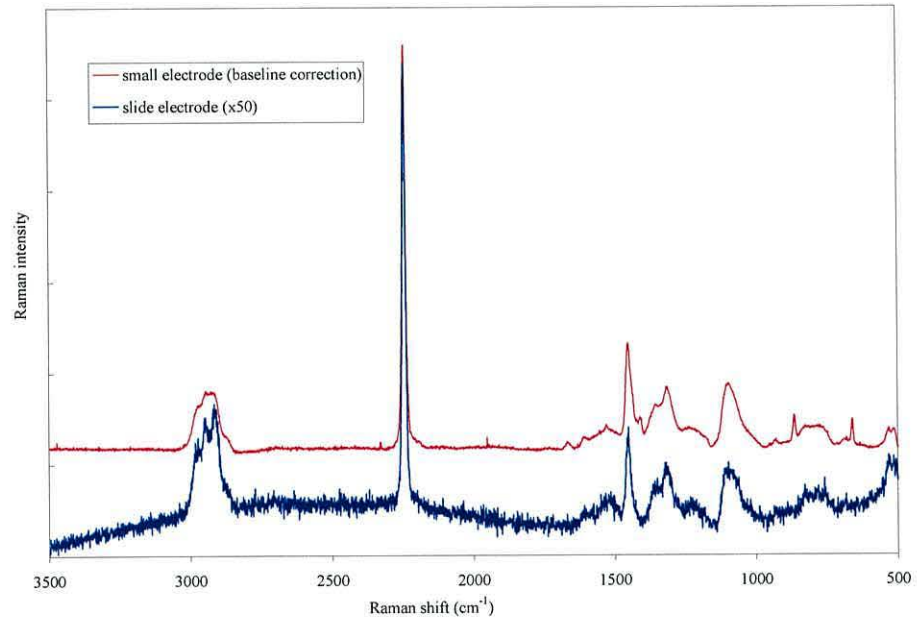

Figure 4.24 *Raman spectra comparing PAN films electrografted on Ag WE under improved condtions (AN 2M, DMF, TEAP 0.05M).*

4.18 Film thickness control

Using the conditions set out in Section 4.14 a range of PAN films were electrografted onto different WE electrodes: 0.2, 0.5, 1 and 2M concentrations. Thickness measurements and RMS roughness analyses were carried out on each film using the AFM. Ellipsometry measurements were carried out on the thicker films (2M) and compared. The results are presented in Figure 4.25 and Table 4.4. A selection of AFM 3D images are presented in Figure 4.26 to illustrate the surface sections used to measure the PAN film thicknesses.

Table 4.4 *RMS roughness measurements of PAN films electrografted onto different WE for different monomer concentrations in DMF and in brackets ACN.*

	0.2M	0.5M	1M	2M
Ag	1.73 nm	-	2.24 nm	1.31 nm
Au	2.86/0.625 nm	2.53/0.818 nm	2.11 nm (29 nm)	1.99nm
Cu	1.43 nm	-	2.5 nm	3.48 nm

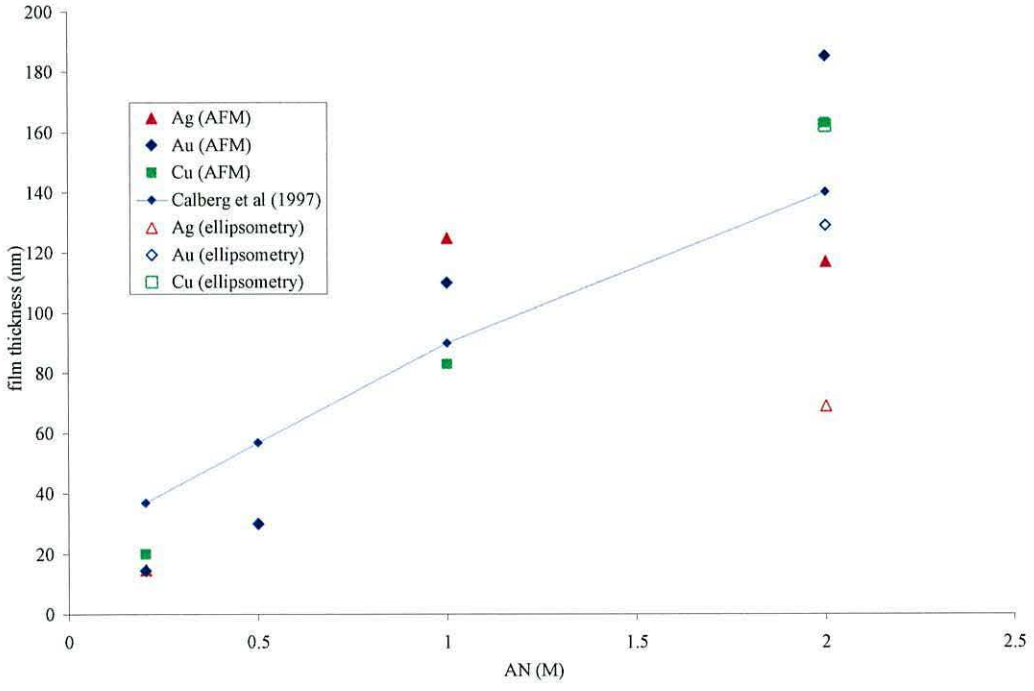

Figure 4.25 *AFM thickness measurements for PAN films electrografted using different AN concentrations and working electrodes.*

Figure 4.26 *AFM images showing the sections of electrografted PAN films used for the thickness measurements.*

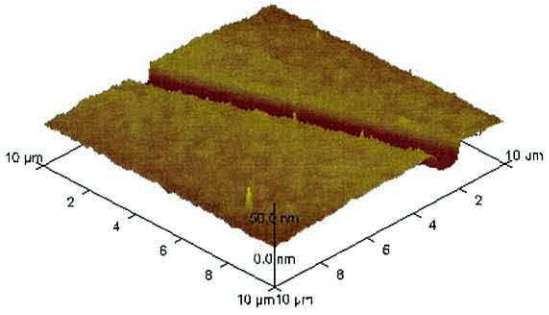

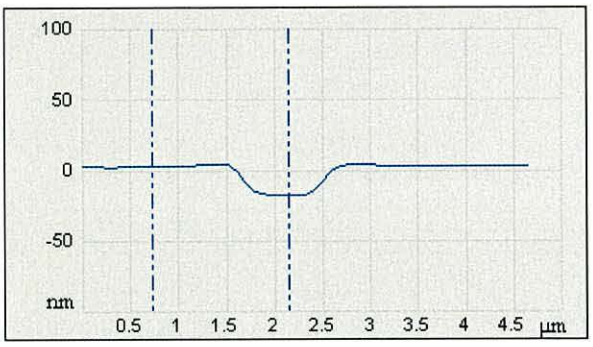

AN 0.2M, Au WE. **PAN film thickness ~ 15 nm**

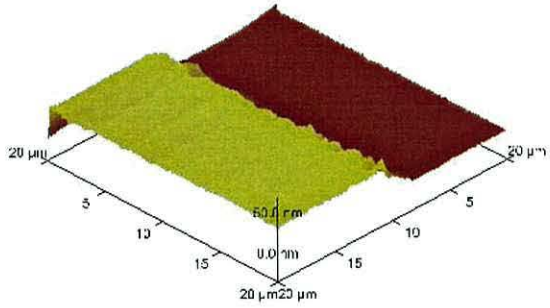

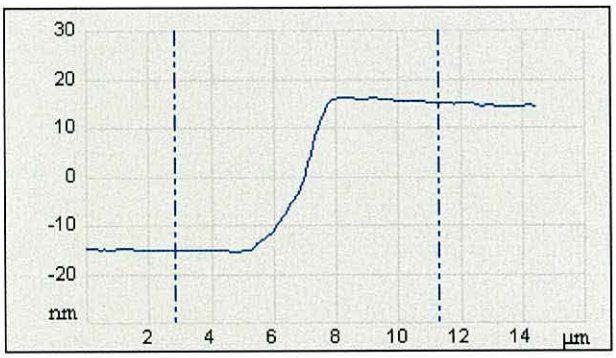

AN 0.5M, Au WE. **PAN film thickness ~ 30 nm**

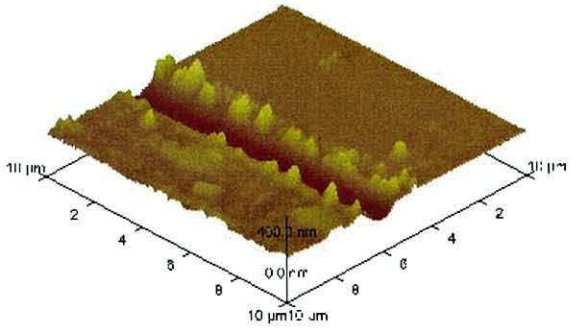

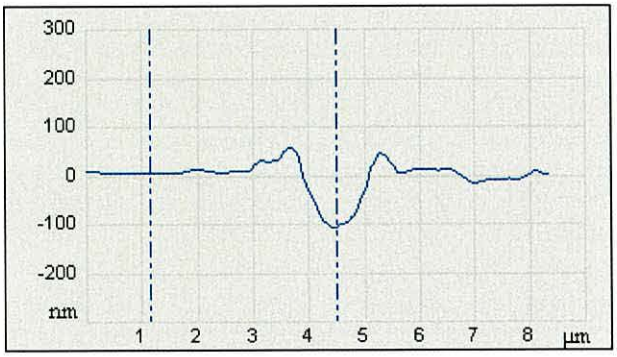

AN 1M, Au WE. **PAN film thickness ~ 110 nm**

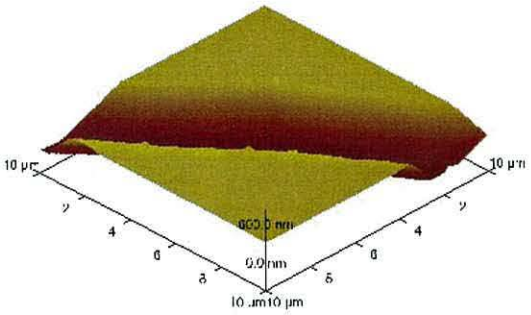

AN 2M, Au WE.

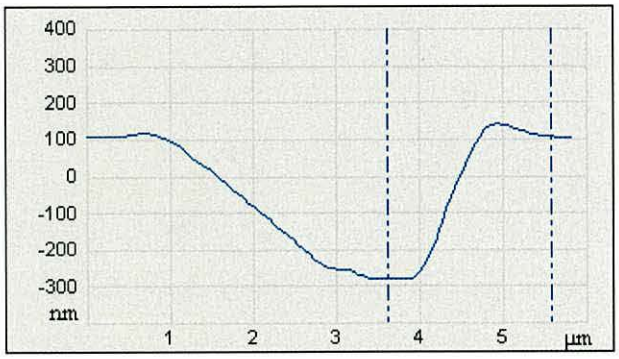

PAN film thickness ~ 185 nm
(including deduction for metal layer)

4.18.1 AFM thickness results

The thickness measurements are only approximate. The PAN films from the lower monomer concentrations were easier to score and the resulting measured thicknesses compared well with those of Calberg et al (1997) see Figure 4.25. However the thicker PAN films from 2M AN concentrations were not so straightforward. AFM thickness measurements for all three PAN films gave values in the order of 330 to 385 nm, these contrasted markedly with those obtained using an ellipsometer for the very same films. One possible suggestion was that the scoring of the thicker PAN films also included the metal electrode layer underneath. A thickness of 200 nm was therefore deducted for the metal layer. The electrodes were evaporated using the Balzer system see Chapter 3, which is a fairly crude process as no quartz crystal was used to measure the deposition rate of the different metals used, so this value is only an estimate.

Another consideration is the ellipsometer model calculations. The refractive indices for PAN on Au and Cu were found to be comparable at 1.432 and 1.453 respectively. In contrast the refractive index for PAN grown on Ag of 1.703 was found to be too high. Interestingly this film shows the largest discrepancy in thickness. Repeating the experiment would confirm the outcome.

4.18.2 AFM RMS roughness analysis

In Table 4.4 two values are given for the roughness of films produced on Au for monomer concentrations of 0.2M and 0.5M. The second lower value was recorded for

PAN films electrografted on electrodes with a thinner keying layer of Cr, see next section. These lower values are comparable to the RMS roughness measurements obtained by Calberg et al (1997): 0.6 nm for 0.2M AN in DMF. The study by Calberg et al also shows a marked change occurred in the roughness as the monomer concentration was increased. This is not the case for all the metal electrodes used in this work. One reason could be the underlying metal electrode. In the present study, the roughness of each substrate was not measured since this would expose the electrode to contamination prior to electrografting. Calberg at al used X-ray reflectivity to measure the roughness of the Ni PAN interface. Values of 1 – 1.9 nm were recorded which compare favourably with the values recorded for films produced here on pretreated Ag.

Of interest, Newton et al (1997) using the alternative solvent ACN measured a RMS roughness of 22.4 nm for an AN concentration of 2.5M and similar therefore to the 29nm measured here for the film grown from 1M AN on Au. These results confirm our findings that ACN produces rougher films, see work using different solvents in Section 4.5.

4.19 Influence of Cr layer

Despite improvements to the potentiostat control from pretreatment of the working electrode, the cyclic voltammograms for AN solutions remained unpredictable. At the lower AN concentrations such as 0.2M, the main indicator for effective electrografting was the signature of electrode passivation. Visible observation of film growth was hazardous due to the risk of de-bonding - the film becomes more visible if blistered during this process. However repeated signs of electrode passivation and no film growth led to concerns that the Cr layer was diffusing through the top metal layer, particularly at the edges and interfering with the electrode surface during repeated cycling of the voltage. An open circuit voltage of 0.25 V measured prior to application of the voltage scan gave some indication of galvanic activity across the bi-metallic junction. Electrodes produced from the Edwards system with an increase in the Au to Cr ratio of 100:1 gave significant results. The open circuit voltage was reduced to 40 mV and the resulting cyclic voltammograms produced during electrografting were similar to those

reported by Mertens et al (1998). Predictable film growth then produced defect free films with no trace of debonding i.e. blistering of the surface.

Out of interest electrodes were also produced with a diffusion barrier of Pd sandwiched between the Au and the Cr and compared. A further drop in the open circuit voltage to 23 mV occurred. The efficiency of passivation was measured using a repeat scan. Any electroactivity measured during the repeat scan was assumed to be either due to poor surface coverage or defects in the film providing access to the electrode surface. Minimal electroactivity was observed see Figure 4.27.

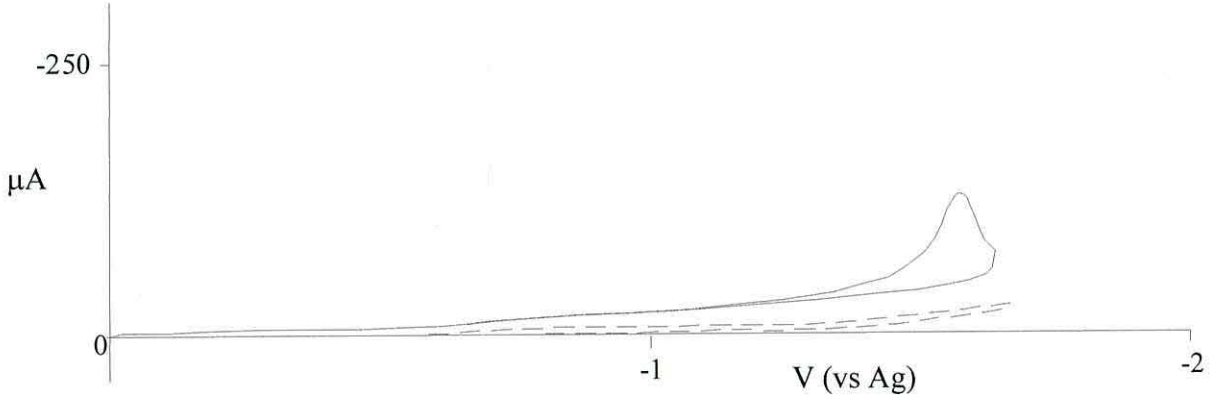

Figure 4.27 *Cyclic voltammogram of the electrografting of PAN onto a Au working electrode with a diffusion barrier of Pd to prevent the diffusion of Cr, Repeat scan (- -) shows electrode passivation (AN 0.5M, DMF,TEAP 0.05M, 20 mV / s scan rate).*

The Raman spectra of a PAN film electrografted using these WE from an AN concentration of 0.5M are given in Figure 4.28. As can be seen, the signals are extremely weak which is not surprising. AFM measurements revealed that the film thicknesses were only 30 nm and fluorescence was a major factor. Spectra were recorded using both the He Ne and argon ion laser with the signal built up using appropriate accumulation times. The use of a laser with a shorter wavelength provides the advantage of less surface penetration thereby reducing the fluorescence in the Raman spectra of thin films.

The spectra obtained using the different lasers are similar especially regarding the intensity and position of the peak at 1520 cm^{-1}. The loss of detail in the fingerprint region of the spectra is due to the limitations of the baseline corrections for the fluorescence (see Section 4.13). However the similarity of the spectra irrespective of the laser used

eliminates resonance enhanced Raman scattering (RERS) as the origin of the anomalous peaks. This type of Raman enhancement occurs when the wavelength of the incident light is equal to an electronic transition of the structure. If the peak at 1520 cm^{-1} was due to a RERS sensitive structure, a difference would be expected between the spectra from the different lasers. Unfortunately the film grown on the WE with the Pd layer was too thin to reveal any spectral information in this region, fluorescence obscured any detail.

Figure 4.28 includes the spectra of one of the PAN films which had been subjected to prolonged exposure to the laser. The appearance of peaks at 1585 and 1375 cm^{-1} show the PAN film is undergoing carbonization as a result of being heated by the laser beam. In their study of the pyrolysis of PAN films to produce carbon films, Renschler et al (1988). assigned these peaks to the ordered and disordered graphite phases respectively.

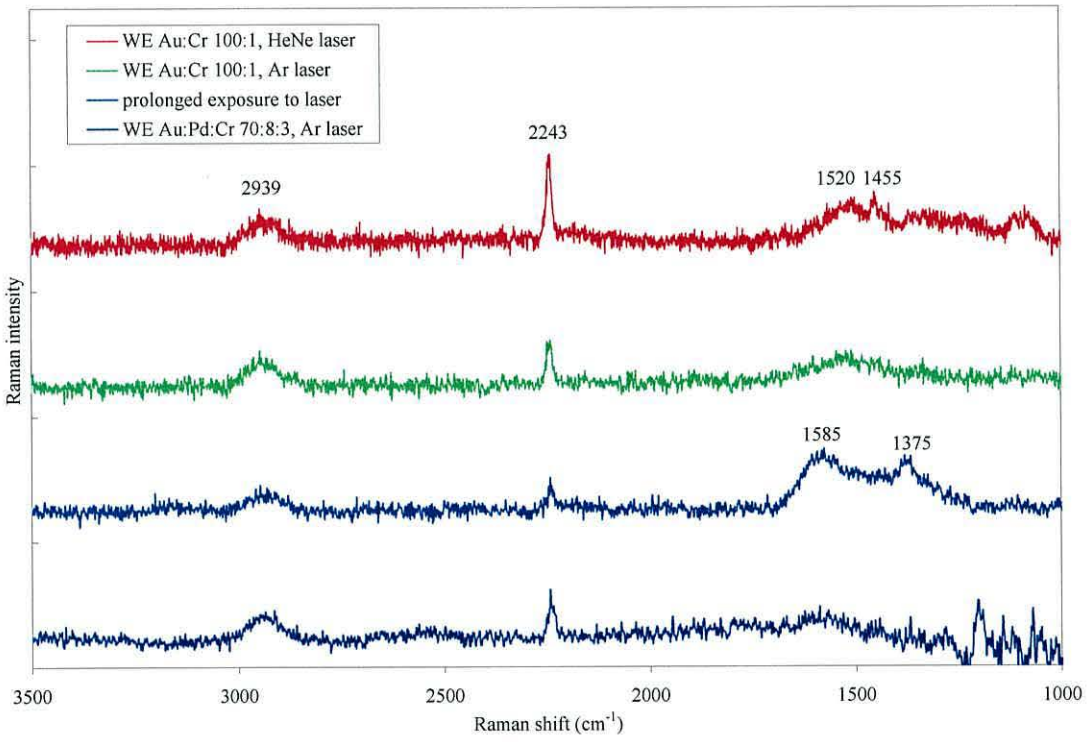

Figure 4.28 *Raman spectra of PAN films grown on Au WE with a thinner Cr adhesion layer and also a Pd blocking layer, AN 0.5M, DMF, TEAP 0.05M (baseline corrections).*

4.20 Laser intensity

In view of the evidence in Figure 4.28 showing that PAN film carbonize during prolonged exposure to the laser; an investigation was carried out to assess the effect of the laser irradiation during normal operation. The Raman spectra of electrografted PAN film samples excited using different laser intensities; high, medium and low were recorded and the results are given in Figure 4.29.

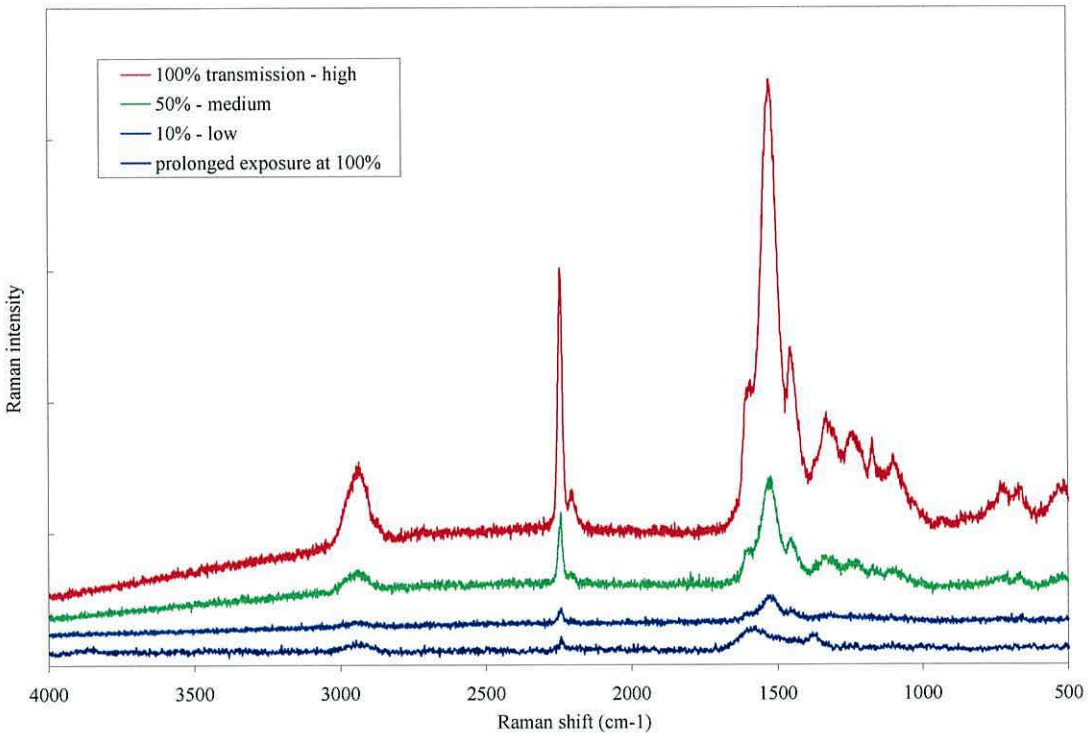

Figure 4.29 *Raman spectra of electrografted PAN films excited with different laser intensities (AN 0.5M, DMF, TEAP 0.05M, Ag WE).*

Numerical analysis of the four main peak intensities; 2940, 2243, 1520 and 1455 cm^{-1}. shows that they increase approximately in proportion to the increase in laser intensity. The spectrum of the PAN film subjected to prolonged exposure is included for reference. Clearly for normal operation there is no indication for the occurrence of structural transformations associated with carbonization even at 100% laser transmission.

4.21 Heat treatment

Exposing PAN films to heat can cause structural transformations, this can be seen in Figure 4.28. A number of studies have been carried out investigating such changes, in particular following the transformation of PAN into a carbon-fibre type structure (see Chapter 2). Using specular reflection infrared spectroscopy Leroy et al (1985) showed that by heating an electropolymerized PAN film on Ni, chemical transformations of the polymer (intra-chain cyclization, inter-chain reticulation, de-hydrogenation and de-nitrogenation) will take place. Another study by Pospisil et al (1998) looked at the structural evolution of pyrolized spun-coated PAN samples using FTIR and UV-visible spectroscopy. The resulting spectra revealed a conjugated structure caused by ring closure involving nitrile side groups.

One consideration regarding the unusual Raman peaks discovered in this work has been the possibility that these peaks are in fact the result of similar structural transformations arising from the applied voltage or the catalytic effect of the metal electrode. In order to explore this further PAN films electrografted onto semi-transparent Au electrodes were characterized before and after heat treatment (225 ^{o}C in a vacuum drying oven for two hours) using Raman, FTIR and UV-visible spectroscopy. The results proved interesting. One noticeable difference was the change of colour in the PAN film from a yellow to a more brown like colouration.

4.21.1. Raman spectral observations

The Raman spectrum of the PAN film prior to the heat treatment was typical of the PAN films seen here in this work for 1M AN concentration (Figure 4.10). The peaks at 1520 and 1600 cm^{-1} were clearly evident and their respective intensities were found to be in proportion to that expected for the monomer concentration. Unfortunately the recording of the Raman spectrum after the heat treatment was unsuccessful. The Raman signal from the sample saturated the detector on each attempt. Various methods were used to reduce the intensity i.e. filter, exposure times, and adjustment of focal point but with no results.

4.21.2. UV-visible spectral observations

The UV-visible spectra recorded before and after the heat treatment were typical of those found for a commercial spun-coated PAN sample in the literature, see Figure 4.30. Pospisil et al (1998) proposed that the change in the absorption spectrum after pyrolysis was due to the formation of a delocalized π-electron structure along the conjugated C=C and C=N bonds.

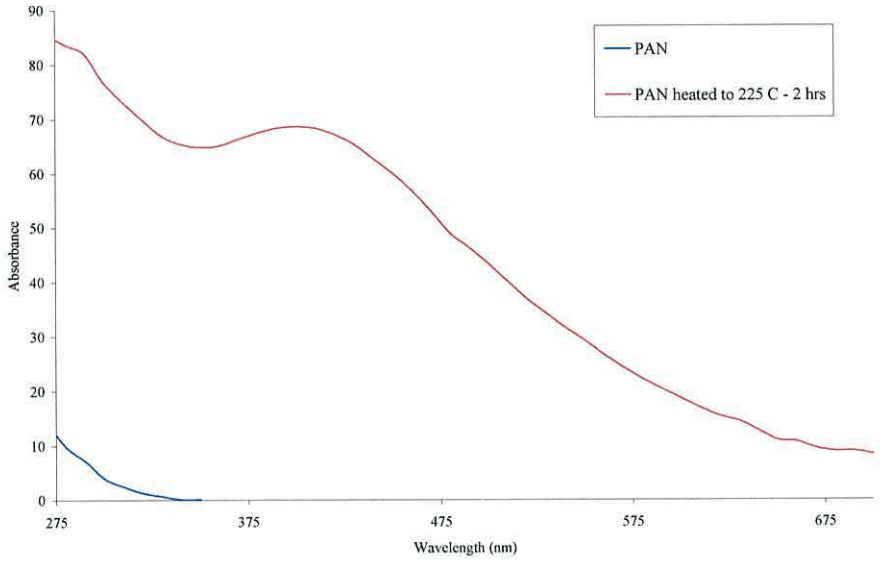

Figure 4.30 *UV - visible spectra of a PAN film before and after heat treatment*

4.21.3 FTIR spectral observations

The FTIR spectra of the electrografted PAN film shown in Figure 4.31 supports the transformations proposed by Pospisil et al (1998). A reduction in the ν (C-H) peak at 2939 cm $^{-1}$ and the ν (C≡N) at 2243 cm $^{-1}$ and the appearance of new peaks which we assign to ν (C=NH) at 2200 cm $^{-1}$, ν (C=C) at 1620 cm $^{-1}$, ν (C=N)n at 1585 cm $^{-1}$and δ sym (CH_3) at 1375 cm $^{-1}$ are consistent with the presence of conjugated imine and ethylene structures. Also worth noting is the disappearance of the peak associated with the solvent at 1666 cm $^{-1}$ which at the temperature applied is likely to have completely evaporated.

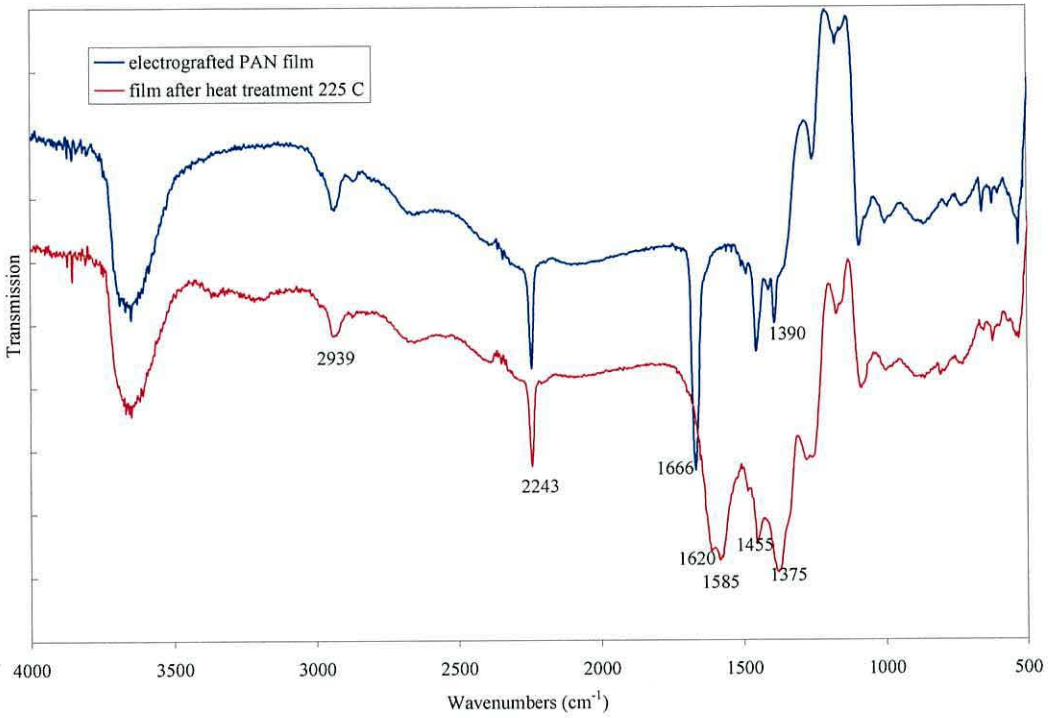

Figure 4.31 *FTIR spectra of electrografted PAN film before and after heat treatment, (AN 1M, DMF,TEAP 0.05M, Au WE, semi-transparent)*

4.22 Conclusion

The results presented in this Chapter have revealed a number of interesting points:

- Poor potentiostat control - Peak I is an unreliable indicator for effective film growth. Repeat scanning to test for passivation after any electroactivity was the only reasonable method for detection. Visibly observing film growth proved to be hazardous as the film visibility increased when it started to de-bond. The main concerns emerging are that the film's insolubility is due to cross-linking as a result of exceeding the grafting potential rather than true electrografting, and the influence of the Cr keying layer on the voltammogram response.
- Raman spectral anomalies at 1520 and 1580 cm^{-1} - FTIR and Raman spectra of electrografted PAN closely resemble a commercial spun-coated sample except for the appearance of these two unusual peaks, never seen before for PAN. There has never been any indication of these peaks in the FTIR equivalent spectra suggesting symmetry of the Raman active stretch making them FTIR inactive.
- Electrografted PAN films have a tendency to trap the solvent DMF indicated by the presence of a strong peak in FTIR at 1670 cm^{-1}. Further analysis of the other peaks present (see Section 5) confirms that this is the case and a slight shift in the carbonyl stretch indicates some complexing of the solvent carbonyl group with the nitrile moiety of the PAN. However the FTIR spectra of electrografted PAN films grown by Calberg et al (1998) using the same solvent show no such peaks.
- The Raman anomalies vary according to the solvent used. The Raman spectra of films grown in ACN show peaks at 1566/1600 cm^{-1} suggesting the type of structural transformations normally seen in the pyrolysis of PAN. This is supported by the deterioration of the nitrile peak and the appearance of peaks at 2190 and 3340 cm^{-1}, whereas the spectra of films grown in DMF show comparatively little deterioration. The anomalies do not appear to be dependent on the quantity of DMF trapped in the PAN film.
- Raman anomalies were found to be dependent on the monomer concentration of the electrografting solution and WE. The peaks were more intense for thinner films and consistently disappeared for thicker films grown at higher concentrations (2M) using the improved experimental conditions. Calberg et al

(1998) reported electrografted PAN to be predominantly isotactic near the surface. This suggests the anomalies are caused by a surface structure encouraged by the isotactic formation of PAN.

- Anomalies are sensitive to the pretreatment of the WE. Application of ORC treatment to Ag prior to electrografting has the effect of significantly reducing the intensity of these peaks. However the appearance of a peak at 1725 cm^{-1} in FTIR suggests the presence of unwanted oxidized species at the electrode surface which probably interferes with the electrografting process. This provides further evidence that the anomalies are associated with a structure near the surface.
- The intensity of these unusual peaks is also sensitive to the WE metal. For instance PAN films grown from a 0.5M AN solution show the strongest intensity for different WE metals according to the following order Pt >Ag > Cu >Au. The use of Pt foil eliminated Cr as a potential cause.
- Fluorescence has become an increasing problem as the quality of electrografted PAN films has improved.
- Heat treatment of the electrografted PAN films either through prolonged exposure to the laser or by more conventional vacuum oven, cause the structural transformations normally associated with the pyrolysis of PAN as evidenced by both the FTIR Raman and UV-visible spectra. Peaks associated with the trapped DMF were effectively eliminated and the Raman anomalies were replaced by the usual peaks associated with graphitization. UV- visible spectra of untreated electrografted PAN films showed no absorption above the wavelength of 300 nm.

These points will be discussed more fully in the next Chapter.

4.23 References

Baute, N., Jérôme, C., Martinot, L., Mertens, M., Geskin, V.M., Lazzaroni, R., Brédas, J.L. and Jérôme, R., *Eur. J. Inorg. Chem.,* (2001), 1097.

Calberg, C., Mertens, M., Jérôme, R., Arys, X., Jonas, A.M. and Legras, R., *Thin Solid Films,* **310,** (1997), 145.

Calberg, C., Mertens, M., Baute, N., Jérôme, R., Carlier, V., Sclavons, M. and Legras, R., *J. Polymer Sci., Part B,* Vol **36**, (1998), 543.

Crispin, X., Lazzaroni, R., Geskin, V.M., Baute, N., Dubois, P., Jérôme, R. and Brédas, J. L., *J. Am. Chem. Soc.,***121**, (1999), 176.

Leroy, S., Boiziau, C., Perreau, J., Reynaud, C., Zalczer, G., Lécayon, G. and Le Gressus, C., *J. Molecular Structure*, **128**, (1985), 269

Mertens, M., Calberg, C., Baute, N., Jérôme, R. and Martinot, L., *J. Electroanal. Chem.,* **441**, (1998), 237

Newton, P., Houzé, F., Guessab, S., Noel, S., Boyer, L., Lécayon, G. and Viel, P., *Thin Solid Films,* **303**, (1997), 200.

Pospisil, J., Samoc, M. and Zieba, J., *Eur. Polym. J.,*Vol 34,7, (1998), 899.

Renschler, C.L., Sylwester, A.P. and Salgado, L.V., *J.Mater.Res.,* **4**, (1988), 452.

Sánchez-Soto, P.J., Avíles, M.A., del Río, J.C., Ginés, J.M., Pascual, J. and Pérez-Rodríguez, J.L., *J. Anal. App. Pyrolysis*, **58**, (2001), 155.

Xue, G., Dong, J. and Zhang, J., *Polymer,* **35**, (1994), 723.

Chapter 5: Discussion of the PAN results

5.1 Introduction

The results obtained in the present work have raised a number of interesting points related to the electrografting of PAN. The main issues, which were summarized at the end of Chapter 4, will be explored in more detail here. For example, the study has provided further evidence concerning the important structural factors e.g. stereo-regularity, thickness control etc, which are used to promote electrografting as a means of functionalizing surfaces with high quality films. The main thrust of the discussion that follows, however, is focused on clarifying the main contradictions that appear in the literature (see Chapter 2) and in aspects of the current work. In so doing a new structure is proposed to explain a previously unreported Raman spectral feature in electrografted PAN.

5.2 Potentiostat control

Throughout this work, using the voltammogram to identify the onset of film growth proved unreliable. Even under the most stringent experimental conditions with a carefully prepared WE, there was no guarantee that a clear signature of electrografting was obtained. Indeed on several occasions, Peak I was not found to be related to film growth. This is not surprising since Bureau et al (1999) had shown mathematically (Section 2.20) that Peak I probably arose from the dynamic effect of polymerization occurring in solution rather than the result of electrode passivation.

Interestingly in another study by Bureau et al (1996) to investigate the interface structure of the anodic electropolymerization of MAN at a platinum electrode, it was found that even though no electroactivity was evident before the oxidation barrier of the perchlorate supporting salt, polymer films were nevertheless formed below this barrier but no corresponding Peak I was observed in the voltammograms.

The main concern in the present work was to identify accurately the electrografting potential to avoid the risk of over-voltages denaturing or de-bonding the film. In the absence of clearly identified electroreduction peaks, the insolubility of the PAN film at the electrode surface when grown in a solvent for PAN, i.e. DMF, was taken

as a positive indication of effective electrografting. A further important indicator was the significant reduction in the cathodic current observed in repeat scans arising from electrode passivation (see Figures 4.12, 4.18, 4.27 and 4.37).

Despite the controversy surrounding the electrochemical visibility of the electrografting reaction, the use of cyclic voltammetry has nonetheless provided an effective means of growing good quality PAN films. The careful preparation of the electrolyte and the electrochemical cell has assured the production of voltammogram responses comparable to those reported by Mertens et al (1996). The appearance of Peak I recognizable by its sensitivity to the monomer concentration and its subsequent disappearance during a repeat scan has been shown generally to be an effective indicator (see Figures 4.12, 4.18, 4.27 and 4.37). The proof of its effectiveness, however, has been in the quality of the resulting PAN films as evidenced by AFM microscopy (see Section 4.18). The confidence in the electrografted nature of these PAN films arises from several qualities, namely, the ability to withstand a peel test, insolubility in DMF, roughness and thickness measurements comparable with those reported by Calberg et al (1997) for the electrografting of PAN using the equivalent conditions i.e. same monomer concentrations, solvent etc.

The experimental preparation and set-up used here has evolved via a series of improvements to a technique used by Mills et al (2000) in line with the preparation and procedures adopted by Lecayon et al (1982) for the electrografting of PAN. Although the requirement for stringent conditions is similar, the simplicity of the current set-up contrasts markedly with previous workers (see Chapter 3). For example the adoption of a simple electrochemical cell employing siphoning techniques has reduced the need for the elaborate glove box procedures thus leading to a cost-effective industrial process. The comparable voltammogram responses and the resulting PAN film quality provide adequate assurance that this approach works.

5.3 DMF in PAN films

The electrografted PAN films produced in this work have a tendency to trap DMF as indicated by the presence of a strong peak in FTIR at 1666 cm^{-1}. This contrasts with the PAN films grown by Calberg et al (1998) using the same solvent which showed no

such peaks. Funt et al (1964) have also reported the presence of a peak at 1670 cm^{-1} when electropolymerizing PAN in DMF but attributed this to cross-linking and did not consider the influence of the solvent. The presence of other peaks at 1570 and 2200 cm^{-1} associated with –C=N- and -$(C=N)_n$ – chains supported their proposed explanation for the insolubility of the cathodic polymer. Several other studies on PAN cite the presence of the 1670 cm^{-1} peak as evidence of cross-linking of PAN via nitrile groups. Badawy et al (2003) ascribed the band at 1670 cm^{-1} to the formation of -CH=N-N=CH- conjugation across the polymer chains as a consequence of radiation induced polymerization of AN. Coincidentally DMF was also used as a supporting solvent.

However, the 1570 and 2200 cm^{-1} peaks reported by Funt et al (1964) are not present in the FTIR spectra of the untreated electrografted PAN films produced in this work from a solution containing DMF. Interestingly, subtracting the characteristic peaks of PAN from the spectrum of an electrografted PAN film reveals not only the peak at 1670 cm^{-1} but a range of other peaks common to DMF. The presence of the three main peaks at 1670, 1388 and 659 cm^{-1} which can be attributed to ν (>C = O), ν (OC – N) and δ (O – C - N) respectively provide clear evidence that the 1670 cm^{-1} peak is more likely to be due to the presence of trapped DMF than to the cross-linking suggested by Funt et al and others. Further confirmation is provided by undertaking a final rinse in acetone (see section 4.6) when all three of the above peaks in the FTIR spectrum were significantly reduced as DMF was removed from the sample.

A comparison of these three peak positions with those of pure DMF show a slight shift suggesting the PAN may have some influence on the solvent spectrum. In an FTIR study Phadke et al (2005) showed that the degree of interaction between DMF and PAN was dependent on the molecular weight of the commercial PAN samples dissolved in the solvent. The shifts in the FTIR spectral peaks were explained in terms of changes to the bond character of the DMF molecule. For pure DMF, the resonance of electrons from the N tends towards the more electronegative O giving the N - C more double bond character whereas the C = O has a more single bond character. Upon adding a low molecular weight PAN A, (M_w = 50 k) the electronegative N of the nitrile group interacts with the relatively electropositive N of the DMF resulting in an increase in the single bond character of the N - CO observed as a red shift while the increase in the double bond

character of the >C = O resulted in a blue shift.. However for a higher molecular weight PAN C (M_w = 250 k), the anti-dipolar alignment of the nitrile is more probable so that less nitrile groups are accessible to interact with DMF resulting in fewer changes in the spectral peaks. In contrast, a PAN B at an intermediate molecular weight (150 k) showed a mixture of shifts. All three PAN samples also show the emergence of a new peak at 667 cm^{-1} Table 5.2 summarises these results and shows how the peak positions vary between pure DMF and that of a range of electrografted PAN (EG PAN) samples grown on different metals and a spun coated commercial PAN sample (M_w = 150 k) from this work. Table 5.1 also includes the respective nitrile stretches to show that PAN is also influenced by the trapped solvent.

Table 5.1 *The effect of PAN and DMF interaction on the IR frequencies (cm^{-1})*

Sample	ν (>C = O)	ν (OC – N)	δ (O – C - N)	ν (C ≡ N)
DMF	1667.3	1390	661.5	-
DMF + PAN A	1673.1	1387.5	658.6, 667	2241.1
DMF + PAN B	1665-1680	1385.8	658.6, 667	2242.1
DMF + PAN C	1660-1670	1392.5	659.6, 667	2242.1
PAN A,B,C	-	-	-	2241-2243
EG PAN on Ag	1664.9	1388.5	659.6	2243.3
EG PAN on Au	1664.4	1389.2	659.7	2243.3
EG PAN on Cu	1666.4	1392	659.9	2241.2
EG PAN on Pt	1664.6	1388.7	661.6	2243
Commercial PAN	1674	1388.6	659.6	2243.1

It is strongly evident from the information given in Table 5.1 that DMF is responsible for the peak at ~1666 cm^{-1}. A comparison of the values suggests that there is some interaction between DMF and PAN. Interestingly, the effect is much weaker in the electrografted PAN than in the commercial PAN.

The FTIR spectra of electrografted PAN films grown by Calberg et al (1998) using low monomer concentrations do not show any solvent residue. However, the isotacticity of these films was found to be comparable to that of PAN produced in urea canals. A study by Minagawa et al (1989) found that isotactic samples of PAN prepared

by canal polymerization of AN with urea using γ ray irradiation were quite insoluble in DMF unless the temperature was increased above 100 °C. If this is correct the amount of trapped DMF in a PAN film could possibly be considered as an indicator of the degree of stereoregularity of the PAN film.

A further study by Minagawa et al (1995) into the steric effect of solvent molecules in the dissolution of commercial PAN samples from different DMF derivatives using Raman spectroscopy shows that the carbonyl band of pure DMF at 1661 cm^{-1} is shifted to 1671 cm^{-1}after the addition of adiponitrile. Since dipolar aprotic solvents associate with each other through strong dipole - dipole interaction (Senoh et al, 1970), the addition of the nitrile group is expected to interfere with this association and hence shift the carbonyl band as observed experimentally.

The tendency of the electrografted films in this work to trap solvent can probably be explained by the inability of the WE surface to be completely accessible for the initiation of the electrografting of polymer chains due to a residual level of contamination remaining both in the electrolyte and on the electrode surface. This contrasts with the films grown by Calberg et al (1998) which progressively repel the solvent from the electrode as the densely packed grafted chains propagate.

From the evidence presented above, it is clear that the electrografted PAN films produced in this work contain traces of the DMF solvent used in film preparation. Therefore, in the discussion that follows no further attention will be paid to the characteristic FTIR bands of DMF which appear at 2930, 2860, 1667, 1500, 1439, 1407, 1389, 1257, 1096 and 660 cm^{-1} nor to the Raman scattering bands of DMF at 2934, 2861, 1661, 1441, 1408, 1096, 867, 660 cm^{-1}. However, the DMF band at 1096 cm^{-1} hides an anomalous Raman scattering band in the electrografted PAN. Evidence for this is seen in Figure 4.8 where little change is observed in the 1096 cm^{-1} Raman band of PAN following a rinse in acetone. This contrasts with the complete removal of the 1096 cm^{-1} FTIR band as DMF is leached out of the PAN film. It is concluded therefore that the 1096 cm^{-1} Raman band is an intrinsic feature of the electrografted PAN that is not seen in the spectrum of solvent free, spin-coated PAN. In the next section, other anomalous Raman bands intrinsic to the electrografted PAN are highlighted and discussed.

5.4 Anomalous Raman bands

The FTIR and Raman spectra of electrografted PAN closely resemble those of commercial spun-coated samples except for the appearance of an unusual broad peak in the Raman spectrum at 1520 cm^{-1}, the shoulder at 1580 cm^{-1} and the peak at 1096 cm^{-1} identified in the previous section. These Raman bands have not been reported previously for PAN. The non-appearance of these peaks in the corresponding FTIR spectra suggest some kind of structural symmetry which allows the stretches to be Raman active yet making them FTIR inactive. The intensity of the Raman bands in the 1500 – 1600 cm^{-1} region appears to depend on the thickness of the PAN films, if it is assumed that the monomer concentration controls the thickness, see Figure 4.10. The ratio of the band intensity to the halfwidth increases as the film thickness decreases. The halfwidthdth of the band can be attributed to the different local structural environments in the polymer influencing the frequency of the vibration. According to Calberg et al (1998) the polymer structure becomes increasingly heterotactic as film thickness increases. The thickness dependence of the band intensity suggests that the vibrations are particularly influenced by the orientation of the PAN chains with respect to the polarization of the incoming light. Tanguy et al (2000) in a study of the electrografting of methyl methacrylonitrile proposed a progressive reorganization of the polymer towards a brush-like conformation as a result of successive cycles of the voltage. It appears therefore that there are two factors which can potentially affect the conformation of these Raman bands namely the tacticity of the polymer chains and the organisation of the tethered chain on the metal surface. The more intense, sharper Raman bands of the thinner PAN films reflect the more isotactic brush-like polymer structure nearer the metal surface.

5.5 Non-characteristic PAN peaks

Whereas the anomalous bands described in the previous section have not previously been observed, there are many examples in the literature of spectral features occurring in PAN that are not characteristic of PAN films. For example, Leroy et al (1985) found that applying an electrografting potential for 2 s and 10 s produced structural differences in the resulting PAN films (AN 0.5M, ACN) which could be seen

in the FTIR spectra. Only cis-type vinylic bonds were recorded for the 2 s sample whereas both cis and trans-type vinylic bonds were observed for the 10 s film. The existence of solely cis-type vinylic bonds in the 2 s sample suggests a high degree of isotacticity in the polymer chains, consistent with Calberg et al (1998) who postulated that a high degree of isotacticity was more probable in the early stages of growth. Increasing the growth duration appears to increase chain segmentation and intramolecular ring formation as evidenced by the increase in vinylic terminal bonds and conjugated imino groups in PAN films grown for 10 s.

Table 5.2 reproduces the list different infrared bands which have been observed for different PAN samples. Only those bands characteristic of pure PAN are common to the FTIR spectra of the electrografted PAN films produced during this work and those presented by Leroy et al (1985).

Table 5.2 *FTIR bands attributable to electropolymerized PAN (Leroy et al,1985)*

Structure	Wavenumber (cm^{-1})	Vibration	PAN film (2 s)	PAN film (10s)
amine	3360	ν NH	w	+ , broadening
amine	3340	ν NH		w
term vinylic	3000	ν CH cis	w	+
term vinylic	2970	ν asym (CH_3)	m	+
PAN	2940	ν asym (CH_2)	m	+
PAN	2890	ν CH	w	+
term vinylic	2880	ν sym (CH_3)	mw	+
PAN	2860	ν sym (CH_2)	w	+
PAN	2240	ν (C≡N)	s	+
imino nitrile	2200	ν (C=NH)	mw	+ , broadening
term vinylic	1640	ν (C=C)	w	+ , broadening
cyclization	1575	ν $(C=N)_n$		m
term vinylic	1460	δ asym (CH_3)		s
PAN	1450	δ (CH_2)	s	+
term vinylic	1420	δ in-plane (CH) cis	ms	+
term vinylic	1370	δ sym (CH_3)		w
PAN	1360	δ (CH)		w
PAN	1325	δ (CH)	w	+ , broadening
PAN	1310	δ wag (CH_2)	w	+ , broadening
term vinylic	1300	δ in-plane (CH) trans		w
PAN	1235	δ twist (CH_2)		w
amine	1175	ν (C-N)	w	+ , broadening
term vinylic	990	δ in-plane (CH) trans		w
term vinylic	770	δ in-plane (CH) cis	w	+

As discussed in Section 5.3, Funt et al (1964) also reported non-characteristic FTIR peaks at 2200, 1670 and 1570 cm^{-1} for an insoluble cathodic PAN produced in DMF and attributed these to cross-linking and the formation of –C=N- and $-(C=N)_n-$ chains. These authors however, failed to recognize the characteristic absorption bands of DMF in the FTIR spectra. On the other hand, the electrografting work carried out in this study using ACN, a non-solvent for PAN does give similar results to Leroy et al (see Figure 4.6) suggesting that the nature of polymer precipitation at the electrode may favour certain transformations.

Using SERS Xue et al (1994) showed that, by adjusting the evaporation rate of the DMF residue of a sample containing commercial PAN, they could influence the degree of cyclization of PAN catalysed by a Ag surface. They proposed that by increasing the evaporation rate, the polymer chains were more likely to pile up on one another randomly on the surface, giving insufficient time for the side groups to orientate thus leading to only partial cyclization of the first monolayer. The degree of cyclization was indicated by a significant reduction of the peak at 2243 cm^{-1} associated with the nitrile stretch and the appearance of new peaks at 2140, 1600, 1575, 1075 and 1000 cm^{-1} typical of aromatic ring vibrations.

Xue et al (2001) again using SERS investigated the adsorption and surface-catalyzed reaction of PAN on Ag. The SERS spectra were recorded from PAN coatings on HNO_3 etched Ag surfaces, where samples were prepared by spreading a solution of PAN dissolved in DMF followed by a controlled evaporation of the solvent. Figure 5.1 shows the resulting spectra. The presence of the 2245 cm^{-1} band in spectra A and B is typical of PAN and is attributed to the free dangling nitrile peak. However the appearance of a broader band at 2160 cm^{-1} in spectrum B was also attributed to a C = N stretch. The authors suggested that the shift and broadening upon adsorption indicated side-on co-ordination between the nitrile group and the Ag surface atoms. They further proposed that the triple bond order of the nitrile is reduced by the back donation of electrons from the metal to the nitrile anti-bonding orbitals as a result of this direct interaction. The roughened Ag surface weakens the CN bond of any adsorbed PAN and catalyses the cyclization of PAN which normally occurs at higher temperatures.

The presence of other bands at 1600, 1580, 1080 and 1000 cm^{-1} were attributed to –(C=C) - or –(C=N) conjugation ring stretching and in-plane C-H deformation frequencies respectively to support the transformation of PAN into a fused ring structure at the interfacial region. The strength of the intensities was attributed to the aromatic ring structure sticking up on the metal surface based on the electromagnetic theory of the SERS selection rule. The difference between spectra B and C was attributed to the time allowed for favourable molecular orientations see section 5.2.

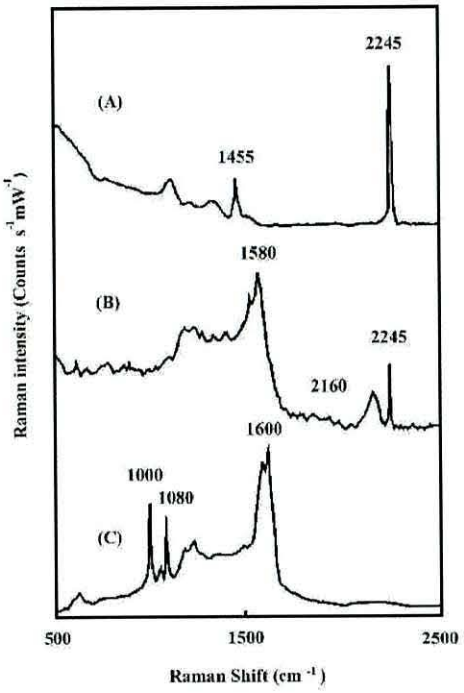

Figure 5.1 *(A) Normal Raman spectrum of PAN on smooth silver foil; (B) SERS spectrum of PAN film on rough silver foil, prepared by fast evaporation of the solvent; (C) SERS spectrum of PAN film on rough silver foil, prepared by slow evaporation of the solvent (Xue et al, 2001).*

These Raman spectral trends are similar to those seen by Leroy et al and others in FTIR for electrografted PAN either following prolonged growth periods or from heat treatment. Table 5.3 lists these spectral findings.

Table 5.3 *Non-characteristic PAN peaks observed in FTIR and Raman spectra, by various authors.*

Authors	PAN + solvent	Spectra Type	Non characteristic PAN spectral bands (cm^{-1})	
			No heat treatment	After heat treatment
Funt et al (1964)	electropolymerized DMF	FTIR	1670, **1570**	
Reynaud et al (1982)	electrografted ACN	FTIR	2980, **2200**, 1425	**1590** – 1680 range
Leroy et al (1985)	electrografted (2s & 10s) ACN	FTIR	3360, 3340, 3000, 2970, 2880, **2200**, 1640, **1575**, 1460, 1420, 1370, 1300, 1175, 990, 770	
Renschler et al (1989)	commercial PAN DMF	FTIR Raman		**1590, 1380** **1580**, 1350
Xue et al (1994)	commercial PAN DMF	Raman (SERS)		2155, 1600, **1580**, 1075, 1000
Deniau et al (1991)	electrografted ACN	FTIR	**2197**, 1719, 1639, 1079, 830	
Mertens et al (1996)	electrografted ACN	FTIR	Only characteristic PAN peaks observed	
Newton et al (1997)	electrografted DMF	FTIR		2190, **1600** + shoulder at 1640, **1385**
Pospisil et al (1998)	commercial DMF	FTIR		2190, 1650, 1360
Calberg et al (1998)	electrografted DMF	FTIR		2190, 1566
Zhou et al (2003)	commercial PAN DMF	Raman (SERS)		1585, **1375** (high intensity laser 200 mW)

In general the majority of authors listed above, all share similar findings in their spectral results. Either the early stages of the structural transformation normally seen during the pyrolysis of PAN are characterised by the appearance of bands at ~ 2190 cm^{-1} and 1566 cm^{-1} or the later stages by bands at 1590 and 1380 cm^{-1}. The variation in the values depends on the type of spectroscopy used. All the spectra reviewed show an increase in the bands attributed to transformations which occurs at the expense of the characteristic PAN peaks at 2940, 2245 and 1455 cm^{-1}. This is in marked contrast to the Raman anomalies found in this work for the PAN electrografted in DMF where no evidence was obtained either in FTIR or Raman, for the growth of a band at 2190 cm^{-1}, to support this type of transformation.

Interestingly though, electrografted PAN films can undergo structural changes at a much lower temperature than previously reported for bulk PAN (Chung et al, 1984). In the present work, heating the electrografted PAN films either by prolonged exposure to a laser or in a conventional vacuum oven were found to cause the structural transformations normally associated with the pyrolysis of PAN (see Renschler et al, Table 5.3) as evidenced by FTIR, Raman and UV-visible spectra results (see Chapter 4). Heating effectively eliminated the peaks associated with trapped DMF and the Raman anomalies were replaced by the usual peaks associated with graphitization (see Table 5.3). Additionally, while UV spectra of electrografted PAN films showed no absorption above 300 nm (Figure 4.30), heated films took on a distinct yellowy brown hue consistent with graphitization.

Laser- induced structural changes in PAN were also investigated by Zhou et al (2003). In their experiments, a Ag layer deposited onto spun-coated PAN films of different thicknesses, was reduced to form colloidal particles a few 10s of nm in size. The Ag layer thus provides a SERS-active overcoating layer. The usual characteristic PAN peaks at 2941, 2245 and 1455 were collected from the thicker 10 μm PAN films. A study of 100 nm PAN films using a 1065 nm laser line at different laser powers showed a dramatic difference in the spectra between 30 mW and 200 mW. The band at 2245 cm^{-1} became rather weak and new bands appeared at 1608, 1393, 1130 and 1005 cm^{-1} indicating structural changes resulting from the higher laser power. These bands were attributed to aromatic ring vibrations and correlated with the FTIR spectra of PAN

subjected to heat treatment (see Table 5.3). A SERS spectrum of a 100 nm PAN film recorded with a 514.5 nm laser line with a power of 200 mW clearly showed that the PAN under the Ag layer had been further converted to a graphite-like structure. Indeed, the spectrum was found to be identical to that obtained by evaporating Ag onto carbon fibres. The characteristic bands of PAN had been replaced by two broad peaks at 1585 and 1370 cm^{-1}. Zhou et al (2003), in agreement with Xue et al (1994), proposed that the Ag colloidal particles catalyse the cyclization of PAN a process which normally occurs at higher temperatures.

Exposure to laser radiation in the present work did not show comparable changes in the Raman spectrum of PAN films (see Figure 4.29). Furthermore, the Raman spectra reported by Zhou et al (2003) do not exhibit the anomalous Raman bands found in this work. The only similarities are the characteristic PAN bands seen in the spectra of Zhou et al's 10 μm PAN films and the two broad peaks at 1375 and 1585 cm^{-1} associated with graphitization of the PAN film which is also seen here following prolonged exposure to the Ar ion laser.

5.6 Dependence of anomalous Raman bands on experimental parameters

The Raman anomalies found in this work vary according to the solvent used. The Raman spectra of films grown in ACN show peaks at 1566/1600 cm^{-1} suggesting the type of structural transformations discussed above. This is supported by the reduction of the nitrile peak and the appearance of peaks at 2190 cm^{-1} (FTIR and Raman) and 3340 cm^{-1} (FTIR). In contrast, the spectra of films grown in DMF show no such behaviour. The Raman anomalies do not appear to be dependent on the quantity of DMF trapped in the PAN film. The FTIR and Raman spectra of PAN films electrografted onto different pretreated metal WE (see Figure 4.13) show that a PAN film (Ag WE) which appears to have significantly more DMF trapped within it does not show a similar increase in the intensity of the Raman bands at 1520 and 1580 cm^{-1}.

The main difference between DMF and ACN is the ability to dissolve any ungrafted PAN in solution. PAN films electrografted in DMF are more likely to be brush-like in conformation as opposed to films grown in ACN which could potentially be a precipitated mixture of grafted and ungrafted chains. AFM images of PAN films

electrografted in different solvents show significant differences. PAN films grown in ACN are quite rough in comparison to the smoother PAN films formed in DMF (see Figure 4.7). Calberg et al (1997) reported that PAN films grown in ACN were much thinner than those grown in DMF. The difference was attributed to the precipitation of growing chains in ACN which hindered further propagation. Calberg et al (1997) also found that PAN films deposited in ACN were more heterogeneous than those prepared in DMF which appeared more uniform and regular. They suggested the difference in the surface characteristics reflected a more homogeneous initiation on the electrode surface in DMF and the solvation of the growing chains during the whole polymerization process in the solvent. This difference in the polymer structure most likely explains the influence of the solvent on the Raman anomalies (see Figure 4.6). If the polymer chains have a tendency to precipitate onto the electrode in ACN, the nitrile moiety is more likely to come into contact with the Ag surface than in the case of DMF, therefore allowing the Ag to catalyse the cyclization of PAN as reported by Xue et al (2001), see Section 5.4.

Raman anomalies were found to be dependent both on the monomer concentration in the electrografting solution and on the WE. The peaks were more intense for thinner films and consistently disappeared for thicker films grown at higher concentrations (2M) using the improved experimental conditions. Calberg et al (1998) reported that electrografted PAN was predominantly isotactic near the surface and attributed this to steric and electrical restraints imposed by the electric field on the initiated chains. PAN films grown in DMF at 0.5M AN were shown by FTIR analysis to exhibit twice as much isotacticity as PAN films grown at 2M using the same conditions. The PAN film grown at the lower concentration was found to be comparable to a stereoregular PAN synthesized in urea canals, whereas the isotacticity of the PAN film at the higher concentration was typical of a commercial PAN. If this is the case and Minigawa et al (1989) are correct, DMF is unlikely to be present in the isotactic region of PAN and therefore cannot be a cause of the anomalous peaks.

It has already been suggested earlier that the more homogeneous initiation of polymerization in a solvent for the polymer can lead to a more orderly, brush like conformation of the polymer chains near the electrode surface. If this is the case, thinner films will have proportionally greater brush-like character than thicker films. Further

support for this view comes from Calberg et al (1997) who showed that overall film thickness depended on the solvent used and the monomer concentration, these factors controlling the degree of tethering and density of polymer chains on the WE. All this suggests that the anomalous bands are caused by a surface structure reflecting the isotactic, brush like formation of PAN near the surface.

The anomalies are sensitive to the pretreatment of the WE. Application of ORC treatment to Ag prior to electrografting has the effect of significantly reducing the intensity of these peaks. However the appearance of a peak at 1725 cm^{-1} in FTIR (Figure 4.11) suggests the presence of unwanted oxidized species at the electrode surface which probably interferes with the electrografting process. This provides further evidence that the anomalies are associated with a structure near the surface.

The intensity of these unusual peaks is also sensitive to the WE metal. For instance the Raman spectra of PAN films grown from a 0.5M AN solution show that the intensity for the different WE metals follows the order Pt >Ag > Cu >Au. The last three coin metal WE were all produced by vapour deposition (see Chapter 3) and required a chrome keying layer. Using a polished Pt foil WE eliminated the Cr adhesion layer as a potential cause of the Raman anomalies. All four metals were subjected to negative cycling prior to the electrografting process. Apart from Pt, the coinage metals reflect the order of the surface plasmon wavelength response to a HeNe laser in the diagram compiled by Schatz et al (2002), see Figure 3.5. If SERS was responsible for enhancing some surface structure, Pt would be expected to be the least effective. The AFM analysis of a Ag surface before and after the pre-treatment shows no indication of the type of surface required for SERS enhancement suggesting that this is not the mechanism for the effect.

As the quality of electrografted PAN films improved i.e. reduction in film defects, the competing phenomenon of fluorescence made it increasingly more difficult to obtain Raman spectral information for the chemical characterization of PAN. Unfortunately the region below 1500 cm^{-1} was particularly obscured in the Raman spectra of electrografted PAN films. Baseline corrections are not effective in recovering information in this region due to the errors involved is estimating the background curve to be subtracted from the raw data. Fluorescence is often attributed to impurities. The enhanced fluorescence

observed in the Raman spectra of improving PAN films then appears to be a contradiction. However the reduction of film defects due to the development of the technique also resulted in a reduction of film thickness, in line with those found by Calberg et al (1997) probably due to a more efficient surface initiation. This is supported by the noticeable increase in passivation efficiency in the voltammogram responses. Any surface impurities at the metal polymer interface would be more accessible to the laser causing fluorescence in thinner films. This is supported by the fact that fluorescence is significantly greater for PAN films grown at lower monomer concentrations.

5.7 Assignment of anomalous Raman band.

Based on the results in Chapter 4 and the foregoing discussion in this Chapter a number of clues as to the cause of the anomalous Raman bands has been uncovered namely:

- Raman and FTIR spectra of electrografted PAN closely resemble commercial PAN except for the unique Raman anomalies and those arising from trapped DMF.
- That the feature is Raman active but FTIR inactive is consistent with a molecular arrangement demonstrating structural symmetry.
- An isotactic, brush-like polymer structure encourages the interaction of nitrile groups in the aligned polymer chains.
- The Raman anomalies are sensitive to orientation of the structure at the surface.
- Raman/ FTIR spectra of heat treated films do not exhibit the same features
- DMF is unlikely to be directly involved.
- No absorption for wavelengths greater than 300 nm was evident in the UV-visible spectra of untreated electrografted PAN films.
- The resilience of the Raman peak at 1096 cm^{-1} in the spectrum of an electrografted PAN film rinsed in acetone.
- No obvious increase in the FTIR spectral peak at 2190 cm^{-1} to support the structural transformations normally seen for PAN.

As a result of these findings the mechanism and structure in Scheme 5.1 are proposed to satisfy the above criteria. The scheme was first suggested by Pethkar et al (2001) for the

γ-Ray induced cross-linking of polyacrylonitrile chains. According to this study, the – C ≡ N consisting of weaker π bonding is more susceptible to forming radicals, which results in the cross-linking of the two polymeric chains through the nitrile group.

Scheme 5.1

Step 1

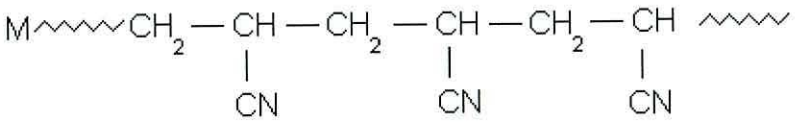

Step 2

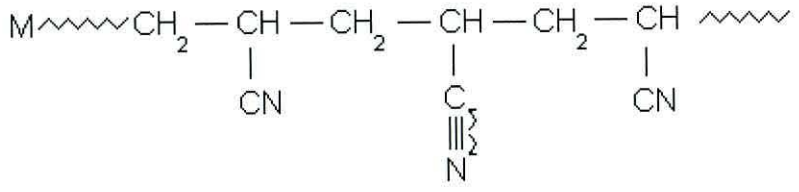

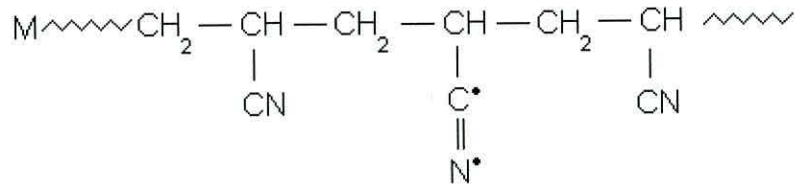

Step 3

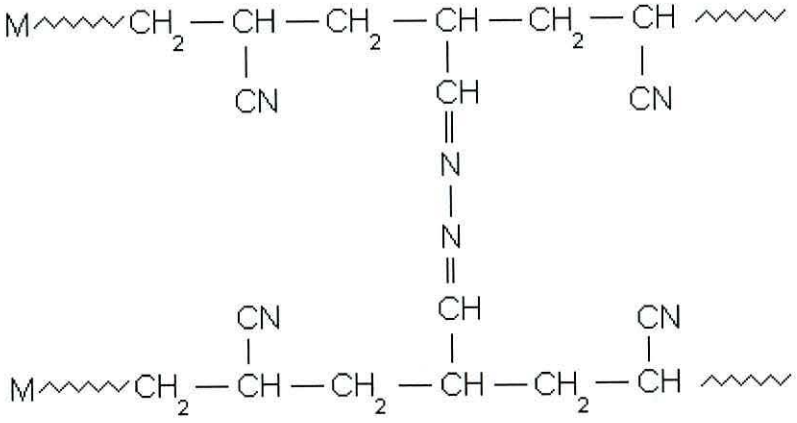

As a result of the interaction between nitrile moieties, azo groups are formed between PAN chains thus creating a ladder type structure. The structure has a symmetrical centre and is therefore expected to have the ν(N - N) and ν_{sym} (C = N)

inactive in IR spectroscopy but active in Raman whereas the ν_{asym} (C = N) will be active in IR and not in Raman. The Raman peak at 1096 cm^{-1} which was hardly affected by the acetone rinse (see Section 5.3 and Figure 4.8) and the Raman anomalies centered at 1520 cm^{-1} with a shoulder at 1580 cm^{-1}, which are not present in FTIR, certainly provide the evidence for the ν(N - N) and ν_{sym} (C = N) respectively. Harada et al, (1991) in a FTIR and Raman study of a stereoregular polymer prepared from propionaldehyde azine observed similar peaks in Raman which were not active in FTIR. Abo Aly (1999) also confirms these findings in a study of the infrared and Raman spectra of some symmetric azines. The studied azines were found to have almost a C_{2h} symmetry and therefore the ν(N - N) and ν_{sym}(C = N) were only observed in the Raman spectra, whereas ν_{asym}(C = N) was observed in FTIR. If the structure described above is present as a result of the brush-like isotactic formation of PAN near the surface, there should be a complementary ν_{asym}(C = N) visible in FTIR. A close inspection of the FTIR spectrum of the film rinsed in acetone (see Figure 4.8) suggests the presence of a possible candidate observed as a shoulder at ~ 1640 cm^{-1} to the intense carbonyl stretch of the DMF.

This ladder type structure is only likely to be present near the surface where the PAN film is predominantly isotactic. The azo type structure would potentially hang quasi -parallel to the surface between two normally aligned polymeric chains. A structure of this nature should be sensitive to the polarization of the incident light. Furthermore, increasing disorder in thicker films would be expected to lead to a thickness dependence of the intensity of the Raman bands observed in Figure 4.10. This approach was also used by Everall (1998) to map gradients through the thickness of uniaxially-oriented poly(ethylene terephthalate) films.

The two Raman active stretches ν(N - N) and ν_{sym} (C = N) of the symmetric azine are sensitive to the adjoining molecular structure. The study by Abo Aly (1999), which reports the vibrational coordinates for a series of conjugated azines, shows how the ν(N - N) and ν_{sym} (C = N) stretches can vary from 1000 to 1218 cm^{-1} and 1525 to 1624 cm^{-1} respectively depending on the nature of the different aryl groups. The breadth of the Raman bands centered at 1520 cm^{-1} with a shoulder at 1600 cm^{-1} reflects the

sensitivity of the vibrational coordinates of the azine to the immediate structural environment.

Pethkar et al (2001) also used UV-visible spectroscopy and solid state NMR to support their proposals. The UV-visible spectra of the electrografted PAN films grown on semi-transparent Au WE for this work provided no such supporting evidence. However this is not surprising since the thickness of the structured layer is unlikely to provide sufficient absorption to be detected by the instrument used in the present work. The main purpose of the UV-visible spectroscopy was to refute the notion that the anomalous Raman peaks arose from a cyclization mechanism such as occurs when PAN is subjected to heat treatment (Pospisil et al, 1998).

5.8 Summary

In this Chapter it has been argued that the electrografted PAN films produced in this work are comparable to those obtained by Mertens et al (1996) and Calberg et al (1998) as evidenced by the AFM and FTIR studies. In this first time Raman study of electrografted PAN films, new previously unreported Raman peaks centered at 1096 cm^{-1} and 1520 cm^{-1} with a shoulder at 1580 cm^{-1}, have been attributed to the formation of a ladder type network of vertically stacked polymer chains connected by azine bridges. It has also been shown that the FTIR absorption bands at ~ 1670 cm^{-1} has been incorrectly assigned by several workers. It is likely to have arisen from entrapped DMF rather than from structural transformations of the type that occur in PAN during heating. No evidence for such transformations was found in the spectra of PAN produced in this work by electrografting in DMF, although similar effects may have occurred when electrografting in ACN.

5.9 References:

Abo Aly, M.M., *Spectrochimica Acta Part A*, 55 (1999), 1711.

Bureau, C., Deniau, G., Valin, F., Guittet, M. J., Lécayon, G. and Delhalle, J., *Surface Science,* **355**, (1996), 177.

Bureau, C., *J. Electroanal. Chem.,* **479**, (1999), 43.

Calberg, C., Mertens, M., Jérôme, R., Arys, X., Jonas, A.M. and Legras, R., *Thin Solid Films,* **310,**(1997), 145.

Calberg, C., Mertens, M., Baute, N., Jérôme, R., Carlier, V., Sclavons, M. and Legras, R., *J. Polymer Sci., Part B,* Vol **36**, (1998), 543.

Chung, C., Schlesinger, Y., Etemad, S., Mac Diamid, A. G. and Heeger, A. J., *J. Polym. Sci. Polym. Phys. Ed.* **22**, (1984), 1239.

Deniau, G., Lécayon, G. and Viel, P. *Langmuir*, **8**, (1992), 267.

Everall, N.J., Appl. Spectrosc., **52**, (1998), 1498.

Funt, B.L. and Williams, F.D., *J. Polymer Sci., Part A,* **2**, (1964),865.

Harada, A., Hirofumi, F. and Kamachi, K., Macromolecules, **24,** (1991), 5504.

Ikeda, R., Chase, D.B., and Everall, N.J., in Handbook of Vibrational Spectroscopy, Vol. 2, Chalmers, J.M. and Griffiths, P.R. (Eds.), John Wiley and Sons, Chichester,(2002),716.

Lécayon, G., Bouziem, Y., Le Gressus, C., Reynaud, C., Boiziau, C. and Juret, C., *Chem. Phys. Lett.*, **91** (1982), 506.

Leroy, S., Boiziau, C., Perreau, J., Reynaud, C., Zalczer, G., Lécayon, G. and Le Gressus, C., *J. Molecular Structure*, **128**, (1985), 269.

Mertens, M., Calberg, C., Martinot, L. and Jérôme, R., *Macromolecules,* **29**, (1996), 4910.

Mills, C.A., Lacey, D., Stevenson, G. and Taylor, D.M., *J. Mater. Chem.,* **10**, (2000), 1551.

Minagawa, M., Takasu, T., Morita, T., Shirai, H and Fujikura, Y., Polymer, **37**, (1996), 463.

Minagawa, M., Miyano, K., Morita, T. and Yoshii, F., Macromolecules, **22**, (1989), 2054.

Newton, P., Houzé, F., Guessab, S., Noel, S., Boyer, L., Lécayon, G. and Viel, P., *Thin Solid Films,* **303**, (1997), 200.

Pethkar, S., Dharmadhikari, J.A., Athawale, A.A., Aiyer, R.C. and Vijayamohanan, K. *J. Phys. Chem. B.*, **105,** (2001), 5110.

Phadke, M.A., Musale, D.A., Kulkarni, S.S. and Karode, S.K., *J. Polymer Sci., Part B; Polymer Physics,* **43**, (2005), 2061.

Pospisil, J., Samoc, M. and Zieba, J., *Eur. Polym. J.,*Vol 34,**7**, (1998), 899.

Renschler, C.L., Sylwester, A.P. and Salgado, L.V., *J.Mater.Res.,* **4**, (1989), 452.

Reynaud, C., Boiziau, C.,Lecayon and Le Gressus, C., *Scanning Electron Microscopy* **111, (**1982), 961.

Xue, G., Dong, J. and Zhang, J., *Polymer,* **35**, (1994), 723.

Zhou, D-S., Xu, N., Li, L., Ji, G. and Xue, G., *J. Phys. Chem. B.*, **107**, (2003), 2748.

Chapter 6: Experiments with other monomers

6.1 Introduction

Following the eventual identification of conditions for the successful electrografting of PAN, the study was extended to a range of related monomers with the structure in Scheme 6.1.

Scheme 6.1

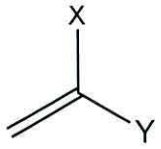

The monomers were synthesized by Rump in Lacey's group in the Chemistry Department, Hull University. The various functional groups incorporated at X and Y are given in Table 6.1. The Y functionalities were included so that further chemistry could be carried out on the functionalized surface once successful electrografting had been achieved.

Attempts to electrograft the monomers followed essentially the same procedures that had proved successful for PAN, see Section 4.14.

Table 6.1 *Range of vinyl monomers tested for their electrografting potential. The X and Y functional groups are given for each monomer.*

Monomer	X functional group	Y functional group
A	CN	OH
B	$CO_2CH_2CH_3$	OH
C	CN	Br
D	CN	OTHP - OH protected using tetrahydropyran (THP)
E	$CO_2CH_2CH_3$	OTHP - OH protected using tetrahydropyran (THP)
F	CN	NB - Carboxyl protected using 4-nitrobenzyl
G	$CO_2CH_2CH_3$	NB - Carboxyl protected using 4-nitrobenzyl

6.2 Results and Discussion

6.2.1 Monomers A, B, C

No success was achieved in the attempts to electrograft A and C on a pretreated Cu WE. The OH group proved highly reactive which prompted the synthesis of monomers D to G by the Hull group. However Monomer B did produce a non-uniform powder-like precipitate during the attempted electropolymerization. The Raman spectrum is given in Figure 6.1. A library spectrum for ethyl acrylate is given in Figure 6.2 for reference. Interestingly monomer B solution was also reported to solidify when left to stand suggesting a tendency to spontaneously polymerize. A Raman spectrum of this solid is included in Figure 6.1. The similarity between the two spectra in Figure 6.1 and the presence of peaks similar to the characteristic bands of polyethyl acrylate at 2983, 1740, 1456 and 1183 cm^{-1} assigned to $\nu(CH_2)$, $\nu(C=O)$, $\delta(CH_2)$ and $\nu(C-O)$ suggest a degree of electropolymerization was achieved. However the absence of peaks assigned to the hydroxide group and high currents recorded in the cyclic voltammogram indicate the decomposition of this required functional group. It was therefore considered necessary to protect this reactive group during the electroreduction process.

All other tests were carried out on monomers with the reactive moieties OH and COOH protected by tetrahydropyran (THP) and 4-nitrobenzyl (NB) respectively.

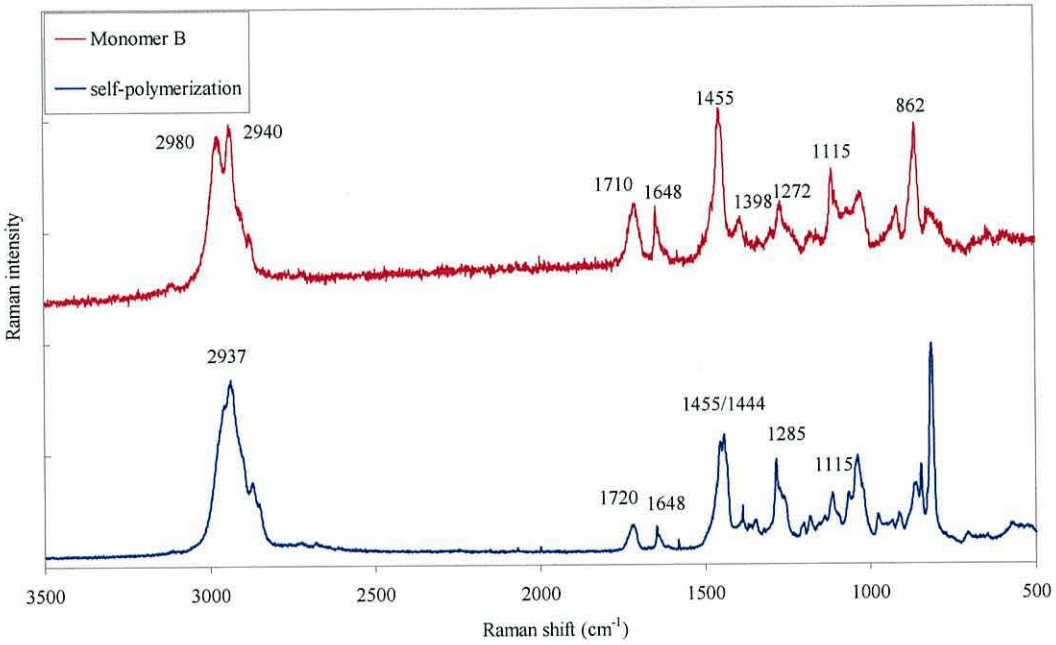

Figure 6.1 *Raman spectra of a precipitate formed from monomer B during attempted electropolymerization (monomer concentration 2M, DMF, TEAP 0.05M, Cu WE)and a sample of the monomer which had polymerized in the storage vial.*

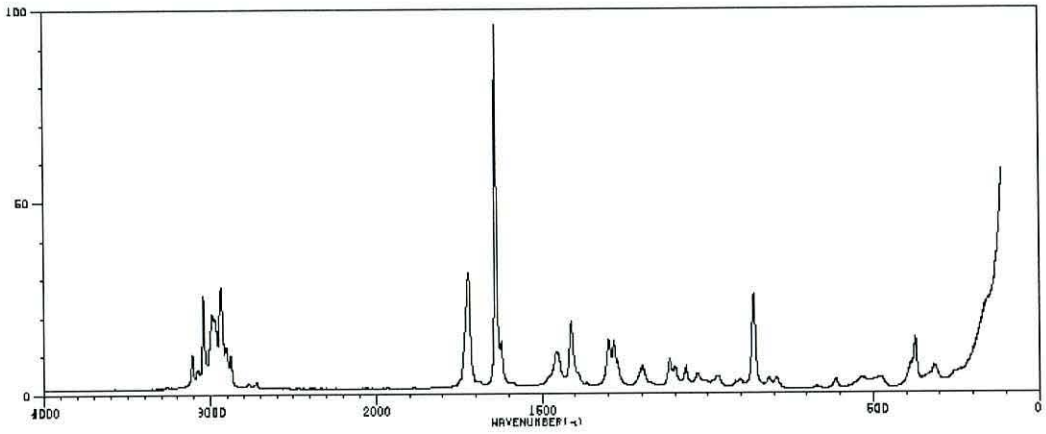

ETHYL ACRYLATE
SDBSNO = 1424 $C_5H_8O_2$ RM-01-00960 : 488OA.200M.LIQUID

3111	10	861	25
3041	25	374	14
2936	27		
2878	10		
1723	31		
1639	96		
1623	13		
1413	18		
1300	13		
1286	13		

Figure 6.2 *Raman spectrum of ethyl acrylate (Spectral database for organic compounds, AIST, Japan).*

6.2.2 Monomers D - G

The cyclic voltammograms of the other monomers D to G suggested that the reduction of water was the dominating reaction. The appearance of electroactivity at lower than expected potentials for the reduction of the monomer indicates there is contamination. Figure 6.3 is an example from the attempted electrografting of monomer E.

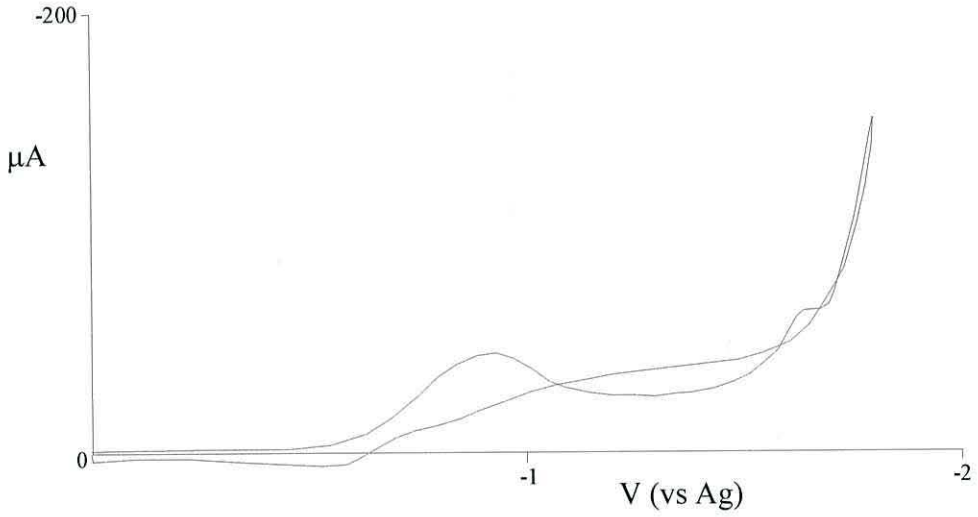

Figure 6.3 *Voltammogram from the attempted electrografting of monomer E (monomer concentration 0.5M, DMF, TEAP 0.05M, Cu WE, 20 mV / s scan rate).*

The electrografting of the model monomer acrylonitrile has been shown to be extremely sensitive to the presence of water. Mertens et al (1998) demonstrated that a water concentration exceeding 400 ppm in ACN and 1000 ppm in DMF has a serious, detrimental effect on the electrografting of PAN. The molar concentrations used for electrografting monomers D - G (0.2M – 2M) meant that the larger mass of monomer required would be expected to introduce relatively more water contamination to the made up electrolyte. This proved to be the case, with water contents ranging from 760 ppm – 3340 ppm being measured by the Hull group using a Coulometric KF Titrator from Denver Instruments. Monomers D - G are likely to be less competitive than AN, suggesting that the water content may need to be even lower than for PAN, in order to provide the right conditions for the monomer to out-compete electrolyte molecules for a place and subsequent initiation of polymerization at the electrode surface.

Following the initial failed attempts, new monomer samples of D to G were synthesized and extensively dried prior to further attempts being made to electrograft onto a Cu working electrode. Monomers F and G behaved very similarly on application of the reduction scan: the working electrode turned blue which disappeared on the reverse scan. The corresponding voltammograms showed redox type peaks indicating some reversibility in the reaction (see Figure 6.4). Analysis of the working electrodes showed no detectable residue.

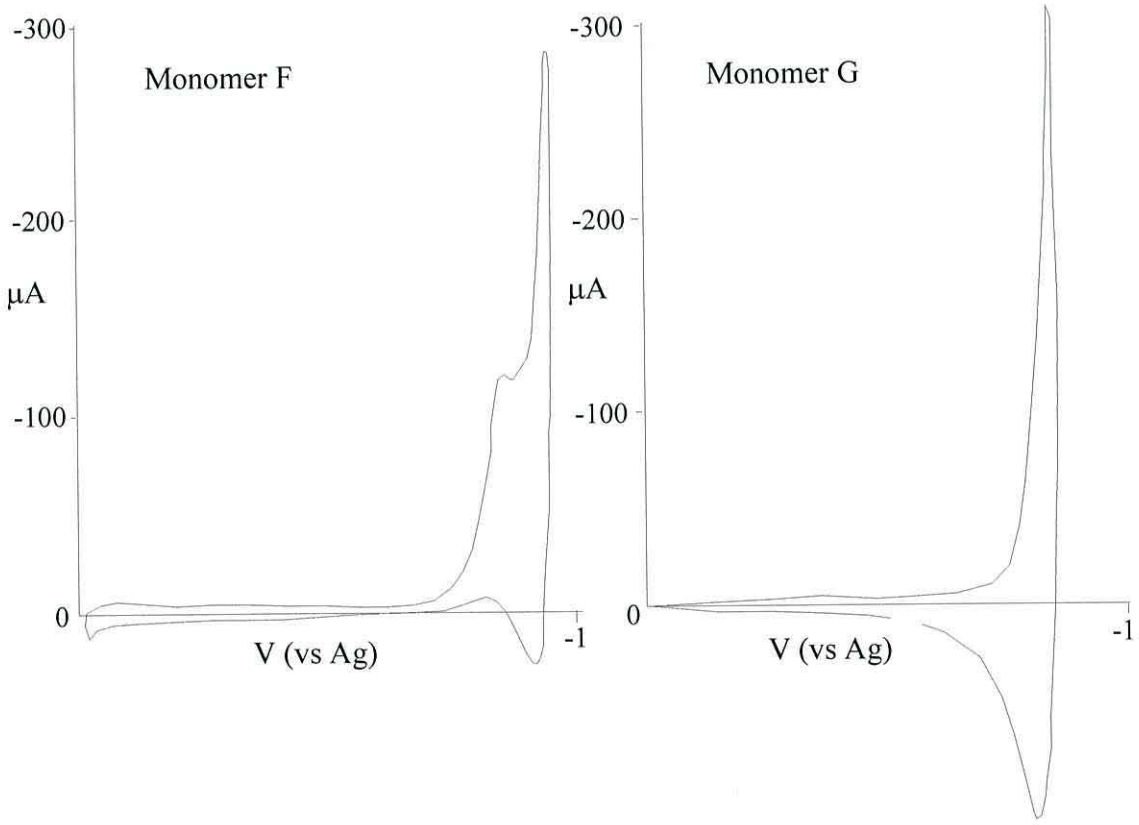

Figure 6.4 *Voltammograms from the attempted electrografting of monomers F and G which contain the carboxyl protecting group 4-nitrobenzyl, (monomer concentration 0.2M, DMF, TEAP 0.05M, Cu WE, 20 mV / s scan rate)*

The cyclic voltammogram of monomer D showed a small current peak followed by no electroactivity during a repeat scan suggesting the blockage of the electrode. In this case, AFM images clearly showed the presence of a film (see Figure 6.5). Unfortunately,

no corroborating evidence was obtained from FTIR or Raman, presumably because the film was too thin (~25 nm, see Figure 6.5(c)). Subsequently the concentrations of all the monomers were increased from 0.5M to 1M or 2M in an attempt to improve surface coverage and thereby encourage the grafting of a thicker, denser film - an approach that had worked for AN (Crispin et al, 1999; Baute et al, 2001, this work Section 4.18).

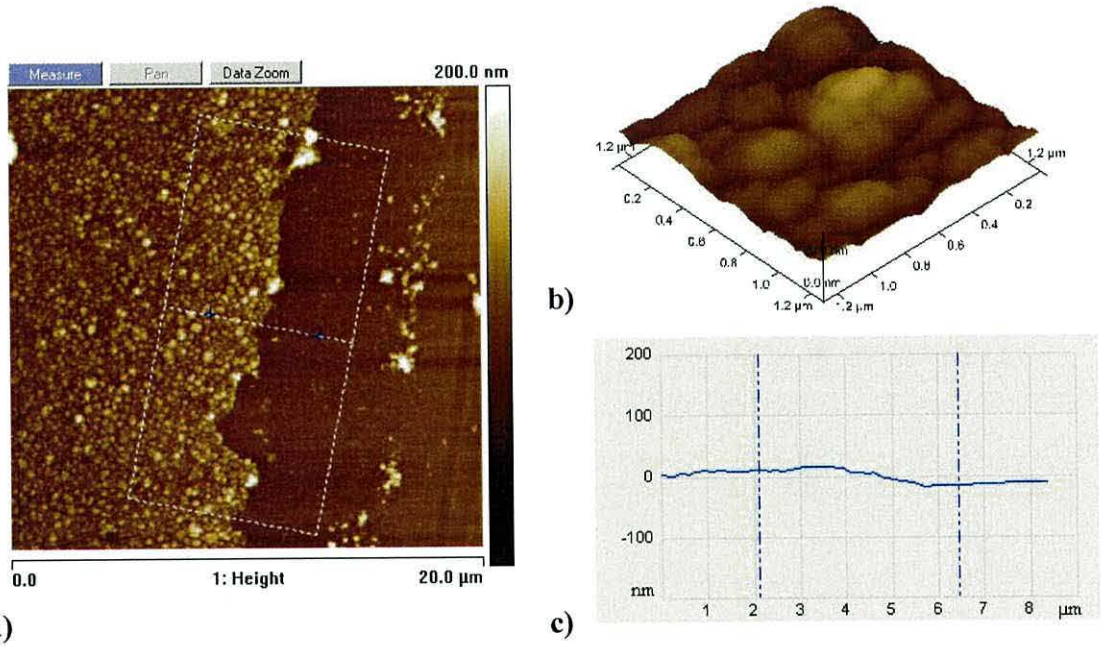

Figure 6.5 *AFM images and thickness measurement of film grown from monomer D, (monomer concentration 0.5M, DMF, TEAP 0.05M, Cu WE).*
a) Topographical and b) 3D AFM images of the film grown from monomer D.
c) Surface profile across the edge of the film which was used to determine the film thickness.

An increase of concentration to 1M for both D and E produced some promising responses from the cyclic voltammograms which showed apparent passivation on the second scan (see Figure 6.6 for monomer E). However once again FTIR and Raman proved too insensitive to detect any film.

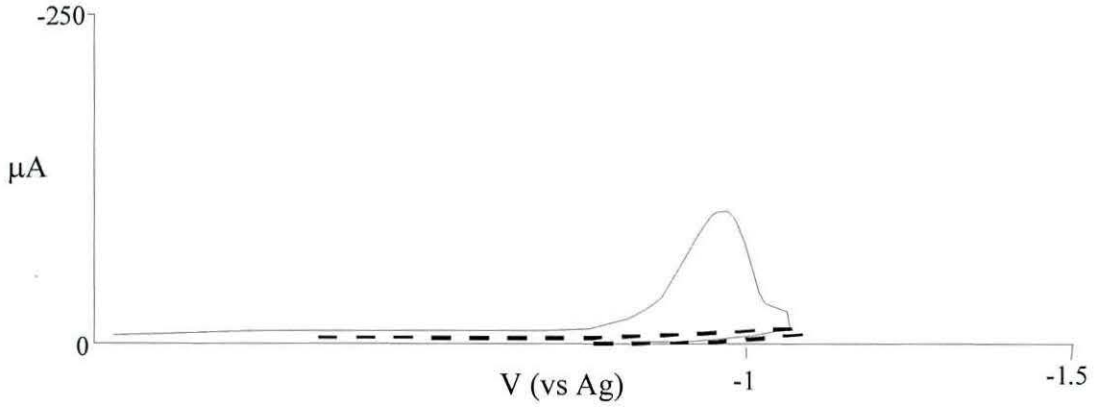

Figure 6.6 *Voltammogram from the attempted electrografting of monomer E. Repeat scan (- -) shows electrode passivation (monomer concentration 1M, DMF, TEAP 0.05M, Cu WE, 20 mV / s scan rate).*

Further increasing the concentration of monomer E to 2M gave similar voltammograms but again produced a film that was only visible to AFM (Figure 6.7). The chemical structure continued to remain illusive to the available Raman and FTIR spectroscopy, the presence of fluorescence obscuring any relevant spectral information in the former.

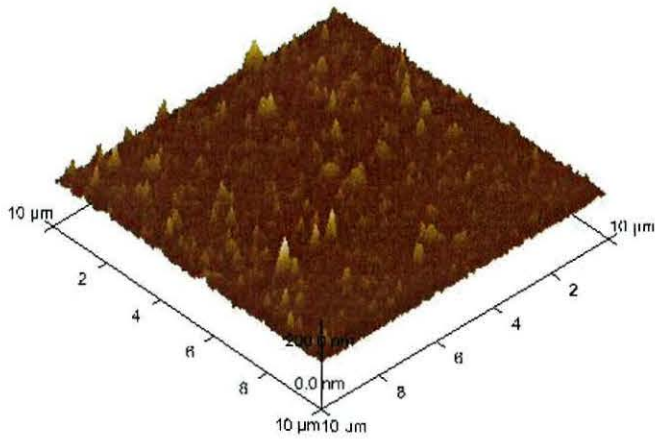

Figure 6.7 *AFM image of film grown from monomer E (monomer concentration 2M, DMF, TEAP 0.05M, Cu WE).*

It was demonstrated in Section 4.19 that a Cr keying layer underlying the Au working electrode had a significant negative effect on the electrografting of AN. Hence trials were carried out using the improved working electrodes (Au:Cr, 100:1). Figure 6.8

gives the resulting voltammogram for monomer D. As before the appearance of a reduction peak on the first scan followed by electrode passivation on the second scan for a 0.5M solution of this monomer suggests film formation. This time, however the film was sufficiently thick to yield a Raman spectrum (Figure 6.9). For comparison the Raman spectra of AN monomer and for electrografted PAN reproduced from Figure 4.24 are also given. Indicators that electropolymerisation has occurred are as follows:

a) No evidence for the unsaturated C–H vibration above 3000 cm^{-1}.
b) Strong signals for the saturated C–H stretch vibrations between 2840 and 3000 cm^{-1}.
c) Presence of some C≡N stretch at 2243 cm^{-1} also a significant fraction red shifted to 2129 cm^{-1}.
d) Significant reduction in C=C at 1609 cm^{-1}.
e) Presence of 1520 and 1600 cm^{-1} peak suggesting formation of azine links similar to PAN.

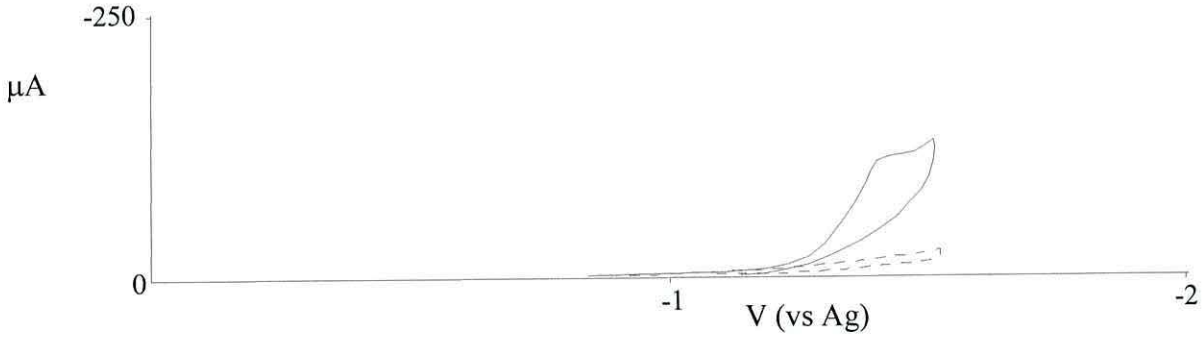

Figure 6.8 *Voltammogram from the attempted electrografting of monomer D using the improved working electrode, Au:Cr, 100:1. Repeat scan (- -) shows electrode passivation (monomer concentration 0.5M, DMF, TEAP 0.05M, 20 mV / s scan rate).*

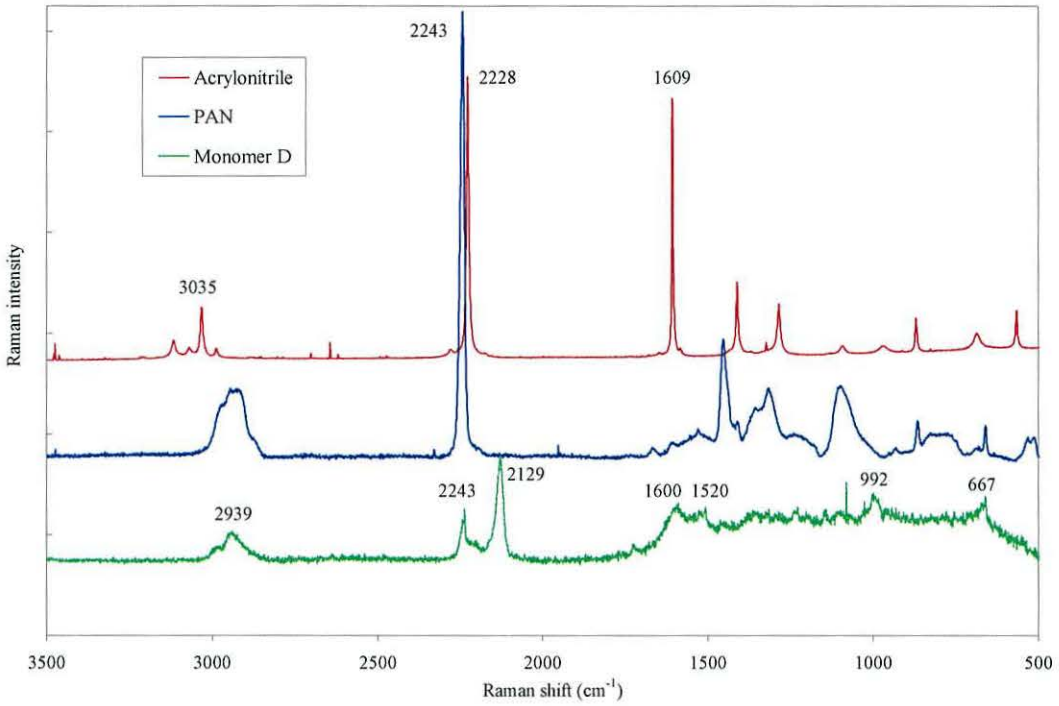

Figure 6.9 *Raman spectra of the film grown from monomer D. (monomer concentration 0.5M, DMF, TEAP 0.05M, WE Au:Cr 100:1).*

6.3 Conclusion

The monomer trials provided some promising results using the improved electrodes. However limitations of current spectroscopy techniques i.e. fluorescence and the spectral sensitivity need to be addressed if films of the order of 30 nm and below are to be characterized more fully. The OTHP appears to have potential as a protection group for the hydroxyl moiety during the electrografting process.

It is difficult to draw any firm conclusions from the available results, however it does appear that monomer D containing the nitrile group shows more promise than monomer E containing the alternative ester group. Baute et al (1998) compared the electrografting of EA to AN (EA has a similar monomer structure to monomer E but with hydrogen as the Y group). The ester group of EA was seen to be less efficient than the nitrile group at triggering electron delocalization and proposed that in the presence of the

strong electron-withdrawing nitrile group, AN would orientate more effectively on the electrode under the influence of an electric field. The β carbon of the monomer would then be in a good position to readily interact with a metal site.

Baute et al (1998) also proposed that the propensity of a monomer to electrograft depends on the electron deficiency of the β- carbon double bond. MMA was observed to be less competitive than EA suggesting the inductive effect of the α - methyl group counterbalances the electron withdrawing effect of the ester group. The electron withdrawing capacity of the X functional group therefore needs to compensate for any inductive effects from the Y functional group. The results here indicate that the nitrile group appears to be a valuable 'engine' for the electrografting process.

6.4 References:

Baute, N., Jérôme, C., Martinot, L., Mertens, M., Geskin, V.M., Lazzaroni, R., Brédas, J.L. and Jérôme, R., *Eur. J. Inorg. Chem.,* (2001), 1097.

Crispin, X., Lazzaroni, R., Geskin, V.M., Baute, N., Dubois, P., Jérôme, R. and Brédas, J. L., *J. Am. Chem. Soc.,***121**, (1999), 176.

Mertens, M., Calberg, C., Baute, N., Jérôme, R. and Martinot, L., *J. Electroanal. Chem.,* **441**, (1998), 237

Chapter 7: Conclusion and Further Work.

7.1 Conclusion

The overall aim of this study was to develop electrografting as a technique to produce functionalized polymeric macrostructures of a desired tactic nature for a range of potential applications. Specifically the study set out to explore the electrografting of a series of vinyl monomers. Of particular interest was the elucidation of how the structure grows from the metal surface, what factors affect the growth of the structure and which metals support electrografting. The objective was to investigate in a systematic manner, a number of monomers that undergo both anodic and cathodic electropolymerization with the purpose of electrografting a polymer with either tactic in-plane or out-of-plane reactive moieties suitable for undertaking further chemical reactions. The preparation of such command surfaces can provide functional groups for the attachment of other active moieties such as sensor units, NLO chromophores etc.

The survey of the literature on the electrografting of acrylonitrile revealed a number of interesting points. All the work reviewed recognized the essential requirement for purity and dryness of the experimental conditions (Lecayon et al, 1982), the need to activate the electrode surface by removal of the metal oxide (Bouizem et al, 1984) and the solvent influence on the surface coverage and quality of films (Mertens et al, 1998). The chemisorption of the monomer, the prerequisite condition for electrografting was found to be dependent on the electrode metal used (Crispin et al, 1999). When electrografting occurred this was shown to influence the tactic nature of the polymer film (Calberg et al, 1998), particularly the early growth of the structure. As a result of this tacticity, cyclization occurs more efficiently when electrografted PAN films are heated compared to solution electropolymerized PAN.

When the technique was extended to other vinyl monomers, the structural differences were shown to significantly influence the electrografting process through their effect on the competitiveness of the monomer for a place on the electrode as assessed through successful grafted surface coverage. An increase in monomer concentration was found to be necessary to compensate for the reduction in monomer competition (Baute et al, 1998). One result of the reduced competitiveness is the

formation of a mixture of grafted and ungrafted chains. Successive scans were also needed to improve surface coverage and thickness (Tanguy et al, 1996).

One of the key features to emerge from the literature survey is the controversy surrounding the limitations of the cyclic voltammetry as a means of identifying the onset of the initiation of electrografting and for controlling the process. Most reports tended to focus on Peak I of the double peak regime as the signature of electrografting. However, Bureau et al (1999) using numerical simulations of voltammograms showed that double peaks can in fact arise as a result of homogeneous polymerization in solution coupled to a charge transfer process. This work questioned whether the footprint of the electrografting reaction can actually be detected using voltammetry. Mertens et al (1998) showed that exceeding the grafting potential led to straining and the eventual debonding of a grafted PAN film. Leroy et al (1985) further showed that prolonged holding of the potential at Peak I can lead to structural changes in electrografted PAN such as chain segmentation and cyclization.

While the work reported here has established the fundamental features of the electrografting technique for the model monomer AN, it has also highlighted the limitations of cyclic voltammetry as the sole technique for controlling the preparation of good quality, well defined macrostructures for academic/industrial use. In particular, observing Peak I is notably unreliable but evidence of electrode passivation on the second scan is a positive indicator of film growth.

Visible observation of film growth also proved to be unreliable. Film visibility increased when it started to debond. It is concluded, therefore, that voltammetry alone is not sufficient to monitor and control the electrografting process. Other techniques such as surface plasmon resonance (see later) which are sensitive to the presence of thin films on electrodes, should be employed in tandem to identify the potential for the initiation of electrografting and film growth.

The initial experiments carried out in this programme adopted a technique used by Mills et al (2000) which was an adaptation from previous work on the electropolymerization of polymeric macrostructures. The technique, using a standard 3-electrode cell connected to a potentiostat, offered great promise as a simple means of functionalizing metal surfaces. Unfortunately, exhaustive attempts to duplicate the Mills

et al (2000) work failed to produce the characteristic electrografted PAN films reported in the literature. Hence, an intensive study was undertaken to investigate the effect of various experimental parameters such as supporting electrolyte, solvent, electrode material and preparation as well as the working environment and potentiostat control. The effect of any changes was monitored electrochemically using cyclic voltammetry. The morphology and chemical structure of successful film growth was evaluated using a combination of Atomic Force Microscopy, Raman Microscopy, FTIR spectroscopy, ellipsometry and UV VIS spectroscopy.

This thorough examination of the procedures involved identified water, oxygen and electrode contamination to be the main inhibitors to the cathodic electrografting process. A series of necessary modifications to the cell design, electrolyte preparation and potentiostat control were then undertaken to establish the essential experimental conditions for the successful growth of quality electrografted films. The work has shown, therefore, that the electrografting process is capable of producing high quality PAN coatings covalently attached to a metal substrate. The films displayed good chemical stability and were of controlled thickness and of well-defined chemical structure. The thickness of the polymer coating was found to be dependent on monomer concentration, type of monomer, solvent, salt and temperature. Film growth could also be affected by side reactions.

Despite the elaborate procedures finally adopted they were, nevertheless, relatively easy to implement and provide a more industrially viable method for electrografting quality PAN films than hitherto reported.

The FTIR spectrum of electrografted PAN closely resembled that of a commercial spun-coated sample. Apart from the presence of unusual, previously unreported peaks centered at 1096 cm^{-1} and 1520 cm^{-1} with a shoulder at 1580 cm^{-1}, the Raman spectrum of PAN electrografted in DMF was also similar to that of spin-coated commercially sourced PAN.

In addition to the unusual Raman peaks referred to above, this study has shown that electrografted PAN films tend to trap the solvent DMF as evidenced by the strong peak in FTIR at 1665 cm^{-1} with related absorption bands at 1388 and 659 cm^{-1}. Further support was provided by DMF peaks appearing in the Raman spectra at 867 and

660 cm^{-1}. A slight red shift of the >C = O stretch band at 1665 cm^{-1} in FTIR suggest some interaction between the solvent carbonyl group and the nitrile moiety of PAN. These findings suggest that the assignment by Funt et al (1964) of the 1670 cm^{-1} FTIR band to –C=N absorption was incorrect, an error that has been perpetuated in several later publications. Interestingly, the FTIR spectra of electrografted PAN films by Calberg et al (1998) using DMF show no evidence for entrapped solvent.

A detailed study of the unusual, apparently anomalous, Raman peaks was then undertaken. Interestingly, the Raman spectra of PAN films grown in ACN did not show these anomalies, but did exhibit peaks at 1566/1600 cm^{-1} suggesting the type of structural transformations normally seen in the pyrolysis of PAN. This is supported by the deterioration of the nitrile peak and the appearance of peaks at 2190 and 3340 cm^{-1}. In contrast the spectra of PAN films grown in DMF showed no such deterioration of the nitrile peak. To eliminate the type of structures arising from the pyrolysis of PAN as the origin of the anomalous features electrografted PAN films were heat treated either by prolonged exposure to the Raman laser or in a conventional vacuum oven. Structural transformations normally associated with the pyrolysis of PAN were identified as evidenced by FTIR, Raman and UV-visible spectra. Peaks associated with the trapped DMF were effectively eliminated and the Raman anomalies were replaced by the usual peaks associated with graphitization.

The Raman anomalies were found to be dependent on the monomer concentration in the electrografting solution and on the WE used. The peaks were more intense for thinner films and consistently disappeared for thicker films grown at higher concentrations (2M) using the improved experimental conditions. The intensity of the peaks was sensitive to the WE metal. For instance PAN films grown from a 0.5M AN solution show that peak intensity for the different WE metals follows the order Pt >Ag > Cu >Au. The use of Pt foil eliminated Cr as a potential cause of the peaks which were also sensitive to the pretreatment of the WE. Application of the ORC treatment to a Ag WE prior to electrografting significantly reduced the intensity of the peaks. However the appearance of a new peak at 1725 cm^{-1} in FTIR suggested the presence of unwanted oxidized species at the electrode surface which probably interfered with the

electrografting process. Taken together, the above evidence points to a structure at or close to the metal surface as the origin of the anomalous Raman peaks.

Calberg et al (1998) reported electrografted PAN to be predominantly isotactic near the surface. The films produced in the present work are comparable to those obtained by Mertens et al (1996) and Calberg et al (1998) as evidenced by the AFM and FTIR studies. It has been argued in the present work, therefore that the Raman peaks at 1096 cm^{-1} and at 1520 - 1580 cm^{-1} which have been identified in this first reported Raman study of electrografted PAN arise from a ladder-type network of vertically stacked polymer chains connected by azine bridges. Either the electrochemistry or the vertical alignment of chains has encouraged the formation of the azine structure which would not normally occur due to the improbability of the nitrile – nitrile association. The complimentary active and inactive bands seen in Raman and FTIR respectively correlate well with the stretch vibration of the azine structure. The complete absence of any spectral peaks normally associated with the usual structural transformation seen in the pyrolysis of PAN in either the FTIR or Raman spectra provides convincing support for the existence of these normally improbable structural transformations.

At first sight, the dense brush-like structure of the electrografted PAN films are ideal for further functionalization. By growing films in a suitable low concentration of DMF, solvent entrapment can be minimized and the growth of a predominantly isotactic structure can be encouraged. However, the formation of the azine network precludes even the limited chemistry that could have been undertaken on the nitrile group. Thus electrografted PAN will be limited to applications based on its passivating properties.

Experiments with monomers capable of a wider range of reactions gave promising results when using the 100:1 Au/Cr electrodes. AFM images of the electrode surface clearly reveal the presence of a film, supporting the signs of passivation seen in the voltammograms. However problems with fluorescence and the Raman spectroscopy detection limits prevented confirmation of electro-polymerization. The OTHP appears to have potential as a protection group for the hydroxyl moiety during electrografting but improvements to the spectroscopy technique need to be addressed to confirm that polymerization has occurred and that the OTHP moiety is fully intact. The apparent difference in behaviour between monomer D and E suggests the nitrile group may well

prove to be a good vehicle to introduce more useful functional groups into the polymer chains of electrografted films.

7.2 Further work

While this study has added significantly to our understanding of the electropolymerization of vinyl monomers, nevertheless a number of areas for further work have been identified. These are discussed briefly below.

7.2.1 Surface Plasmon Resonance

Identifying the potential at which electrografting is initiated and monitoring the subsequent propagation into quality polymer films has been one of the main challenges in this study. Surface plasmon resonance (SPR) offers a potential solution. This optical technique is extremely sensitive to adsorbate changes at the substrate electrolyte interface and if coupled with the electrochemistry could provide a valuable window to decipher the electrografting signature. One of the main advantages of SPR is that it focuses on the optical changes that occur in the close vicinity of the metal. Unlike an electrochemical quartz microbalance these changes are not obscured by what is happening in the rest of the electrolyte.

In principle electrochemical surface plasmon resonance spectroscopy (ECSPR) can monitor in real-time the electrografting of AN and other vinyl monomers onto Ag/Au electrodes. Ehler et al (1999) showed in-situ SPR can effectively be used to follow the sequential multi-layer electropolymerization of a pyridine derivative onto a thin gold electrode. The in-situ technique could potentially provide an insight into the formation and structure of the electrografted polymer and investigate the relationship of the double peak regime with the electrografting process.

Initiation and propagation of the polymer is expected to cause refractive index changes resulting in shifts and band shape changes in the plasmon spectrum (reflectivity versus incident angle). These changes could also provide a sensitive marker for monitoring changes to a functionalized macrostructure on exposure to an analyte.

For not so competitive monomers that require successive voltage scans, each cycle can produce a plasmon spectrum for interpretation. SP analysis of the angular shifts

can yield estimates of thickness and the refractive index of the growing polymer film. Thickness changes of ~20 Å have been detected using Au films.

7.2.2 Functionalising macrostructures

Electrografting of polymers onto conducting surfaces by electropolymerization of a vinyl monomer containing functional groups X and Y have the potential to functionalise polymeric macrostructures. The X substituent is used to help facilitate the polymerization and the Y is reserved for the monomer functionalization. This work produced some promising results using a vinyl monomer with nitrile as the X group and OTHP as the Y. The OTHP is made up of the hydroxyl group protected with tetrahydropyranyl. The hydroxyl group is quite reactive so deprotection could allow the introduction of some useful functional moieties. Schemes for attachment of these moieties are complicated because these polymers ideally will not only have groups attached to the surface of the structure but also along the polymer backbone as far as the surface attachment point.

Further work could investigate the effect of attachment using low angle X-ray diffraction and low angle neutron diffraction to interrogate and provide information on the depth and coverage of the deprotected hydroxyl group and if successful extend the evaluation to the attachment of more sophisticated (biological) and low energy protection moieties. SPR could also be used to monitor these macrostructure changes.

7.2.3 Fluorescence

The attempts to electrograft vinyl monomers containing the OTHP certainly produced films as evidenced by AFM images. Unfortunately only the film grown from the electropolymerizing of monomer D (see Chapter 6) containing the nitrile and OTHP group produced any readable Raman spectra. Raman spectroscopy is a convenient tool for identifying functional groups and confirming polymerization. However it has limitations. During the latter stages of this work in the production of thinner films (<50nm) fluorescence became an increasing problem, obscuring the important spectral information particularly in the fingerprint region. Readily available structural feedback is essential if further work in this subject is to continue. A number of possible solutions to

reduce the problem of fluorescence is to explore the effect of using an infrared laser at 780nm which has been found to be effective but at the expense of a loss of scattering efficiency (scattering decreases as the fourth power of the wavelength of the scattered radiation) or alternatively exploit the selective capability of the instrument's true confocal configuration.

7.2.4 NLO structures

The small π conjugation imparted by cross-linking through –C=N across the PAN chains potentially lends some interesting nonlinear optical properties to an otherwise passive surface. The alignment of these azine links parallel to the surface in ladder-like columns is ideal. However the centrosymmetric structure as evidenced from the complimentary FTIR inactive and Raman active bands, prevents the required asymmetric molecular electron distribution in the presence of an intense optical field required for nonlinear optical responses. Interestingly the Raman spectra of the film produced from electropolymerising monomer D also shows the possibility of similar structures. If polymerization has occurred with the OTHP fully intact and some of the nitrile groups have formed azine bridges this potentially opens up the possibility of an asymmetric structure suitable for NLO studies. Deprotection of the OTHP and attachment of a polar group could potentially change the symmetry of the azine structure and induce the appropriate electron distribution.

7.3 References:

Baute, N., Teyssie, P., Martinot, L., Mertens, M., Dubois, P. and Jérôme, R., *Eur. J. Inorg. Chem.,* (1998), 1711.

Bouizem, C., Chao, F., Costa, M., Tadjedinne, A. and Lécayon, G., *J. Electroanal. Chem.,* **172**, (1984), 101.

Bureau, C., *J. Electroanal. Chem.,* **479**, (1999), 43.

Calberg, C., Mertens, M., Baute, N., Jérôme, R., Carlier, V., Sclavons, M. and Legras, R., *J. Polymer Sci., Part B,* Vol **36**, (1998), 543.

Crispin, X., Lazzaroni, R., Geskin, V.M., Baute, N., Dubois, P., Jérôme, R. and Brédas, J. L., *J. Am. Chem. Soc.,***121**, (1999), 176.

Ehler, T.T., Walker, J.W., Jurchen, J., Shen, Y. Morris, K. Sullivan, B.P. and Noe, L.J., *J. Electroanal. Chem.,* **480**, (2000), 94

Funt, B.L. and Williams, F.D., *J. Polymer Sci., Part A,* **2**, (1964),865.

Lécayon, G., Bouziem, Y., Le Gressus, C., Reynaud, C., Boiziau, C. and Juret, C., *Chem. Phys. Lett.*, **91** (1982), 506.

Leroy, S., Boiziau, C., Perreau, J., Reynaud, C., Zalczer, G., Lécayon, G. and Le Gressus, C., *J. Molecular Structure*, **128**, (1985), 269

Mertens, M., Calberg, C., Martinot, L. and Jérôme, R., *Macromolecules,* **29**, (1996), 4910.

Mertens, M., Calberg, C., Baute, N., Jérôme, R. and Martinot, L., *J. Electroanal. Chem.,* **441**, (1998), 237

Mills, C.A., Lacey, D., Stevenson, G. and Taylor, D.M., *J. Mater. Chem.,* **10**, (2000), 1551.

Tanguy, J., Deniau, G., Zalczer, G. and Lécayon, G., *J. Electroanal. Chem.,* **417**, (1996), 175.

Conferences and Meetings

Materials Research Society (MRS) Spring Meeting 2003,

San Francisco, USA, April 2003

Poster presented: *The Electrografting of Polyacrylonitrile to Noble Metals – A Spectroscopic Study*